COMPARISON OF IGS TROPOSPHERE ESTIMATIONS

Gerd Gendt
GeoForschungsZentrum Potsdam, Aufgabenbereich 1,
Telegrafenberg A 17, D-14473 Potsdam, Germany

INTRODUCTION

Water vapor is a crucial parameter in atmospheric modeling. It has a very inhomogeneous distribution and a high variability. Continuous and well-distributed measurements of water vapor are therefore of fundamental interest both for short range weather predictions and climatology.

The GPS is a cost-effective technology to provide dense, globally distributed and nearly continuously measured water vapor. Even if we get only the (vertical or lateral) integrated values, this is important information.

There are two approaches in the application of the GPS to meteorology with following characteristics:

Ground-based GPS meteorology:

- Networks of ground-based GPS receivers are used to estimate the vertically integrated water vapor (IWV).

  The great advantage is the nearly continuous measurement of IWV. The spatial distribution depends on the density of the network. (For dense networks lateral gradients of IWV can be deduced)
- Over the oceans good coverage can never be reached.

Space-based GPS meteorology:

- GPS receivers on board a Low Earth Orbiter (LEO) satellite observe very short (- 1 minute) atmospheric occultations (-500 per day) which provide a vertical refractivity profile (laterally integrated over -150-200 km) .
- The water vapor profile can be deduced if the temperature profile is known, and vice versa.
- It is not continuous at a point, but has a good global distribution.

  Problems may occur in monitoring lower troposphere in the vicinity of high mountains.

These two approaches are not competing but complementary to each other. The IGS is based and focused on the analysis of the global network of ground receivers and can therefore be part of the ground-based GPS meteorology.

Typically the refraction parameter is estimated in form of the total zenith path delay **(ZPD),** presuming the elevation depending mapping function is known, the wet component changes little over short periods of time and simultaneous measurements in different elevations exist, The ZPD is the sum of the hydrostatic and wet components. Knowing the surface pressure to 0.5 mbar it is possible to remove the hydrostatic zenith delay with an accuracy of a few millimeters or better and to get the zenith wet path delay (ZWD) without introducing any additional error. Furthermore the error in the mapping function for elevations >15 degrees is not a significant part of the error budget for the ZWD. The parameter of interest for the meteorologist is not the ZWD but the vertically integrated water vapor in terms of precipitable water vapor (PWV). With the knowledge of the surface temperature only, this transformation from ZWD to PWV may be done with an accuracy of 2%. From a variety of experiments the PWV accuracy can be estimated to about 1 mm.

Table 1. Error budget for PVW Estimation (units: mm)

Error Source	Pwv	ZPD	Comment	
Estimation error				
orbit	0.2	1.3	10 cm error, 1000 km baseline	a
coordinates	0.5	3.0	1 cm height error	a
multipath	0.3	2.0		a
RSS	0.6			
Conversion error				
Barometric press.	0.2	1.2	0.5 mbar, normal wind	b
Con. ZWD-PWV	0.4	-	2% error (for 20 mm PWV)	b
Physical constants	0.25	1.5		b
RSS	0.5			

a Rocken et al., 1995 b Runge, et al., 1995

The 7 IGS Analysis Centers (AC) routinely analyze more than 50 global distributed IGS tracking stations. To produce the IGS products - precise orbits, earth rotation parameters and station coordinates - the tropospheric refraction has to be modeled and a zenith path delay (ZPD) correction must be adjusted. Up to now the ZPD itself is not a product and therefore the routine analysis is not optimized to get best estimates for it. Nevertheless, the accuracy of its determination is high and converted to precipitable water vapor content its a valuable information for meteorology.

To look into the stability of ZPD determination, comparisons of CODE and GFZ tropospheric estimates were presented already at the last IGS Workshop (Data from 3 weeks in northern winter 1994/95). The general consistency was about ±10 mm for the stddev and ±6 mm for the bias. The result was encouraging and stimulated to think about a new IGS product, the IGS mean of PWV, provided that the IGS tracking sites are equipped with automated meteorological packages. In preparation of such a new product the IGS Governing Board recommended to accomplish a more comprehensive comparison including all ACS and choosing 3 weeks during northern summer (August 1995), to have for the majority of sites not so dry air as in northern winter.

DATA, SOFTWARE

The main features for tropospheric parameter estimation in the software package of all ACS are given in Table 2. There are very different approaches. It should be pointed to those differences, which could be responsible for differences in the tropospheric parameter estimation. A great influence may have the elevation cutoff angle, which varies from 15 to 20 degrees. Whereas all other ACS solve for ZPD independent from interval to interval, EMR and JPL introduce constraints within their Kalman procedure. For poor observed sites and time intervals the constrained solution is naturally smoother, compared to the unconstrained case.

During routine analysis most ACS estimate ZPD parameters in intervals of 4 to 6 hours, so that for this comparison the test weeks had to be reprocessed to get a sampling rate of 2 hours, which was agreed on. For the comparison the GPS weeks 812 to 814 (July 30 to August 21, 1995; DoY211 to231; MJD 49928 to 49948) were chosen. The sites used vary from AC to AC, their number can be seen in Table 3. Only those sites analyzed by at least 3 ACS were compared, which reduces its number to about 40.

There were some problems in the calibration of ESA and NGS series, which couldn't be identified and removed. For the NGS estimates this may probably be explained by the fact that NGS is the only AC applying elevation dependent antenna phase corrections. Because of these large biases some results are therefore presented without these two centers.

Table 2. Characteristics of the software packages

	CODE	EMR	ESA	GFZ	JPL	NGS	SIO
Method	doub.diff.	undiff.	doub.diff.	undiff.	undiff.	doub.diff.	doub.diff.
MetData	Hei.-dep. nominal P,T,H	Global constant	Global constant	Hei.-dep. nominal P		Lat. -Hei- DoY Model	Global constant
Tro. Model	Saastam.			Saastam.		Saastam.	
Mapping F.	1/cos(z)	Lanyi	Willmann	I/coS(z)	Lanyi	Niell	Davis
Elev. cutoff	20	15	20	20	15	15	20
Sampl. Rate (Data; rein)	2	7.5	6	6	5	0.5	2
Sampl. Rate Tro. Estim.	120	7.5	120	120	5	120	60
Constraints	No	Yes	No	No	Yes	No	No

Table 3. Number of sites and time interval for tropospheric parameter estimation

	No. STA	Tropospheric Estimation (minutes)	Weeks analyzed 812	813	814
CODE	58	120.	+	+	+
EMR	28	7.5	+	+	+
ESA	48	120.		+	+
GFZ	47	120,	+	+	+
JPL	35	5.	+	+	+
NGS	41	120.		+	+
S10	15	60,	+	+	+

COMBINATION OF MEAN ZPD SERIES

The files used by the individual ACS for storing their tropospheric estimates are different in format and philosophy. To handle all comparisons and the combinations a SINEX-like format for tropospheric series was defined and applied throughout this investigation.

The individual series have of course biases between each other. If a straightforward mean would be computed then gaps in one of the biased input series would produce a jump in the mean series. This is why the following 2-step procedure is used to derive the mean series for a defined interval, e.g. 1 day or 1 week:

- A mean ZPD-file is computed by combining the estimates of all ACS. This file is named IGS-Trop-File.
- No weights are used in the combination.
- The 2-step procedure has the following main steps and works site by site:

A 1 Computation of a preliminary IGS-Trop-File.
Mean trop values are computed for those epochs, where **all ACS** have ZPD estimates (to get no jump in the mean by missing ACs).

A2 Computation of the bias between the preliminary IGS-Trop-File and each AC.

B 1 Computation of IGS-Trop-File.
Mean ZPD values are computed, where the AC estimates are corrected by the bias from step A2. This way all epochs can be used and a gap in the series of one AC will not result in a gap for the IGS-Trop-File. Outliers are eliminated. The number of contributing ACS is coded for each ZPD value. A series of a single AC is copied into the IGS-Trop-File too.

B2 Computation of stddev and bias between the IGS-Trop-File and each AC. Only epochs are used where at least 3 ACS have contributed. Outliers are eliminated (with 2.5*stddev)

RESULTS

First of all differences in pairs were computed to get an insight into the consistency between the individual ACS. This was done using daily and weekly biases for each site, Tab. 4. The stddev for the ZPD-differences is about ±9 mm. The weekly bias has no significant systematic shift and its stddev over all sites is about ±5 mm. The consistency between CODE and GFZ is the same as it was obtained in the comparison with data from northern winter 1994/95 (Gendt and Beutler, 1995). From this one may conclude that the accuracy will not depend on the absolute water vapor content. The best agreement is between EMR and JPL, which may be due to the constrained estimation and 15 degree elevation cutoff angle in both series.

There is a high stability in the daily repeatability of the bias for a site, but also a significant site-dependent shift from AC to AC. This high repeatability explains that the improvement in the stddev of ZPD differences is only marginally (-1 mm) if daily instead of weekly biases are used. Therefore, to have no jump at the day boundaries by missing sites for a single AC for a single day, weekly biases were computed for the determination of the IGS mean series. In Fig. 1 the daily repeatability of the bias between JPL and other ACS are shown for selected sites. The repeatability is in most cases better than ±2 mm. The reason for the systematic effects, which reaches values of 1 cm, is not fully explained. Some effects may come from different a priori models, meteorological values and station heights, e.g. 1 cm height change gives 3 mm bias in ZPD. Even having the same coordinates, e.g. for fiducial sites, cutoff angles and software, like EMR and JPL, biases of some 5 mm can be seen. To eliminate all possible sources of biases the coordinates (and so the heights) of as many sites as possible should be agreed on. The higher resulting consistency makes only sense if these coordinates have a high accuracy and will therefor not give systematic errors. For climate research a high long stability is of crucial importance and this implies that significant station height changes should be avoided, at least documented for possible PWV corrections.

Statistics of the ZPD differences between the individual ACS and the IGS mean can be seen from Figs. 2. The stddev and bias are about ±6 mm and ±4 mm, respectively, which gives an rms of ±7-8 mm and corresponds to ±1.3 mm PWV.

In Figs. 3 some tropospheric series are shown. No bias corrections are performed. It can be seen that the accuracy in the estimations does not depend on the amount of fluctuations in the total ZPD. Even such high fluctuations of -200 mm within hours as for ALGO are reflected in all ACS series with an accuracy comparable to ±1 mtn PWV.

SUMMARY

These comparisons demonstrate the high consistency in the tropospheric estimations between the 'IGS Analysis Centers, although there are systematic effects which have to be investigated.

The IGS is ready to produce time series of vertical integrated water vapor, provided the meteorological surface parameters are measured within the IGS network. Many of the sites have already meteorological packages installed for other collocated techniques, like VLBI, PRARE, DORIS, SLR. The last step to use these measurements on a regular basis and to install additional meteorological packages should be pushed forward within the IGS, hopefully still in 1996.

Acknowledgement, This comparison was only possible by the support of all IGS Analysis Centers. Thanks to all of them for reprocessing the test weeks 812 to 814 and making available their tropospheric estimates with the agreed upon sampling rate.

REFERENCES

Gendt, G., G Beutler, 1995, Consistency in the tropospheric estimations using the IGS network, in *Proceedings of the IGS Workshop 'Special Topics and New Directions',* Potsdam, May 1995, editors G Gendt and G Dick, 1996, pp. 115-127

Rocken, Ch, F S Solheim, R H Ware, M Exner, D Martin, M Rothacher: Application of IGS data to GPS sensing of the atmosphere for weather and climate research, in *Proceedings of the IGS Workshop 'Special Topics and New Directions',* Potsdam, May 1995, editors G Gendt and G Dick, 1996, pp. 93-103

Runge, Th., M Bevis ,Y Bar-Sever, S Keihm: Accuracy evaluations of ground-based GPS estimates of precipitable water vapor. *Paper AGU Fall Meeting,* Dec. 12, 1995, San Francisco.

Table 4a. Consistency of ZPD estimates between the Analysis Centers for week 813. (units: mm)

		Weekly bias		Daily bias	
	No.Sta	Bias (mean of sta)	sdev.	sdev.	Bias (daily repeat.)
CODE-EMR	24	-0.2±6.6	8.9	8.0	*3.9
CODE-GFZ	45	-0.3*3.7	10.6	9.8	*3.7
CODE-JPL	35	-1.1*4,9	8.6	7.8	*3.8
EMR-GFZ	24	-0.9±7.0	8.2	7.6	*3.4
EMR-JPL	21	-1 .9±3.6	6.8	6.4	±2.6
GFZ-JPL	31	-0.9*4.9	9.5	9.0	±3.2

Table 4b. Continued, but only for fiducial sites (units: mm)

		Weekly bias		Daily bias	
	No.Sta	Bias (mean of sta)	sdev.	sdev.	Bias (daily repeat.)
CODE-EMR	12	-0.1±4.0	8.2	7.6	±2.8
CODE-GFZ	12	0.4*1 .7	9.7	9.4	±2.5
CODE-JPL	12	-0.9±2.3	8.0	7.5	±2.6
EMR-GFZ	12	0.3±4.2	7.8	7.4	*2,1
EMR-JPL	12	-1 .0±3.0	6.1	5.8	*1.9
GFZ-JPL	12	1.3±2.3	9.1	8.9	±1.5

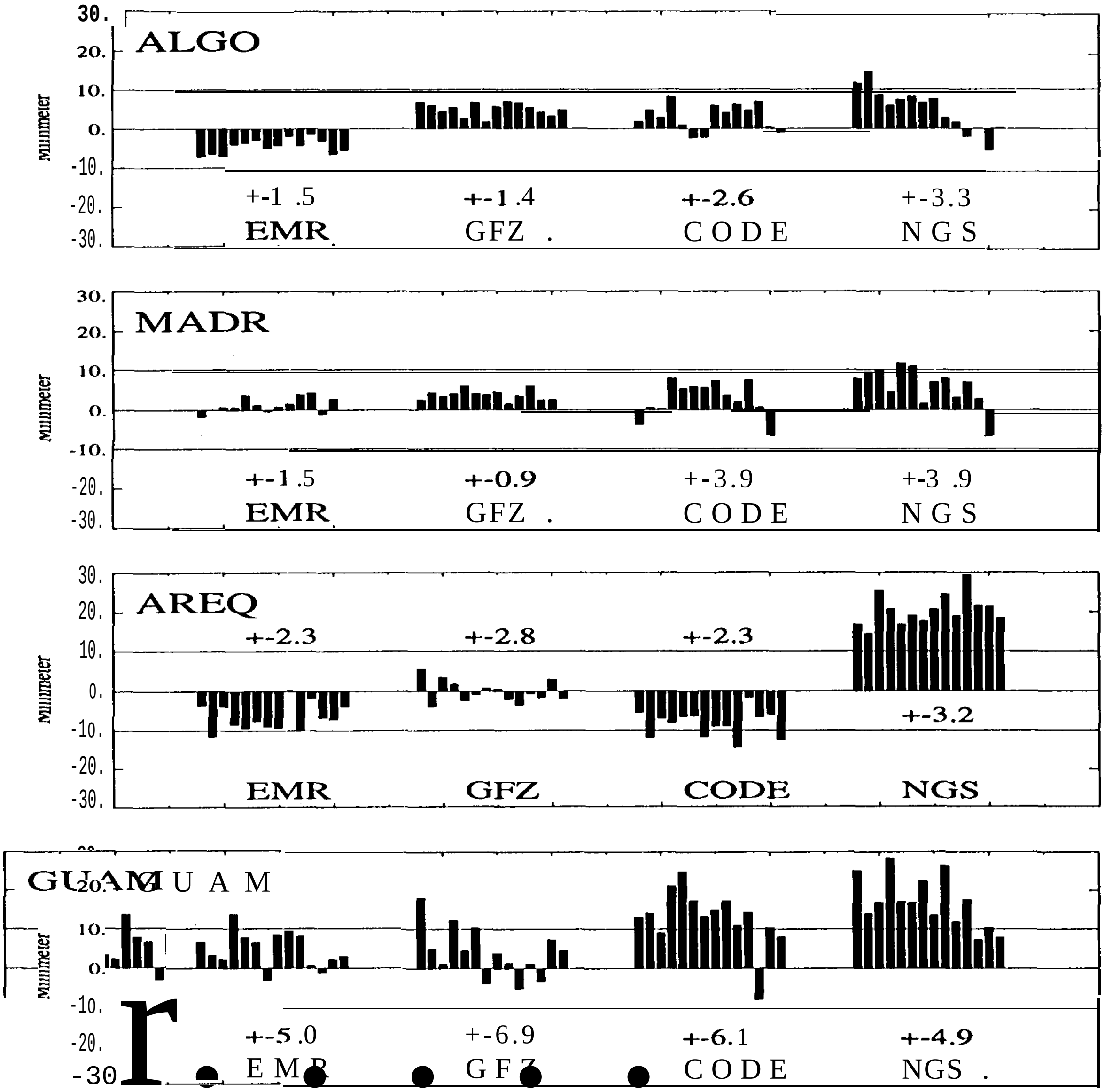

Fig. 1. ZPD biases between JPL and the other **IGS** Analysis Centers for selected stations with their repeatability in mm

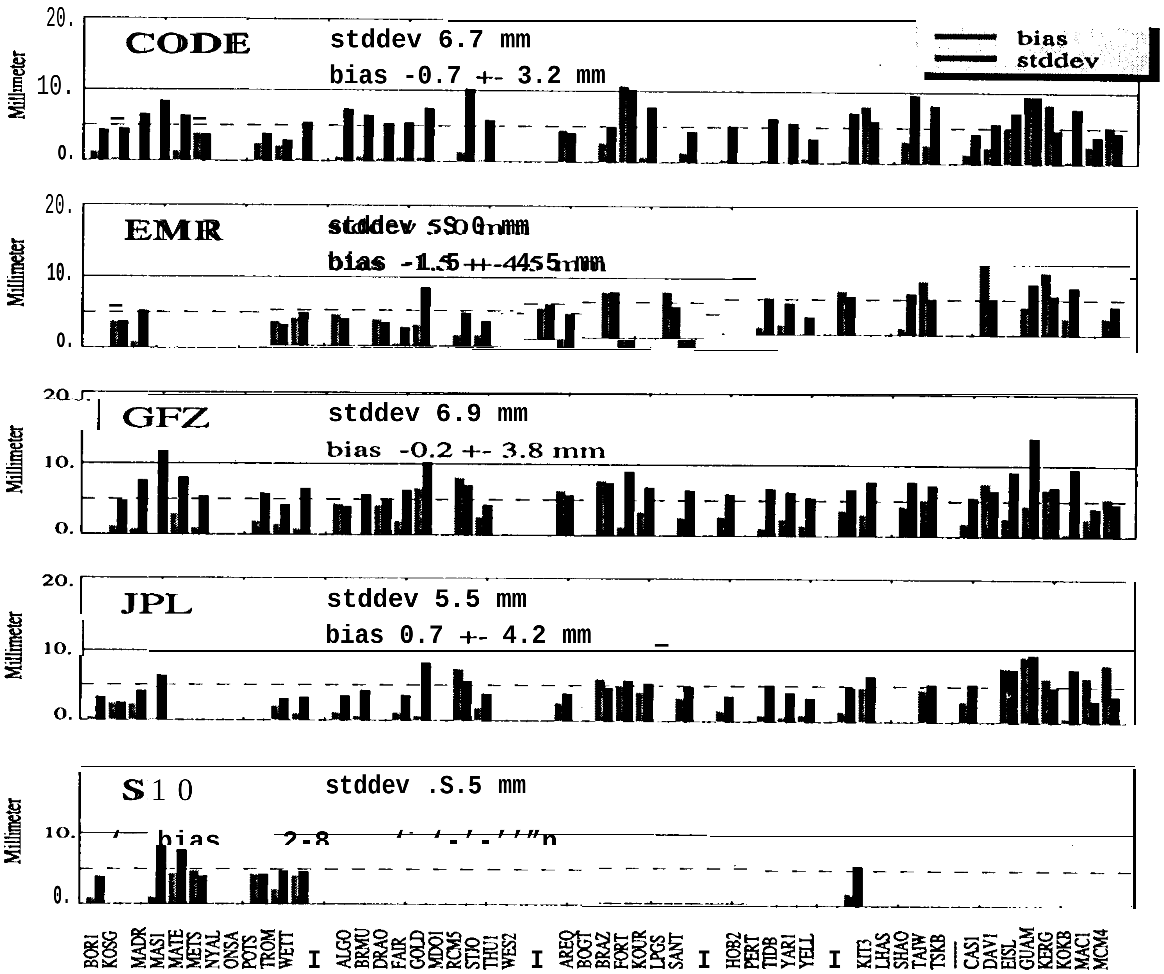

Fig. 2a. Stddev and bias of ZPD differences between the ACS and the IGS Mean, Week 812

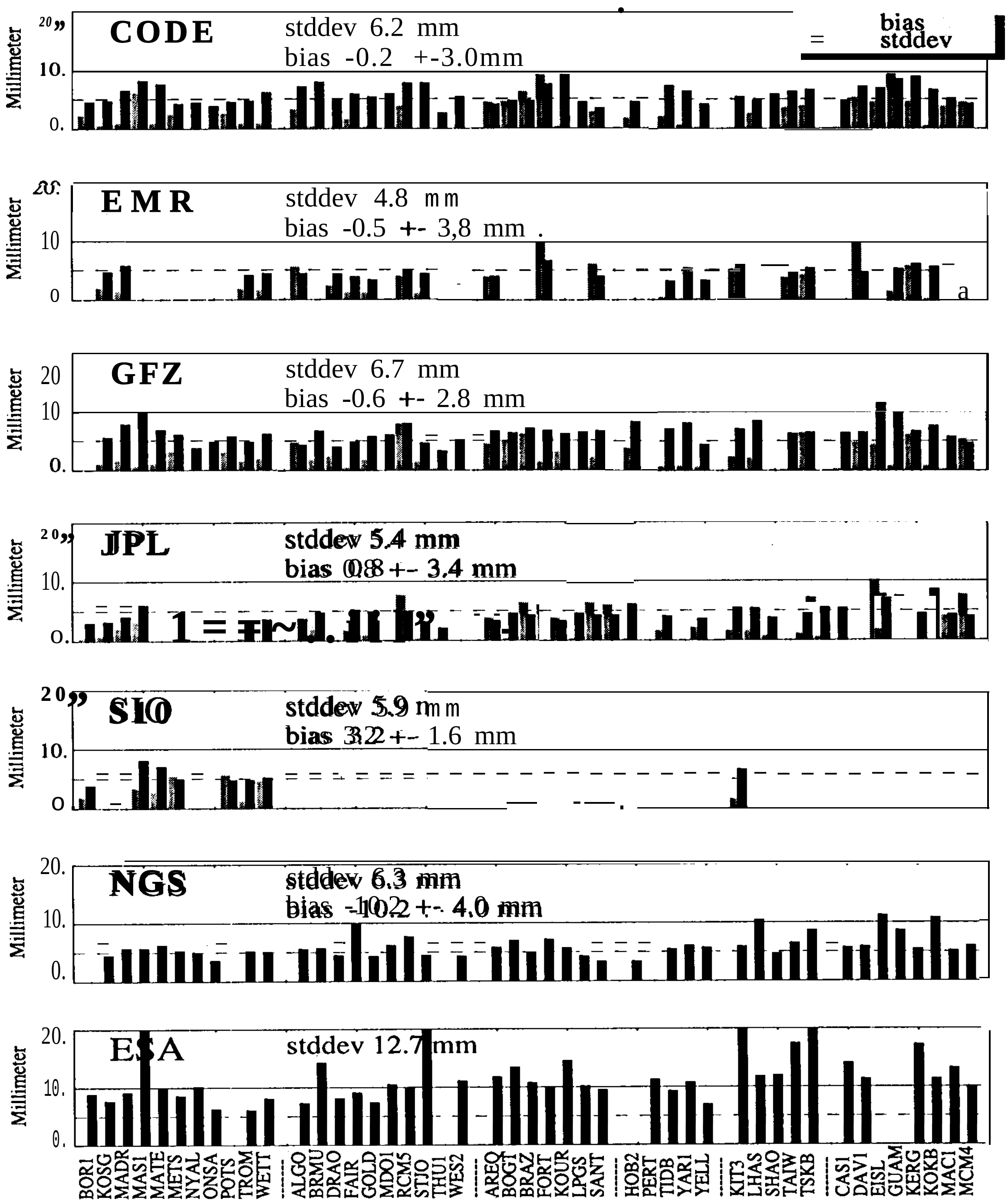

Fig. 2b. Stddev and bias of ZPD differences between the ACS and the **IGS** Mean, Week 813

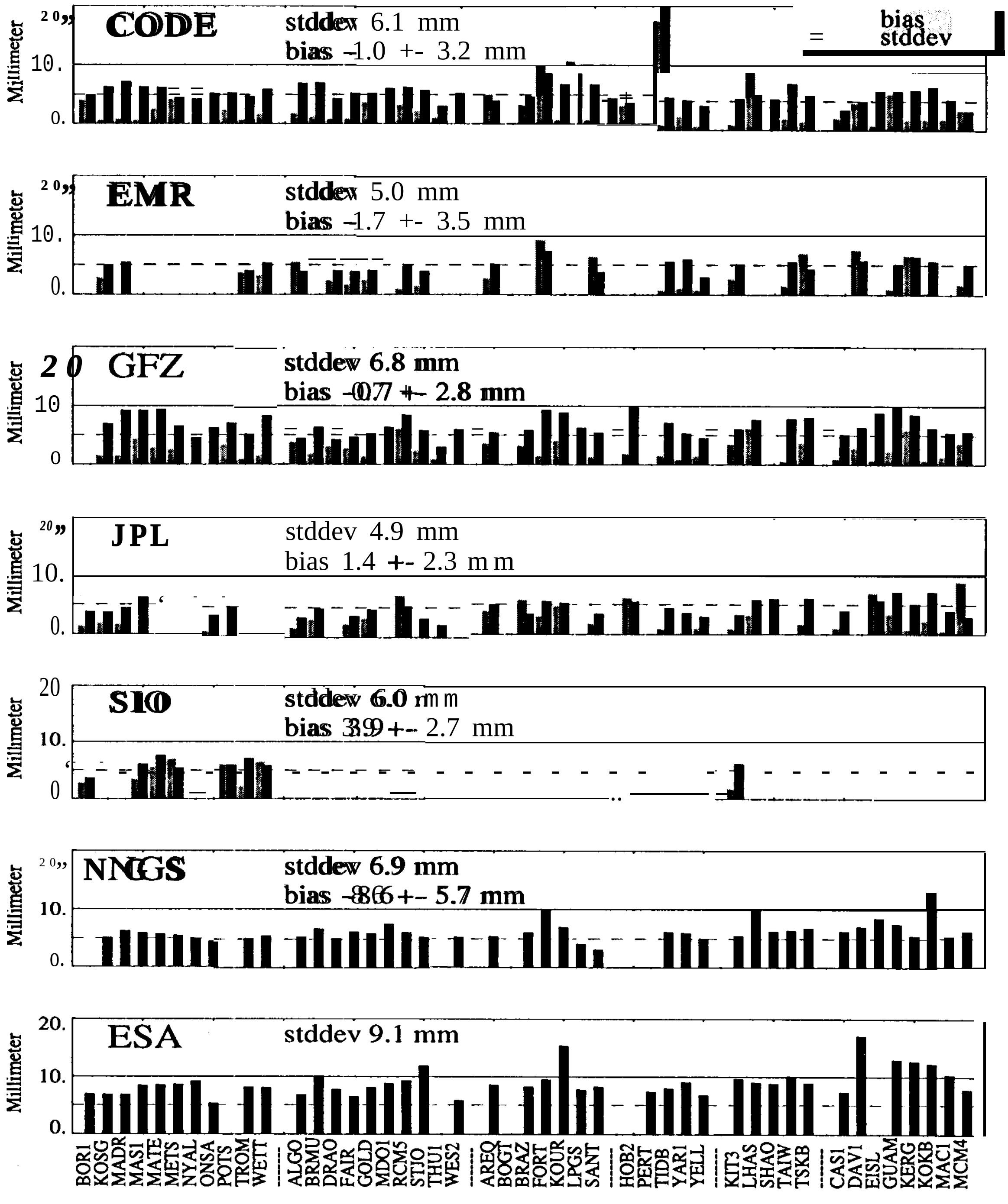

Fig. 2c. Stddev and bias of ZPD differences between the ACS and the IGS Mean, Week 814

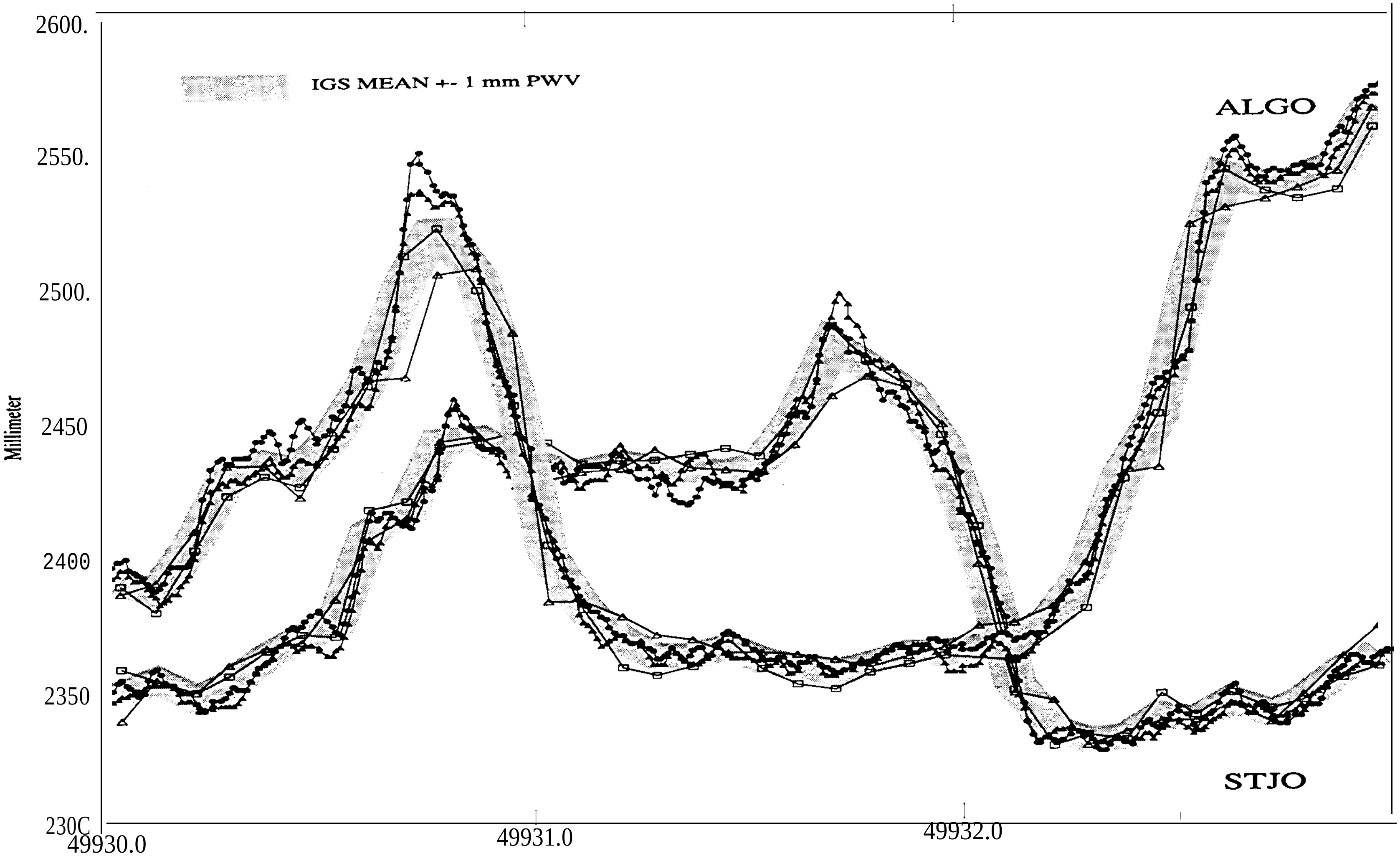

Fig. **3a.** Total zenith path delay series of all ACS for ALGO and STJO with given **IGS-Mean** for selected 3-day interval

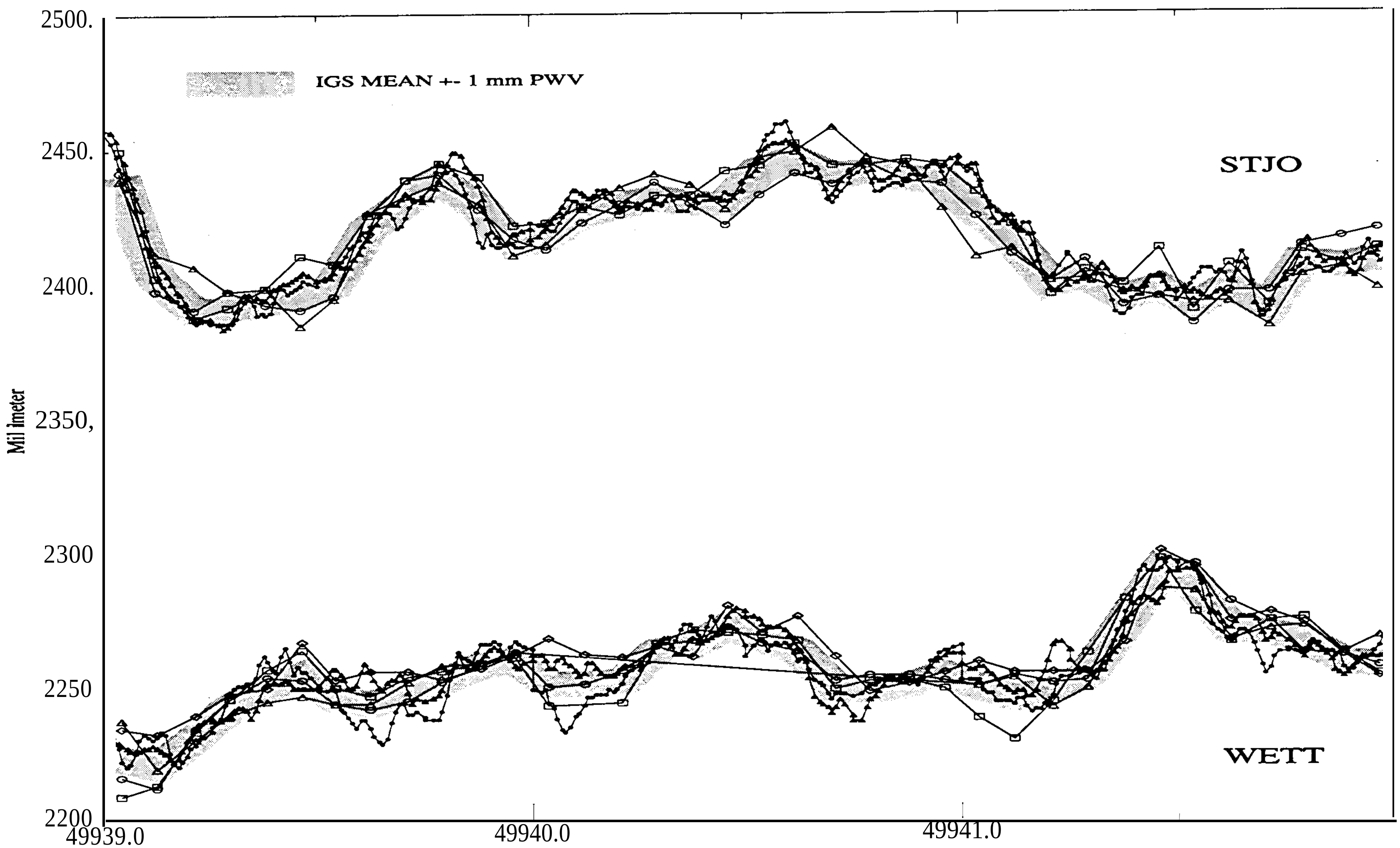

Fig. 3b. Total zenith path delay series of all ACS for STJO and WETT with given IGS-Mean for selected 3-day interval

Strategies for Near Real Time Estimation of Precipitable Water Vapor

Yoaz E. Bar-Sever
Jet Propulsion Laboratory, California Institute of Technology
Pasadena, CA 91109

INTRODUCTION

Traditionally used for high precision geodesy, the GPS system has recently emerged as an equally powerful tool in atmospheric studies, in particular, climatology and meteorology. There are several products of GPS-based systems that are of interest to climatologists and meteorologists. One of the most useful is the GPS-based estimate of the amount of Precipitable Water Vapor (PWV) in the troposphere. Water vapor is an important variable in the study of climate changes and atmospheric convection (Yuan et al., 1993), and is of crucial importance for severe weather forecasting and operational numerical weather prediction (Kuo et al., 1993).

A ground-based GPS system does not produce estimates of PWV directly. PWV is inferred from a direct estimate of the Total Zenith Delay (TZD), with the help of some ancillary information. The TZD quantifies the atmospheric delay for a GPS signal coming from the zenith direction. It is mapped to the elevation angle of a particular satellite-receiver link by means of an appropriate mapping function, assuming horizontal symmetry. The TZD can be separated into two components, Zenith Dry Delay (ZDD) and Zenith Wet Delay (ZWD). The ZDD is caused by the propagation delay and ray bending due to the dry gases in the troposphere. It can be accurately inferred by using precise measurements of atmospheric pressure at ground level, and removed from the total delay. The remaining ZWD is nearly proportional to the quantity of PWV integrated along the zenith direction. The total PWV can be extracted from the ZWD to an accuracy of a few percent given measurements of the temperature at ground level. (Bevis et al., 1994, Rocken et al., 1993, Yuan et al., 1993). In the absence of pressure or temperature measurements on site, they can be approximated by means of an appropriate climate model. Verification of accuracy of GPS-based estimates of PWV is typically done by comparison with estimates based on the more established techniques of radiosondes and Water Vapor Radiometers (WVR). Several recent comparisons demonstrated that GPS can provide millimeter-level accuracy in measuring PWV (Businger et al., 1996, Elgered et al., 1995, Rocken et al., 1995, Chiswell and Businger, 1995). The current level of accuracy of GPS-based estimates of TZD is believed to be better than 1 cm. The extracted PWV is believed to be 1-2 mm accurate.

It is well known that water vapor has significant small-scale variations in time and space (Lilly and Perkey, 1976). The high temporal and spatial resolution of GPS-based estimates of PWV makes the GPS technology unique in its ability to augment the sparse measurements from the radiosondes network. For example, the JPL routine processing of GPS data from the IGS network produces estimates of TZD every five minutes. The only other existing technology for PWV retrieval with high temporal resolution is based on Water Vapor Radiometers (WVR), but their global distribution is extremely sparse due to their high cost. This fact highlights a crucial advantage in exploiting the vast network of GPS ground receivers, namely, its very low cost.

Another unique advantage of GPS-based PWV estimates is the potential availability of data from ground receivers in Near Real Time (NRT), allowing for timely assimilation of the estimates into numerical weather prediction schemes. However, producing PWV estimates from NRT processing of GPS data poses a challenge. Usually, high accuracy estimates are available after processing data from a relatively large global network of receivers. In NRT, only data from a small number of stations is expected and their distribution is unlikely to be global, at least in the near future.

In this paper we discuss various aspects of the process by which ZWD is estimated from GPS data and describe a very simple estimation strategy for NRT applications.

EVALUATING GPS-BASED ESTIMATES OF ZWD

In order to analyze various estimation strategies for ZWD from GPS data we set up an experiment by which we compared GPS-based estimates of PWV with those obtained from a collocated water vapor radiometer. The GPS data used in this experiment was obtained from an 8 channel, dual frequency, TurboRogue GPS receiver that is in continuous operation at a site located at the Jet Propulsion Laboratory. Simultaneous surface pressure and temperature measurements were obtained from a Paroscientific Model 6016B pressure sensor with a stated accuracy of 0.01% of the nominal atmospheric pressure at the comparison site. Surface temperatures were obtained from a temperature sensor contained within the pressure sensor. The water vapor radiometer used in this comparison was a 3 channel design developed at JPL (Keihm, 1991). During the period of the intercomparison, the WVR operated continuously in a fixed scanning pattern. Measurements of the sky brightness temperature were made at a number of elevation angles to allow necessary gain corrections to be made to the WVR signal. PWV estimates used in this comparison were obtained from the WVR measurements made at zenith.

The GPS-based estimates of PWV were obtained by processing the data with the GIPSY/OASIS 11 software system using the technique of precise-point-positioning (Zumberge et al., 1995). The GPS orbits used in the precise-point-positioning technique were those produced routinely at JPL for the International GPS Service (IGS). The measurement interval is five minutes. Pseudorange measurements are carrier-smoothed and carrier phase measurements are simply decimated to the five minutes mark. The troposphere is modeled as a random walk with a sigma of approximate y 1 $cm/\sqrt{hour}$. Estimates of ZWD are produced every five minutes.

The experiment spanned the months of August and October, 1995. We will describe results from 18 days during August. WVR measurements from the rest of the month were excluded due to the existence of clouds. WVR measurements were available again for most of October but the result of the comparisons is similar.

When considering the results below, it must be remembered that there are inherent limitations to the accuracy of both WVR and GPS-based estimates of PWV. A simple analysis of major error sources (Runge, 1995) has estimated that the uncertainty in GPS-based estimates of PWV is approximately 1.1 mm for PWV values in the range of 20 mm. Similarly, due to uncertainties in instrument calibrations and retrieval algorithms, the accuracy of WVR measurements of PWV, is currently limited to 1 to 1.6 mm.

EFFECTS OF ELEVATION ANGLE CUTOFF

In this experiment we tested the effect of the GPS receiver elevation angle cutoff on the quality of the ZWD estimates. The results are summarized in Figure 1. We found that the standard cutoff of 15 degrees gave rise to a significant bias between the GPS-based estimates of ZWD and PWV and the WVR-based estimates. This bias was reduced dramatically when the elevation angle cutoff was reduced to 7 degrees. An illustration of the different estimates during the first three days in August is presented in Figure 2. Similar behavior was observed with the October data.

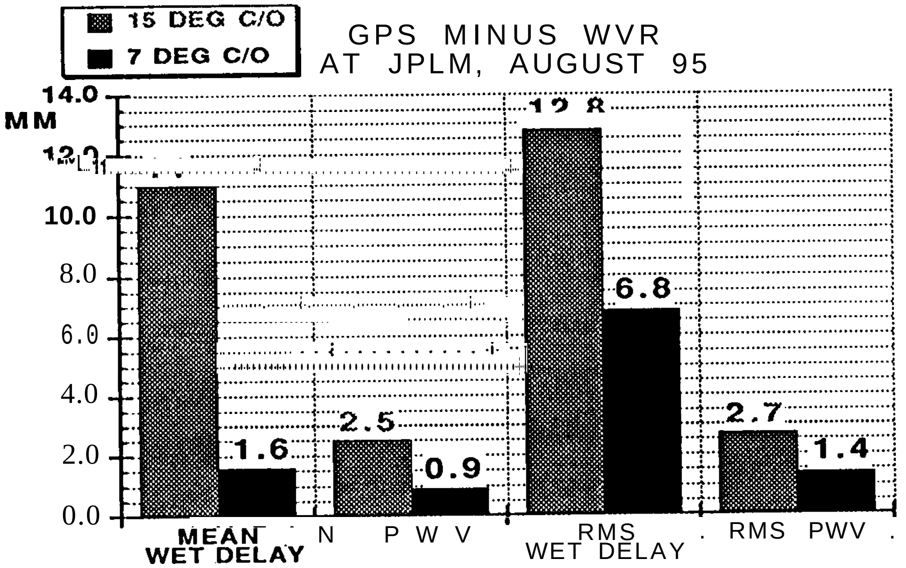

*Fig 1. **Effects** of elevation **angle** cutoff on difference between **GPS-based** estimates of ZWD and WVR estimates. Statistics were based on 18 days in August 1995.*

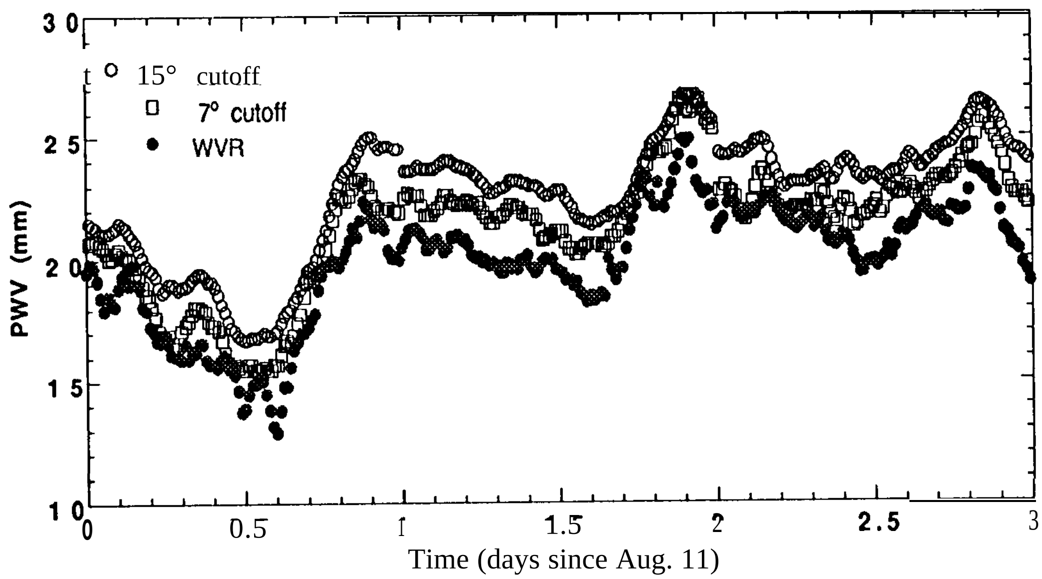

***Fig** 2. Comparing PWV estimates from WVR and from GPS with two elevation angle **cutoffs** for three days in August, 1995, at the JPLM site.*

Accompanying the bias in ZWD between GPS estimates with different elevation angle cutoffs was a bias in the estimated geodetic height of the station. This bias can be observed in Figure 3, depicting the daily geodetic height estimate over the whole month of August with the two elevation angle cutoff values. The mean bias is 2.5 cm.

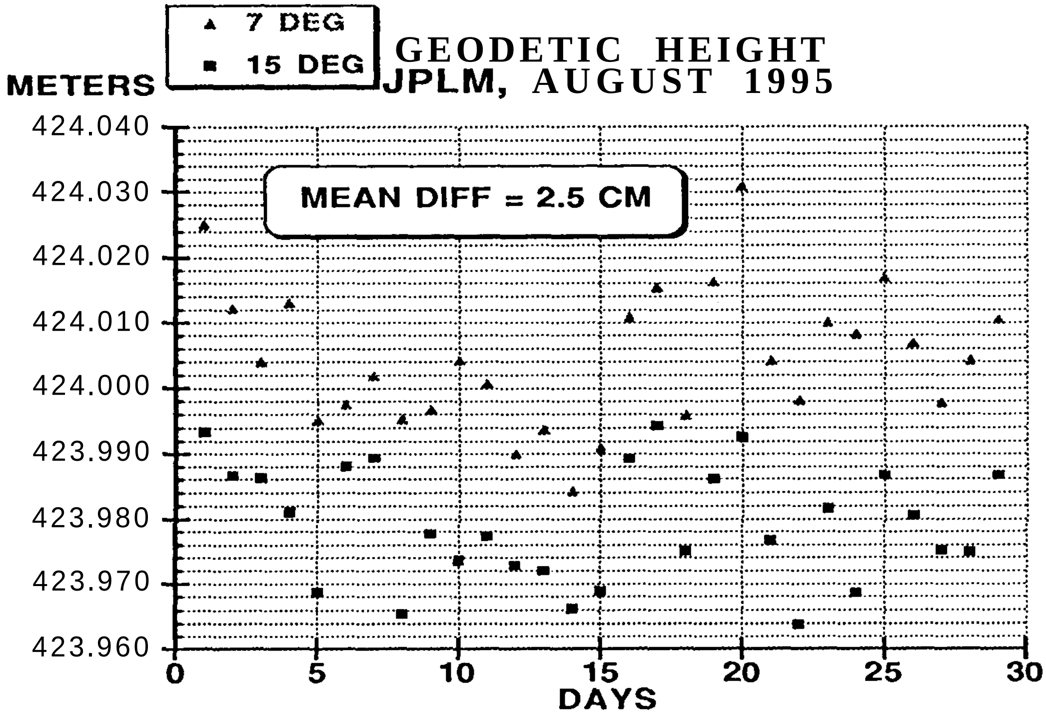

Fig. 3. *Estimated geodetic height of JPLM with two elevation angle cutoff values.*

Although WVR estimates were not available there, we compared GPS-based estimates of ZWD with the two elevation angle cutoffs for several other sites during January, 1996. We found that the size of the bias between the estimates varies from site to site and it can often be insignificant (less than 5 mm) for many. The largest bias was found at Fortaleza, Brazil (FORT) which is a relatively wet site. (See Figure 4.)

We hypothesize that the improvement in ZWD estimates at lower elevation angle cutoff, as observed at JPLM during August and October, 1995, is due to the reduction in the correlation between ZWD and station height. More experimentation is required in order to establish that this phenomenon is not site/receiver dependent.

In general, lowering the elevation angle cutoff did not have a detrimental effect on station position repeatabilities over a month. It suggests that carrier phase multipath may not be very darnaging at 7 degrees elevation.

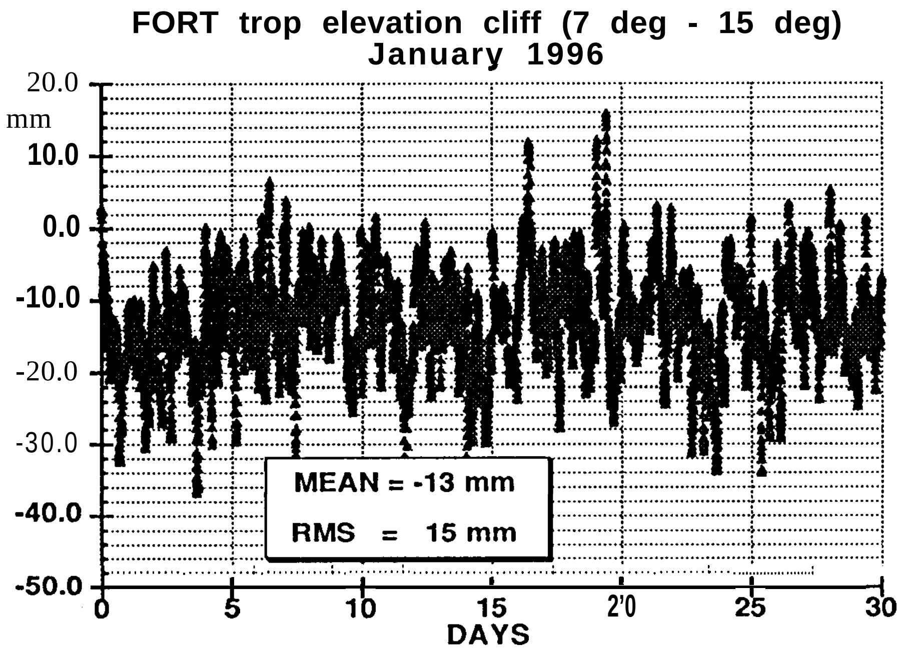

Fig. 4. Difference in ZWD estimates obtained with elevation angle cutoff values of 15 degrees and 7 degrees.

EFFECTS OF GPS YAW ATTITUDE MISMODELING

GPS satellites display a rather complicated yaw attitude behavior during crossing of the Earth shadow (Bar-Sever et al., 1996, Bar-Sever, 1996). Mismodeling this behavior is especially harmful in precise-point-positioning. In this experiment we estimated ZWD at various sites twice: Once with the new yaw attitude model (Bar-Sever, 1996) and once with the old yaw attitude model (the basic ROCK model) that is still in use in many geodetic software systems.

Assuming now that the TZD estimates obtained with the new yaw model are "truth", and subtracting these estimates from estimates obtained with the ROCK yaw model, there are many cases where the differences significantly exceed 1 cm. Figure 5 depicts examples for FORT and BRMU. TZD values for BRMU (after subtracting the mean), estimated without the yaw model, are also presented in Figure 1 in order to demonstrate that the peaks in the error figure are indeed associated with anomalous features in the estimated value. All the peaks in Figure 1 correspond to epochs of observing an eclipsing satellite during its yaw maneuver. These errors may be unacceptably large for some applications. Errors in TZD are equivalent to errors in ZWD.

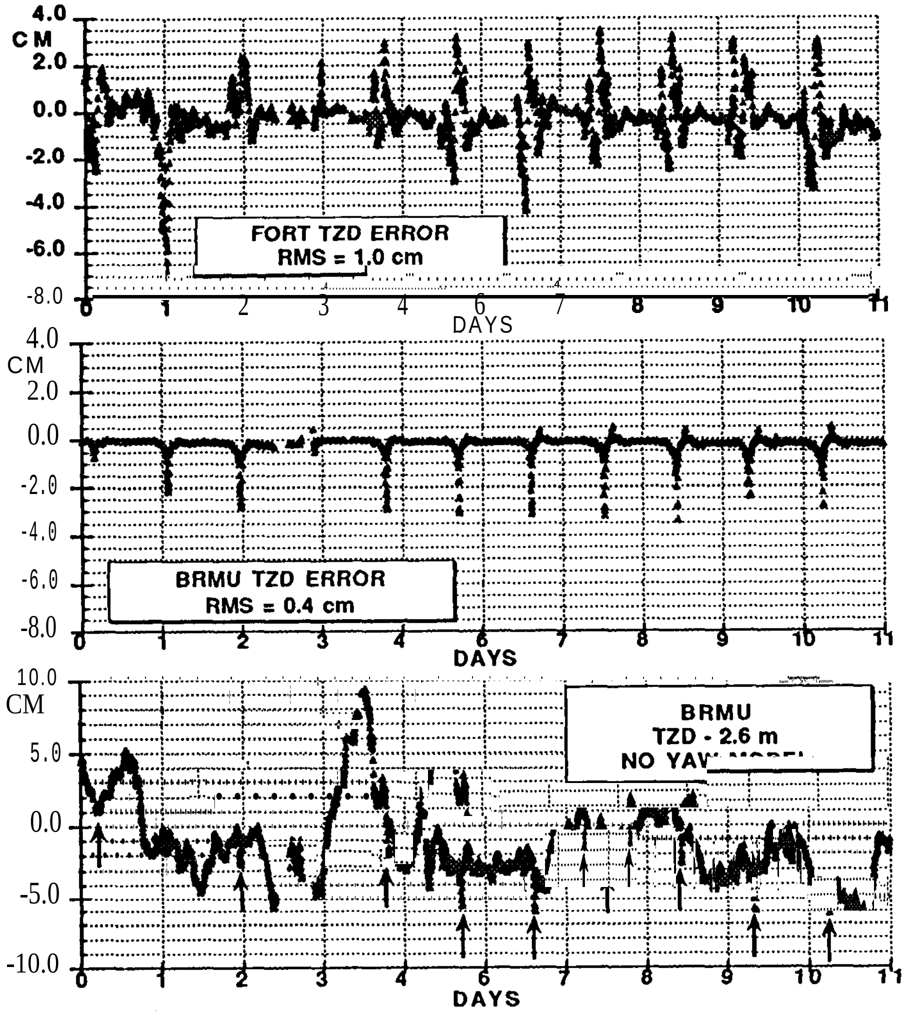

Fig. 5. Effects of omitting the GPS yaw model on estimates of total troposphere zenith delay (TZD) for FORT and BRMU. Estimates of TZD with the full yaw model (with estimated yaw rates) are considered truth. Top: TZD errors for FORT. Middle: TZD errors for BRMU. Bottom: estimated TZD for BRMU after a mean of 2.6 m was taken out and when GPS yaw model was not used. The arrows indicate the anomalous features of the estimates that correspond to the peaks in the error middle figure.

EXTRACTING A SIGNAL FROM THE POST-FIT RESIDUALS

It is a common notion that some tropospheric signal is still present in the carrier phase post-fit residuals. In order to test this notion and its utility for ZWD retrieval, post-fit residuals from receiver-transmitter links with elevation angles greater than 60 degrees were added to the estimated ZWD. If more than one link exists at an epoch, the residuals from all the links were averaged. Crude editing was used to exclude residuals larger than 8 mm. The "corrected" ZWD estimates were then compared to the WVR estimates. This experiment was carried out for the 15 degrees elevation cutoff case (that had a large bias wrt the WVR estimates) and for the 7 degrees elevation cutoff case. The results are summarized in Figure 6. Epochs for which no corrections were available were removed from the statistics.

When residual corrections were applied, the biases with respect to the WVR estimates decreased in both cases, more so for the 15 degrees elevation cutoff case. But in both cases the RMS increased. For the 15 degrees elevation cutoff case the bias decreased for each individual day out of the 18 days in August. In the 7 degrees elevation cutoff case the bias decreased on most individual days. These results support the notion that there is tropospheric signal in the carrier phase post-fit residuals but they also demonstrate that there is a considerable level of noise there. The noise level in the correction may be reduced perhaps, with a more sophisticated editing scheme, but there is no doubt that there is not enough signal in the post-fit residuals to offset the large bias in the estimates. Low elevation angle residuals, though, could be more useful in correcting line-of-sight wet delay because they are expected to contain larger tropospheric signal, in proportion to the larger air mass the signal traverses.

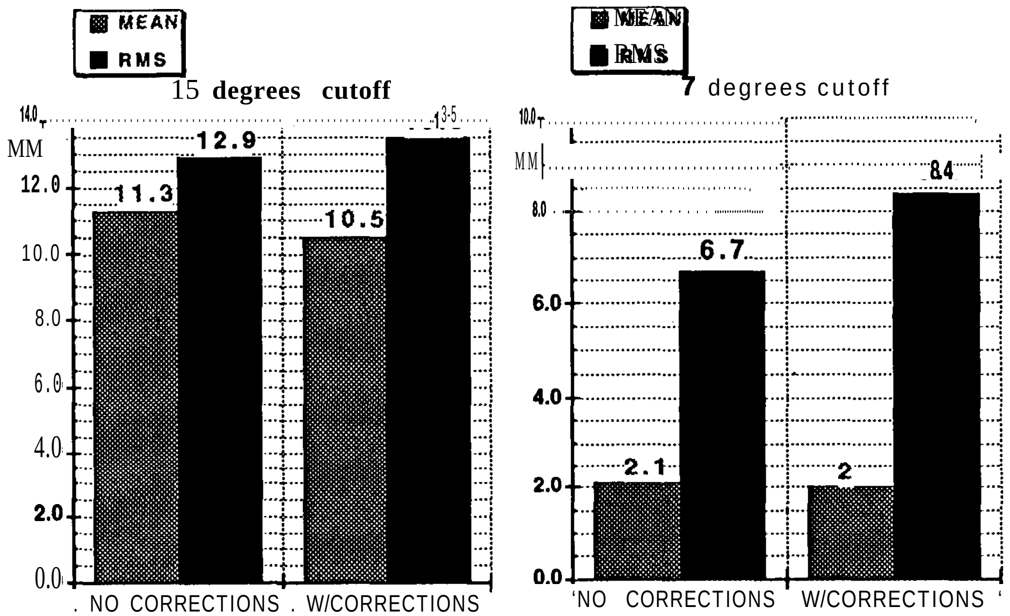

Fig 6. Effects of adding "zenith" residuals to ZWD estimates on the difference between the GPS-based estimates and the WV. estimates.

NEAR REAL TIME ESTIMATION STRATEGIES

To serve as useful input to numerical weather prediction models, the GPS-based estimates of PWV would need to be available within several hours after the data have been collected. In contrast, GPS-based PWV estimates described in the previous sections were produced using precise GPS orbits and clock obtained by processing data from a global network of -30 GPS receivers and are available 2-4 days after data has been collected. Therefore, it is currently not possible to use precise GPS orbits and clocks as the basis for a system to provide NRT PWV estimates. For this reason, we have investigated the use of "predicted" GPS orbits as an alternative. It should be clear that the results cannot be as accurate as those obtained with precise orbits and clocks. The minimal level of accuracy demanded from the NRT PWV is application-dependent and has not been established yet. In this study, rather arbitrarily, we set the accuracy goal at 2 mm RMS for PWV (approximately 12 mm RMS for ZWD).

The degradation in the quality of the predicted orbit causes, in turn, a degradation in the quality of the ZWD estimated (Figure **8).** It is desired, therefore, that the prediction period be minimized. If orbit errors are potentially too large, a third station can be brought in. The three-station differential solution has enough data strength to adjust the GPS orbit. Moderate baselines between all three stations should be maintained for best results. (Figure 9.)

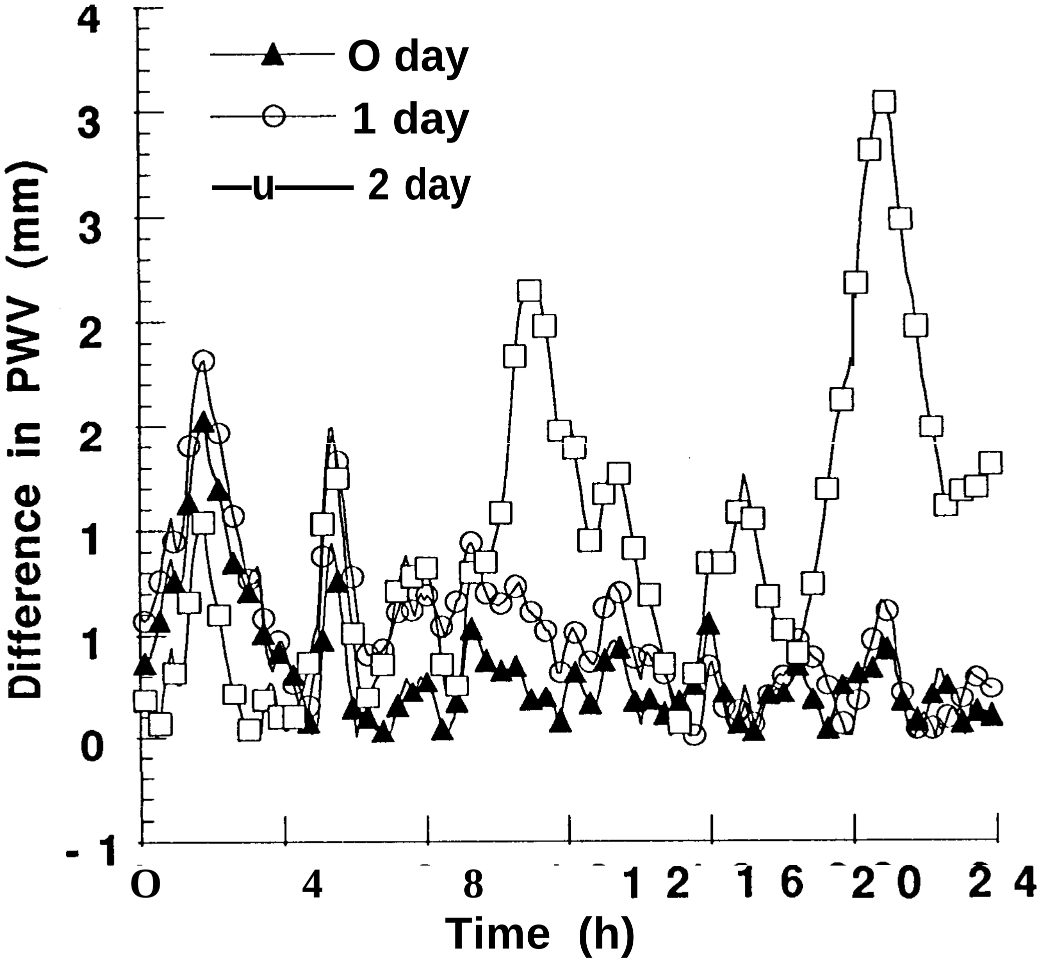

***Fig* 8.** *The effect of GPS orbit prediction period on the accuracy of the PWV estimates. The "0 day" graph corresponds to estimates obtained with precise GPS orbits and clocks and no prediction. The "1 day" graph corresponds to estimates obtained using GPS orbits predicted 24 hours, The "2 day" graph corresponds to estimates obtained using GPS orbits predicted 48 hours.*

In NRT applications data will arrive at the processing center in small batches. If the batch length is too short there will not be enough data to resolve the ZWD properly, given the temporal correlation of the troposphere delay model. In our test, a minimum of three hours was required to resolve the ZED reasonably well (Figure 10). "Processing short batches is possible with proper initialization of the covariance matrix with the covariance of the previous batch, The predicted GPS orbits used in this study were obtained by fitting an orbit to four consecutive days of precise daily solutions, adjusting for 6 epoch state parameters and eight additional empirical parameters. The solution was then extrapolated forward using the satellite's dynamics. Orbit error increased quadratically, in this scheme, up to a level of two meters RMS after two days.

Because of Selective Availability (SA) satellite clocks cannot be extrapolated. Hence the need to estimate them (or difference them out). This requires the simultaneous processing of at least two ground stations. We have found that, under certain circumstances, no more than two stations are needed. This forms the simplest scheme for NRT retrieval of ZWD.

When one clock is held as a reference it is possible to solve for the other station clock as well as the ZWD for both stations, and all observed GPS clocks, with a technique equivalent to double differencing. This technique imposes some constraints on the selection of the second station. One of the stations is considered the target of the ZWD estimate. The other is brought in to provide clock resolution. Its ZWD may, or may not, be desired. The two stations should not be too far apart. If they are, they will fail to form enough double differences. They should also not be too close. If they are, the normal equations will tend to be singular and troposphere at the two stations will be strongly correlated. We have found that separation of 200 km -1000 km usually works well (Figure *7).*

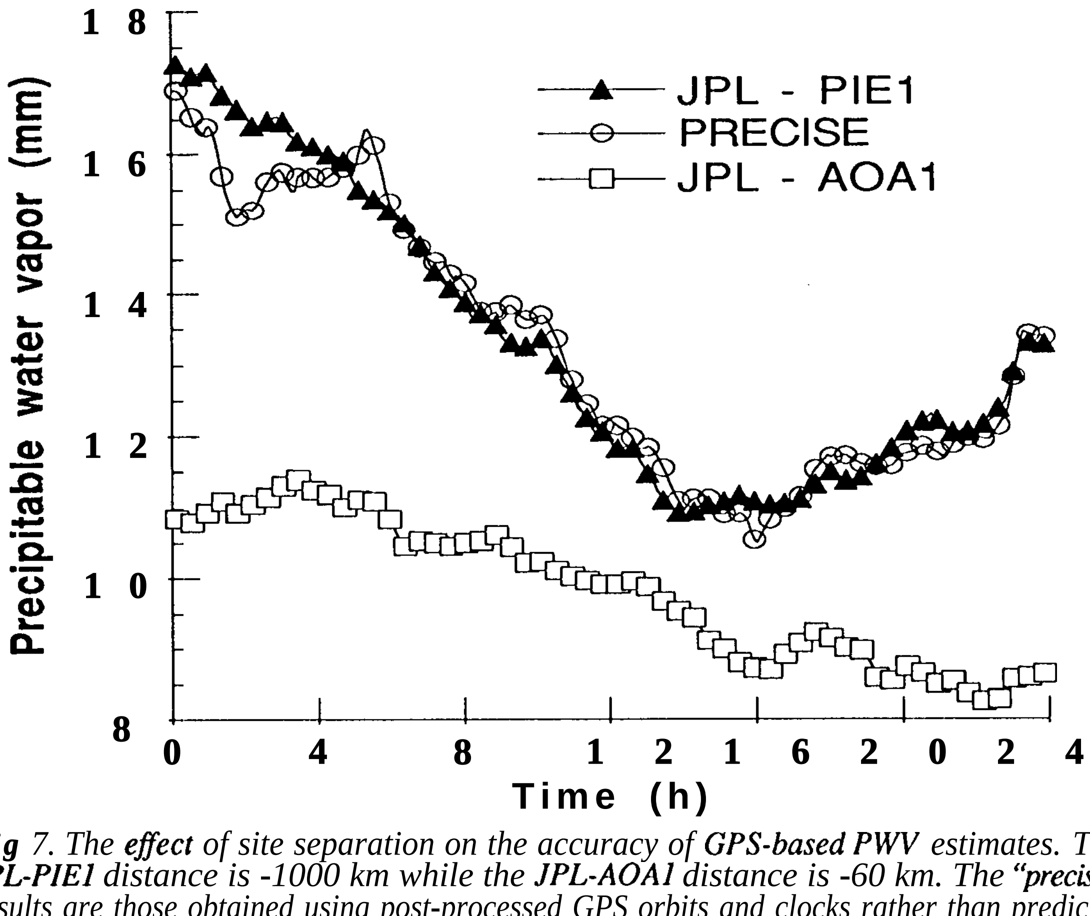

Fig 7. The effect of site separation on the accuracy of GPS-based PWV estimates. The JPL-PIE1 distance is -1000 km while the JPL-AOA1 distance is -60 km. The "precise" results are those obtained using post-processed GPS orbits and clocks rather than predicted orbits.

ACKNOWLEDGMENT

The work described in this paper was carried out in part by the Jet Propulsion Laboratory, California Institute of Technology, under contract with the National Aeronautics and Space Administration.

REFERENCES

Bar-Sever, Y.E., Anselmi, J. A., Bertiger, W.I. and Davis, E. S., Fixing the GPS Bad Attitude: Modeling GPS Satellite Yaw During Eclipse Seasons. Navigation, Spring 1996.

Bar-Sever, Y.E., A New Yaw Attitude Model for GPS Satellites. To appear in J. of Geodesy, 1996.

Bevis, M., S. Businger, T.A. Herring, C. Rocken, R.A. Anthes and R.H. Ware, 1992, GPS Meteorology: Remote Sensing of Atmospheric Water Vapor using the Global Positioning System, *J. Geophys. Res., 97, 15787-15801.*

Bevis, M., Businger, S., Chiswell, S., Herring, T. A., Anthes, R. A., Rocken, C. and Ware, R.H., GPS Meteorology: Mapping Zenith Wet Delays onto Precipitable Water, Journal of Applied Meteorology, Vol. 33, No. 3, March 1994.

Businger, S., Chiswell, S. R., Bevis, M., Duan, J., Anthes, A., Rocken, C., Ware, R. H., Exner, M., VanHove, T., Solheim, F. S., The Promise of GPS in Atmospheric Monitoring, Bull. Am. Met. Sot., Vol. 77, No. 1, January, 1996.

Chiswell, S. R., Businger, S., Improved Severe Weather Forecasts Using GPS, IUGG XXI General Assembly, Boulder, CO, July, 1995.

Davis, J.L., T.A. Herring, 1.1. Shapiro, A.E.E. Rogers, and G. Elgered, 1985, Geodesy by radio inteferometry: Effects of atmospheric modeling errors on estimates of baseline length, *Radio Science, 20, 1593-1607.*

Elgered, G., Johansson, J. M., Lindgren, B., Using the Swedish GPS Network to Monitor the Atmospheric Water Vapor Content, IUGG XXI General Assembly, Boulder, CO, July 1995.

Keihm, S. J., 1991, Water vapor radiometer intercomparison experiment, Platteville, Colorado, March 1-14, 1991, Final Report for Battelle Pacific Northwest Laboratories on behalf of the Department of Energy, Jet Propulsion Laboratory, Internal Document, Dec. No. D-8898, Pasadena, CA.

Kuo, Y. H., Guo, Y.R. and Westwater, E. R., Assimilation of Precipitable Water Vapor into a Mesoscale Numerical Model, Monthly Weather Review, Vol. 121, No. 4, April 1993.

Lilly, D. K., and Perkey, D. J., Sensitivity of Mesoscale Predictions to Mesoscale Initial Data, Sixth Conference on Weather Forecast and Analysis of the Amer. Meteor. Sot., Albany, NY, 1976.

MacMillan, D. S., Atmospheric gradients from Very Long Baseline Interferometry Observations, Geophys. Res. Lett., Vol. 22, No. 9, May 1995, pp 1041-1044.

The degradation in the quality of the predicted orbit causes, in turn, a degradation in the quality of the ZWD estimated (Figure **8).** It is desired, therefore, that the prediction period be minimized. If orbit errors are potentially too large, a third station can be brought in. The three-station differential solution has enough data strength to adjust the GPS orbit. Moderate baselines between all three stations should be maintained for best results. (Figure 9.)

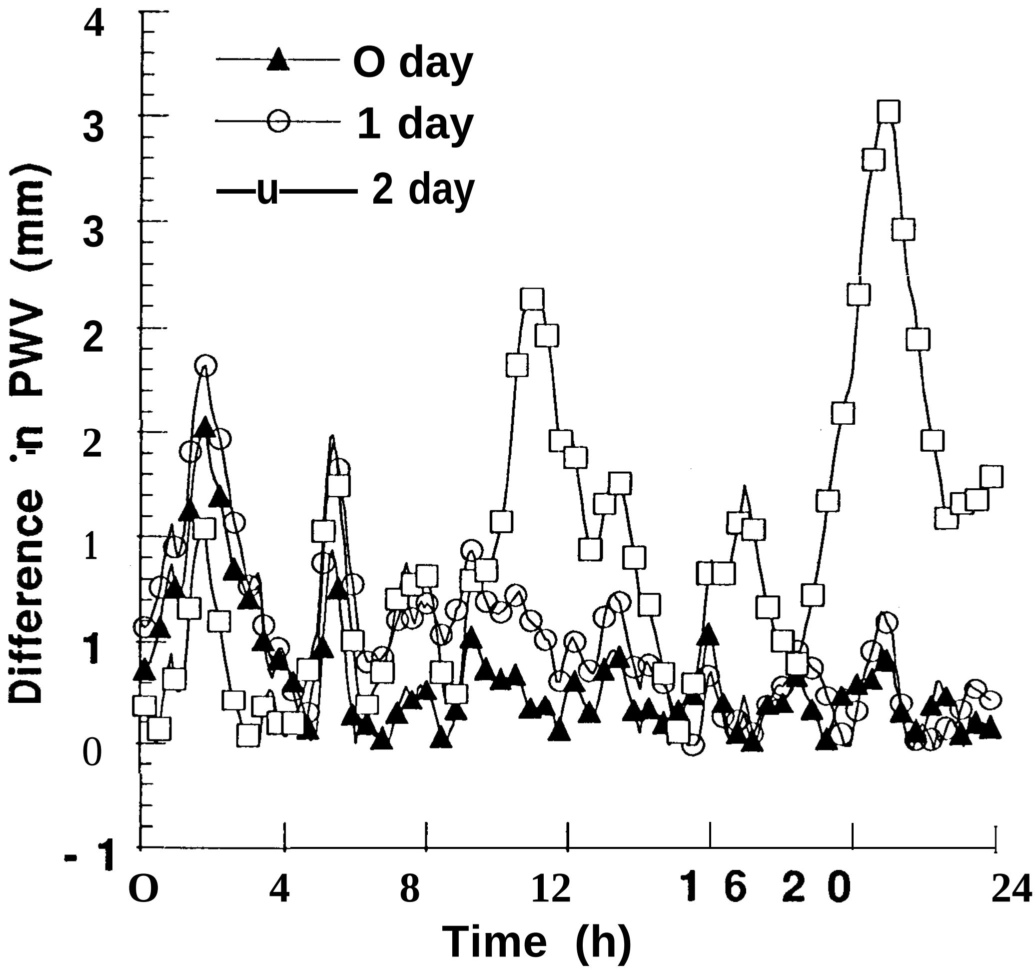

Fig 8. *The effect of GPS orbit prediction period on the accuracy of the* ***PWV*** *estimates. The "0 day" graph corresponds to estimates obtained with precise GPS orbits and clocks and no prediction. The "1 day" graph corresponds to estimates obtained using GPS orbits predicted 24 hours. The "2 day" graph corresponds to estimates obtained using GPS orbits predicted 48 hours.*

In NRT applications data will arrive at the processing center in small batches. If the batch length is too short there will not be enough data to resolve the ZWD properly, given the temporal correlation of the troposphere delay model. In our test, a minimum of three hours was required to resolve the ZED reasonably well (Figure 10). Processing short batches is possible with proper initialization of the covariance matrix with the covariance of the previous batch.

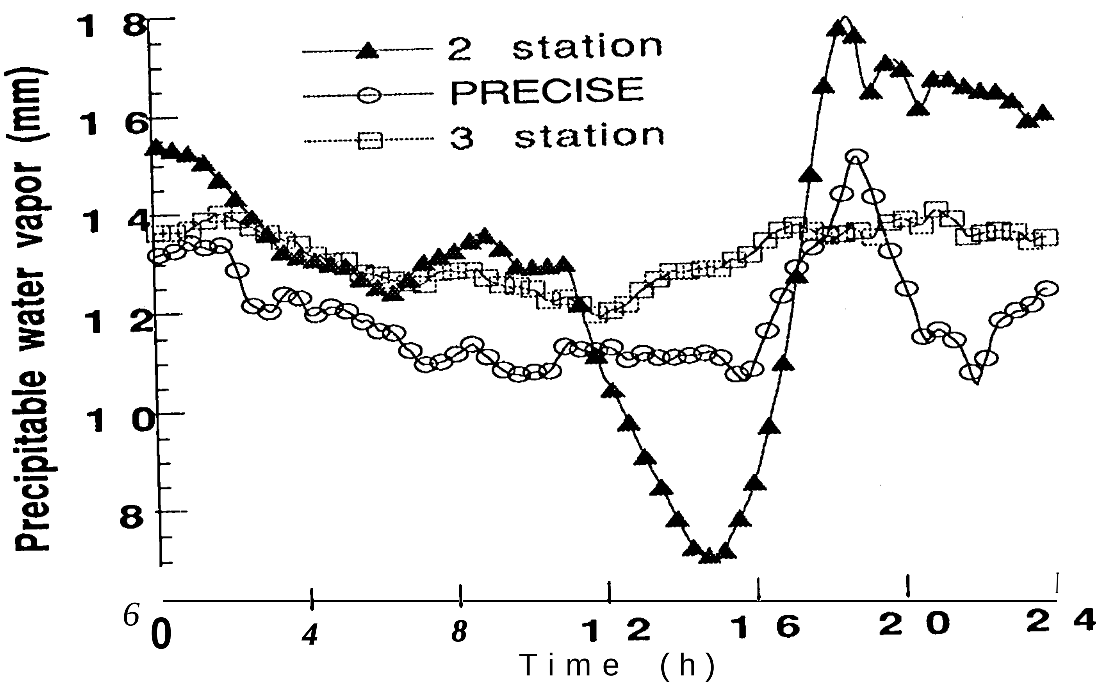

Fig **9.** *The effect of adding data from a third GPS receiver and adjusting the GPS orbits when estimating PWV values. The two station case used JPL and* ***Pietown,*** *and the three station case added data from LEXI.*

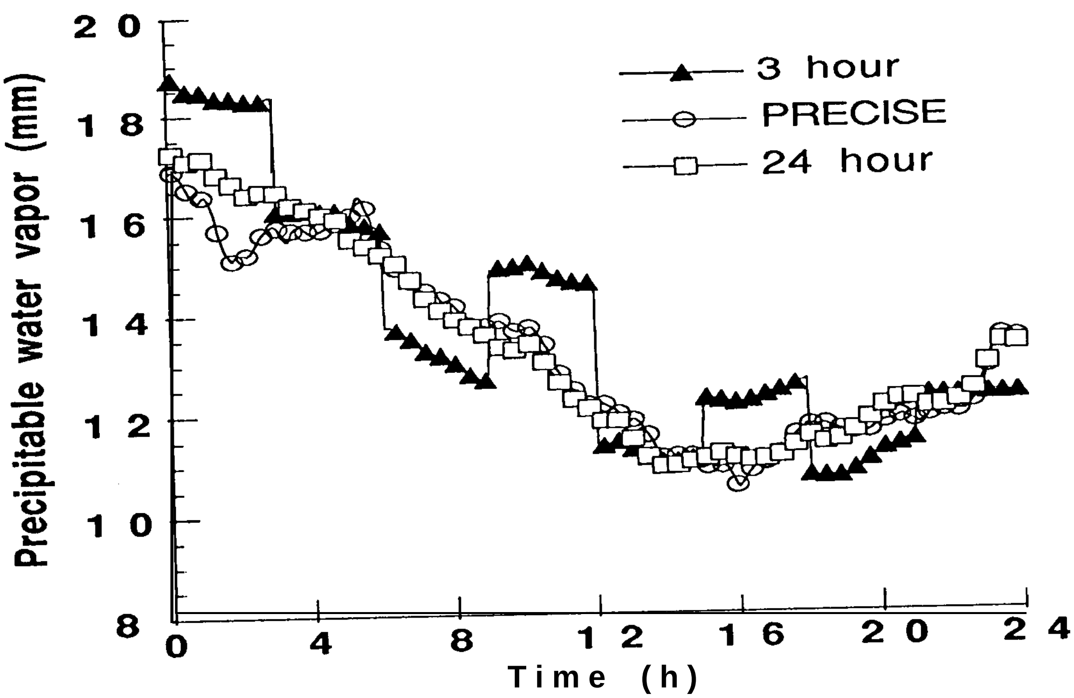

Fig ***10.*** *The effect of decreasing the span of the data on the accuracy of GPS-based estimates of* ***PWV.*** *These results were obtained from data recorded at the JPL and* ***Pietown*** *sites.*

Rocken, C., Ware, R., VanHove, T., Solheim, F., Alber, C., Johnson, J., Bevis, M. And Businger, S., Sensing Atmospheric Water Vapor With the Global Positioning System, Geophys. Res. Lett., Vol. 20, No. 23, 1993, pp 2631-2634.

Runge, T.F., P.M. Kroger, Y.E. Bar-Sever and M. Bevis, 1995, Accuracy Evaluation of Ground-based GPS Estimates of Precipitable Water Vapor, *EOS Transactions,* American Geophysical Union, 1995 Fall Meeting, Vol. 76, F146.

Yuan, L., Anthes, R. A., Ware, R.H., Rocken, C., Bonner, W., Bevis, M. and Businger, S., Sensing Climate Change Using the Global Positioning System, J. Geophys. Res. Vol. 98, No. 14, pp 14925-14937, 1993.

Zumberge, J.F., Heflin, M. B., Jefferson, D. C., Watkins, M.M. and Webb, F.H., IGS Analysis Center 1994 Annual Report, JPL Publication 95-18, Jet Propulsion Laboratory, Pasadena, CA, September 1, 1995.

Ionosphere Maps - A New Product of IGS ?
- Summary -

J. Feltens

EDS at Orbit Attitude Division, ESA, European Space Operations Centre,
Robert-Bosch-Str. 5, D-64293 Darmstadt, Germany

The IGS workshop in Silver Spring was the first IGS workshop where a sub-session was dedicated to the ionosphere. The sub-session's aim was to find out how ionosphere products could enter into the IGS service palette. In preparation for this IGS workshop an intercomparison of ionosphere products computed at the different Analysis Centers was organized to provide material for the discussion.

A position paper was prepared by J. Feltens, and it was agreed between the different Analysis Centers to concentrate in each of their presentations on a special aspect that is relevant to the development of a common IGS product. Accordingly, the topics of the distinct presentations were widely spread:

- The presentation of CODE concerned the long-term analysis of routinely produced ionosphere maps and experiences made.
- The presentation of UNB provided an analysis of the effect of shell height on high precision ionosphere modeling.
- The presentation of JPL dealt with global ionosphere mapping using GPS.
- A second presentation of JPL pointed out the relevance of GPS/MET data for ionosphere modeling, namely for ionospheric profiling.
- The presentation of DLR showed comparison results of GPS-derived TEC maps with independent ionospheric probing techniques.
- The final presentation, that of ESOC, condensed the first results that came out of the intercomparison and pointed out related aspects of software developments at ESOC.

During the discussion that followed the presentations, four points crystallized out as the most important for next steps to progress. These points are listed in the following sections:

1 Completion of the 5 weeks intercomparison

The intercomparison is not yet complete in two aspects:

1) Until now only a general comparison was made to verify overall agreement between the ionosphere products that were computed at the different Analysis Centers. However, a detailed look has still to be made to find out reasons for systematic trends in disagreement and for high levels of disagreement and abnormal behaviour that appeared sometimes. Explanations must be found for those phenomena. Based on the knowledge earned from this closer analysis, repetitions of processing under changed conditions may become necessary, at least for representative parts of the 5 considered weeks.

2) Some Analysis Centers did not deliver their results for all 5 weeks yet; they should complete their products.

Finally it was agreed that the intercomparison should be completed within the next few months.

2 Agreement on common standards

The intercomparison showed, that a lot of different assumptions are made in the ionosphere processing at the different Analysis Centers. To achieve a unique IGS product, general standards must be agreed upon among the different Analysis Centers. Relevant topics that were identified in this direction are:

- An official ionosphere product format (IONEX) must be defined.
- A common reference frame (probably solar-magnetic) should be agreed upon.
- A reliable thin-shell elevation angle mapping function should be investigated for, since this could be a significant source of error (e.g. for the discrepancies detected in the satellite/receiver differential delay values between the Analysis Centers - as first intercomparison results show).
- A common ionospheric shell height should be agreed upon which would possibly take into account the temporal and spatial variation of the ionospheric shell height.
- A common elevation cutoff angle might be agreed upon.
- It must be found out in which form ionosphere products shall be provided to the IGS user community, e.g. VTEC values in the form of maps or in the form of model coefficients (VTEC maps in a geographic grid were favoured - model coefficients would necessitate providing also the reference frame). Does it make sense to distibute also differential delay values to IGS users (the majority opinion was not to distribute them)?
- Of the many mathematical models that are currently used only a few should be favoured for presenting global, regional and local VTEC.
- Grid distances must be agreed upon. Grid sizes must be selected so that no interpolation will be necessary to compare different VTEC maps (e.g. 3 degree grid size for global models and 1 degree grid size for regional and local models).
- Time delays in providing products and update times must be agreed upon (near-real time processing will be an important aspect).
- Some accuracy measures must be defined to give information about the VTEC map reliability. It is very essential that the GPS-derived VTEC maps are also verified regularly with respect to independent ionosphere probing techniques over a wide spread geographical area.
- Criteria, e.g. on weighting, must be defined on how to combine the VTEC maps of the different Analysis Centers to produce one official IGS VTEC map that will be provided to the IGS users.

The most efficient way to come to common standards is to delegate certain topics of the above list to dedicated working groups which will work out a proposal for the topic entrusted to them. Each proposal will be presented to the other groups for agreement. E.g. representatives of two Analysis Centers will have the task to work out a concept of the IONEX format, while members of other Analysis Centers will establish a proposal for a common reference frame. Then the proposals will be exchanged to achieve overall agreement. Once agreement is obtained, corresponding software should be exchanged between the Analysis Centers. This method will have two benefits: 1) Not everybody must take care of everything - which saves working time. 2) By the exchange of software it is ensured that everybody uses the same standards, e.g. for the coordinate transformation to transform into and out of the solar-magnetic reference frame, or to produce identical l y formatted IONEX files.

3 Continuation of e-mail discussion of results & coordination of future work

Considering the above two Sections 1 & 2, the e-mail discussion should be continued in two corresponding directions:

1) The analysis and interpretation of the intercomparison results shall encircle weak points in current ionosphere modeling and remove them.

2) Regarding the aspects stated under the above Section 2, and considering the experience that comes out of the intercomparison, common standards and requirements for each product must be defined.

Responsibilities for the Analysis Centers should be defined, depending on their experiences and interests. A timetable should be worked out for the different tasks to perform.

4 Preparation of a pilot phase in which ionosphere products are processed under pre-operational conditions

When tasks stated in the above Sections 2 & 3 are completed, a pilot phase shall be prepared in which ionosphere products are computed at the different Analysis Centers and combined into a common IGS product under quasi-operational conditions. This will also necessitate the establishment of related software. Once this works, the next step after this pilot phase will then be the routine processing and the official distribution of ionosphere products, i.e. making the ionosphere information really a new IGS product.

Additional remark

Additional input for the discussion in form of an e-mail message was provided by DLR, since no one from that Analysis Center could attend the IGS workshop. And there is one important remark in this message that was not covered in the above four sections:

- The designation "ionosphere models" in relation to the GPS-derived VTEC maps may create confusion, since they are not "models" like IRI or Bent, etc. "TEC mapping" or "ionospheric TEC information" are better expressions.

DAILY GLOBAL IONOSPHERE MAPS BASED ON GPS CARRIER PHASE DATA ROUTINELY PRODUCED BY THE CODE ANALYSIS CENTER

Stefan Schaer, Gerhard Beutler, Markus Rothacher, Timon A. Springer
Astronomical Institute, University of Berne
CH-3012 Bern, Switzerland

ABSTRACT

The Center for Orbit Determination in Europe (CODE) -- one of the Analysis Centers of the International GPS Service for Geodynamics (IGS) - produces orbits, Earth orientation parameters, station coordinates, and other parameters of geophysical interest on a daily basis using the *ionosphere-free* linear combination of the doubly difference GPS carrier phase observations.

Since January 1, 1996, daily global ionosphere maps are routinely estimated as an *additional* product by analyzing the so-called *geometry-free* linear combination, which contains the information on the ionospheric refraction. The Total Electron Content (TEC) is developed into a series of spherical harmonics adopting a single-layer model in a sun-fixed reference frame. For each day a set of TEC coefficients is determined which approximates the average distribution of the vertical TEC on a global scale.

After re-processing all IGS data of the year 1995, a long-time series of TEC parameters is at our disposal indicating that reasonable *absolute* TEC determination is possible even when applying an *interferometric* processing technique. The global ionosphere maps produced are already used in the CODE processing scheme to improve the resolution of the initial carrier phase ambiguities. Spaceborne applications (e. g. altimetry) may benefit from these rapidly available TEC maps. For ionosphere physicists these maps are an alternative source of information about the *deterministic* and *stochastic* behaviour of the ionosphere, that may be correlated with solar and geomagnetic indices and compared to theoretical models.

CODE TEC MAPPING TECHNIQUE

Let us briefly review the TEC modeling features as developed by (Wild, 1994) and those currently used by the CODE Analysis Center for the global (and regional) applications. GPS-derived ionosphere maps are based on the so-called *single-layer* or *thin-shell* model with a simple mapping function. It is assumed that all free electrons are concentrated in a shell of infinitesimal thickness. The height of this idealized layer is usually set to the height of the maximum electron density expected. Furthermore the electron density E --

the surface density of the layer is assumed to be a function of geocentric latitude β and sull-fixed longitude s.

The *local* ionosphere models presented by (Wild, 1994) were described with a two-dimensional Taylor series expansion. Such local TEC models have proved their usefulness on many occasions. Nevertheless, this TEC representation is *not* well-suited for *global* models because of limitations in the (β, s)-space. Therefore we decided to develop the global TEC into spherical functions. We write the surface density $E(\beta, s)$ representing the TEC distribution on a global scale as

$$E(\beta, s) = \sum_{n=0}^{n_{\max}} \sum_{m=0}^{n} \tilde{P}_{nm}(\sin\beta) \cdot (a_{nm} \cos ms + b_{nm} \sin ms) \qquad \text{with } t \in [t_i, t_{i+1}] \tag{1}$$

where

$n_{\max}$ is the maximum degree of the spherical harmonic expansion,

β is the geocentric latitude of the intersection point of the line receiver- satellite with the ionospheric layer,

$s = t + \lambda - \pi$ is the *mean* sun-fixed longitude of the ionospheric pierce point, which corresponds to the local mean solar time neglecting an additive constant π (or 12 hours),

t is the Universal Time UT (in radians),

λ is the geographic longitude of the ionospheric pierce point,

$[t_i, t_{i+1}]$ is the specified period of validity (of model number i),

$\tilde{P}_{nm} = A(n, m) \cdot P_{nm}$ are the *normalized* associated Legendre functions of degree n and order m based on the normalization function $A(n, m)$ and the unnormalized Legendre functions P_{nm}, and

a_{nm}, b_{nm} are the unknown TEC coefficients of the spherical functions, i. e. the global ionosphere model parameters to be estimated.

Another essential modification of our TEC measurement technique has to be emphasized. The CODE Analysis Center of the IGS produces precise orbits and Earth orientation parameters on a daily basis by analyzing the *ionosphere-free* linear combination of doubly difference phase observations. As a result oft his, *cycle-slip-free* portions of L1 and L2 phase observations are readily available for every day. Consequently the zero-difference observable was replaced by the double-difference phase observable due to operational considerations. We are fully aware of the fact that by using *double-* instead of zero-differences we loose parts of the ionospheric signal, but we have the advantage of *clean* observations. Moreover, we are *not* affected by the degradation of the code measurements under the regime of Anti-Spoofing (AS). This advantage may be "lost" when the next generation of precise code receivers will become available. To get more information about the "new" TEC mapping technique we refer to (Schaer et al., 1995).

IMPLEMENTATION INTO THE CODE PROCESSING SCHEME

The computation of Global Ionosphere Model (GIM) parameters has been completely integrated into the Bernese GPS Software (Rothacher et al., 1996a). The scripts to automate the GIM production were prepared at the end of 1995.

Since January 1, 1996, the GIM estimation procedure is running in an operational mode. Several GIM products are derived every day (Rothacher et al., 1996b):

(i) Atnbiguity-free one-day GIMs arc estimated right prior to the ambiguity resolution step. These GIMs arc subsequently used to improve the resolution of the initial carrier phase ambiguities on baselines up to 2000 kilometers.

(ii) Improved GIMs (ambiguity-f fixed, with single-layer heights estimated) arc derived after ambiguity resolution.

At present, the GIM files containing the TEC coefficients for onc day arc available with a delay of 4 days.

The main characteristics of the daily GIMs produced by the CODE Analysis Center may be summarized as follows: The gcon?etrg-free linear combination of double-cliffcrcncc carrier phase observations is processed performing a least-squares adjust ment of the observations of the complete IGS network to extract the global TEC information. Onc observation epoch pcr 3 minutes is processed using an elevation cut-off angle of at present 20 degrees. Note that ---- even under AS *no* restrictions concerning receiver types or satellites have to be made in our approach. The global TEC dist ribution is represented over 24 hours by spherical harmonics up to degree 8 in a geographical reference frame which is rotating with the *mean* Sun. We adopt a spherical ionospheric shell in a height of 400 kilometers above the Earth's mean surface.

Let us mention that we estimate furthermore *regional* ionosphere maps for Europe based on about 30 European IGS stations in a fully automatic mode since December 1995. These ionosphere maps arc used in the processing scheme of the European cluster to support the Quasi-Ionosphere-Free (QIF) ambiguity resolution strategy, too. A description of the QIF strategy is given in (Mervart and Schaer, 1994) and (Mervart, 1995). The European TEC maps are *not* discussed in this article.

Re-Processing of the Year 1995

Supported by the Bernese Processing Engine (BPE), six parallel CPUs, and a powerful data archive systcm, the re-processing of the entire IGS data set of the year 1995 GIM products only - could be performed without major problems within eight days.

LONG-TIME SERIES OF DAILY GLOBAL IONOSPHERE MAPS

At present (March 1996), the CODE Analysis Center is processing the data of about 75 globally distributed stations of the world-wide G I'S tracking network of the IGS. Figure 1 shows the stations used by CODE.

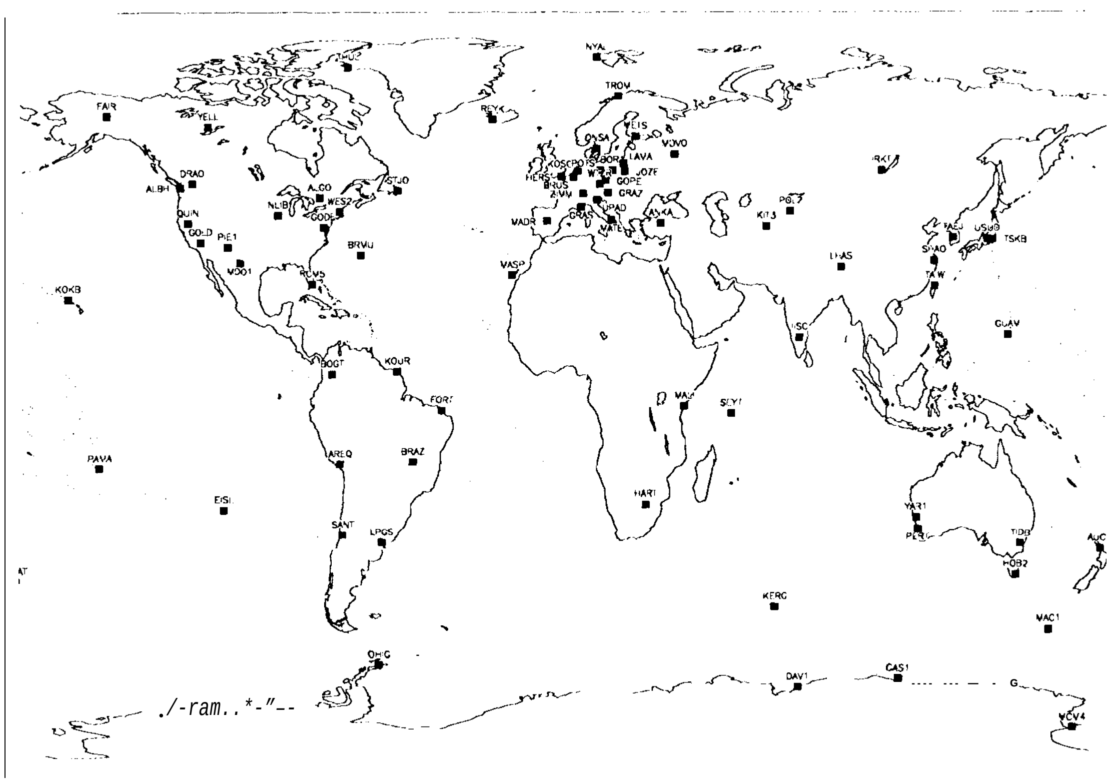

Figure 1. IGS stations used by CODE in 1996.

After re-processing all IGS data of the year 1995 and gathering already generated 1996 GIMs, we may interpret a long-time series of daily global ionosphere maps covering a time span of 427 days, from day 001, 1995 to day 002, 1996 (GPS weeks 782 to 842). This GIM series is represented by thousands of parameters, hence we have to limit the following discussion to few *special* TEC parameters, only.

Important TEC Parameters Describing the Deterministic Part

We already showed in (Schaer et al., 1995) that the zero-degree TEC coefficient a_{00} may be interpreted as the *mean* TEC E_0 per square meter which can be easily converted to the *total* number of ionospheric electrons in the shell. For that reason the quantity E_0 is an excellent parameter to roughly describe the deterministic part of the ionosphere. Figure 2 brings the evolution of the global TEC into focus showing the mean TEC E_0 and, in addition, the *maximum* TEC which has also been extracted from the CODE GIMs. The TEC values are given in so-called TEC Units (TECU), where 1 TECU corresponds to 10^{16} free electrons per square meter. Remember that our one-day GIMs approximate an average TEC distribution over 24 hours, hence our maximum TEC values have to be interpreted accordingly. The three non-AS periods within the time period considered are indicated by dashed lines.

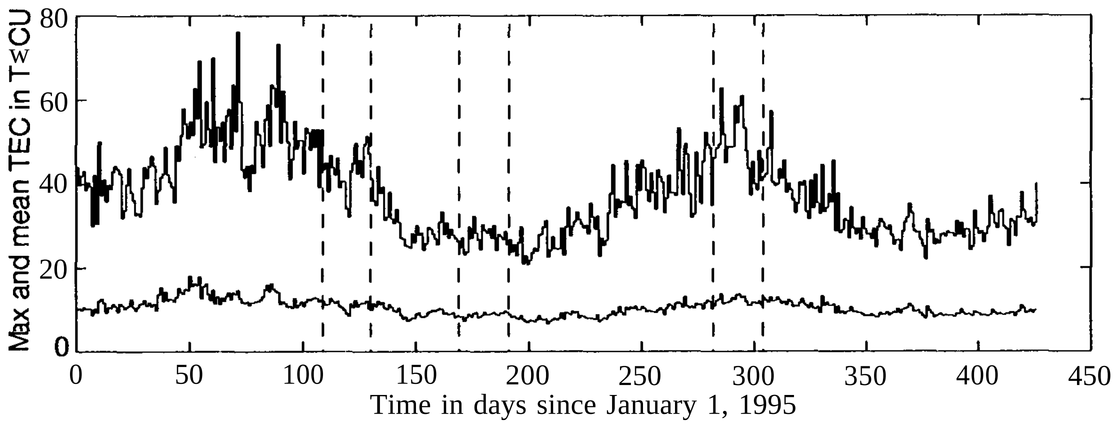

Figure 2. *Maximum* and *mean* TEC extracted from the CODE GIMs roughly describing the deterministic part of the ionosphere.

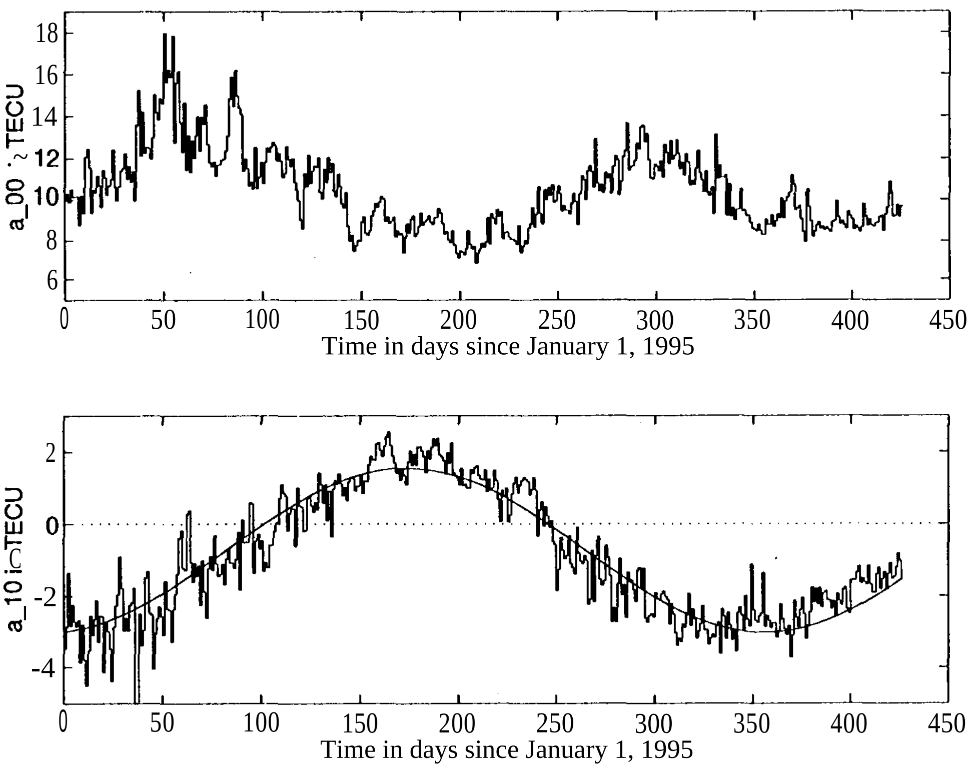

Figure 3. (a) zero-degree TEC coefficient a_{00} (*mean* TEC E_0) and (b) the first-degree coefficient a_{10} which mainly describes the zonal variation.

Figure 3 shows two special TEC parameters of the GIM representation (1) namely the coefficients a_{00} and a_{10}. The zero-degree coefficient a_{00} which corresponds to the recall

TEC E_0 already shown in Figure 2 is plotted in a larger scale here. The variations of the mean TEC even under low-activity conditions is quite impressive. Minima and maxima correspond to 6.8 and 18.0 TECU respectively, or, expressed in number of free electrons, to 3.9 . 10^{31} and 1.030 10^{32} free electrons. The first-degree coefficient a_{10} which describes the latitudinal variation of the global TEC distribution is shown in Figure 3b. The annual variation caused by the inclination of the equatorial plane with respect the ecliptic plane may be seen easily.

A newer example of a CODE GIM (with 64 contributing stations) given in the solar-geographical coordinate system is shown in Figure 4, where the latitude range covered is indicated by two dashed lines. Each individual GIM is parametrized with 81 TEC coefficients.

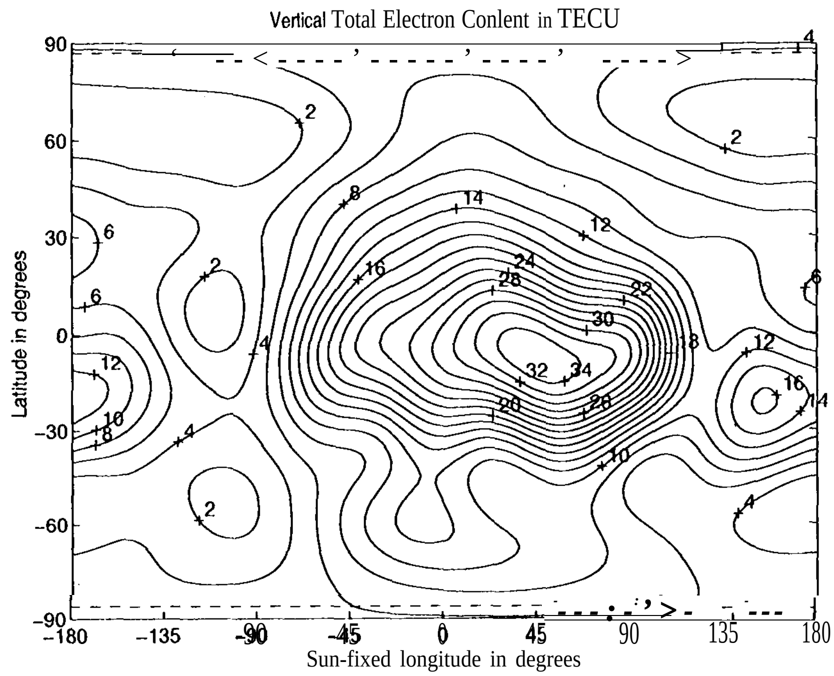

Figure 4. Global ionosphere Map (GIM) for day 073, 1996.

Derivation of Mean Ionosphere Maps

Let us extract *mean* ionosphere maps e.g. monthly maps from our daily results. Such maps may be easily derived by averaging the TEC coefficients a_{nm} and b_{nm} over certain time periods. An example is given in Figure 5. Mean GIMs primarily contain average TEC information as visualized in Figure 6 which shows an equatorial cross-section of the mean TEC structure of Figure 5 and in addition the temporal derivative of $E(0, t)$. Here we may recognize for instance that (a) between the end of evening twilight and the beginning of morning twilight the zenith TEC is statistically decreasing with more or less a constant rate or that (b) the maximum TEC is reached at about 2 hours after midday on average, confirming a well known phenomenon.

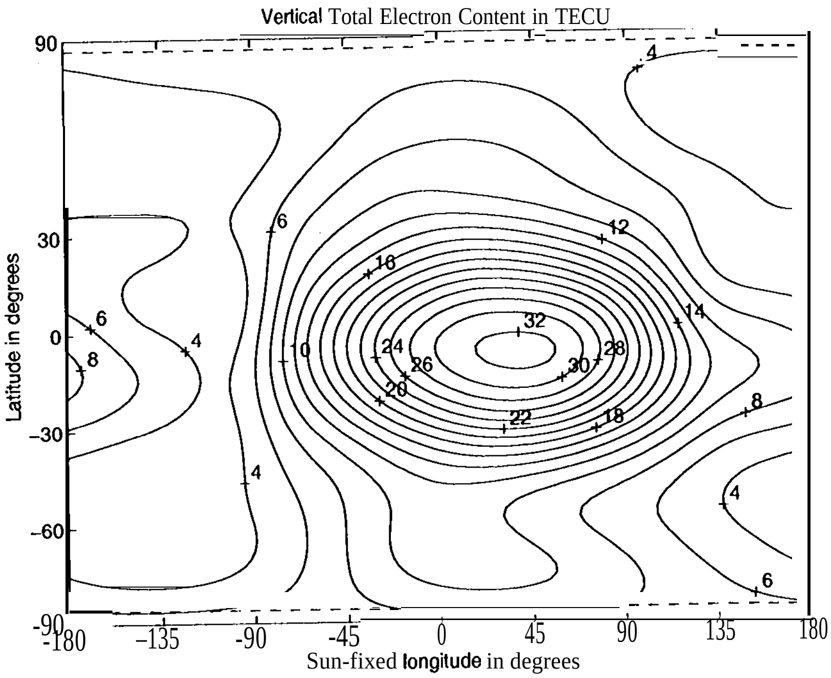

Figure 5. *Mean* global ionosphere map averaged over all 427 days (61 weeks).

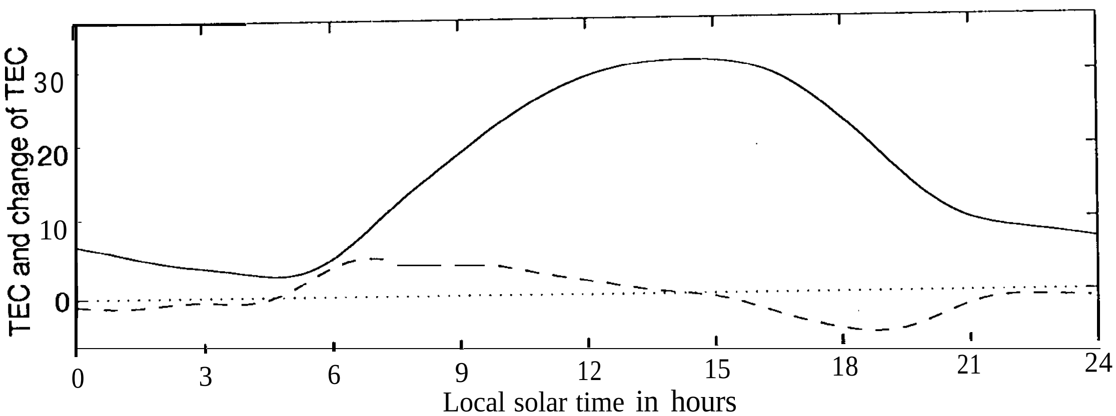

Figure 6. TEC (in TECU) and change of TEC (in TECU/hours) for an average equatorial TEC profile.

Monitoring of the Stochastic Part

At present only one parameter describing the "agitation" of the ionosphere is at our disposal, namely the a posteriori RMS error of unit weight of the least-squares adjustment, which mainly reflects the ionosphere-induced noise of the geometry-free phase observable caused by ionospheric disturbances. The resulting RMS values converted from meters to unitsof TECU are shown in Figure 7. Notice that we cannot detect any jumps in thee evolution of this quantity at the boundaries of the three non-AS periods indicated by dashed lines. This fact again confirms that the quality of CODE GIMs is *not* affected by Anti-Spoofing.

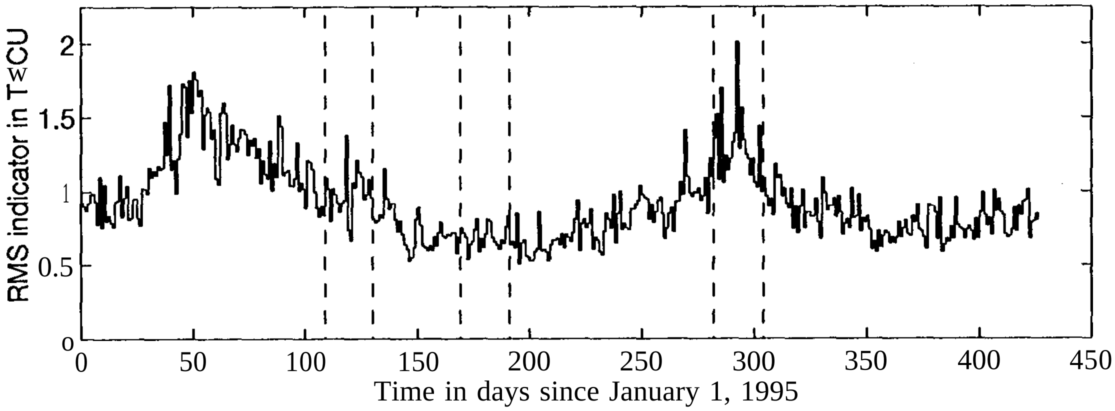

Figure 7. RMS indicator, characterizing the *stochastic* part of the ionosphere on a global scale.

Estimation of Global Shell Heights

We mentioned already that we also derive global ionosphere models where in addition to the TEC coefficients the shell height of the ionosphere is set up as an unknown parameter. In this case the parameter estimation problem is no longer a linear one, which means that we have to improve the GIMs iteratively starting from an initial adjustment. Our daily estimates of the shell height are shown in Figure 8. The dotted line indicates the a priori value used and the solid line shows a linear approximation which lies significantly above the 400-kilometer level generally adopted. We recognize a small linear trend, but this should be interpreted with care because it is based on a trivial shell height model and a mapping function which has to be refined. General considerations concerning the shell height may be found in (Komjathy and Langley, 1996).

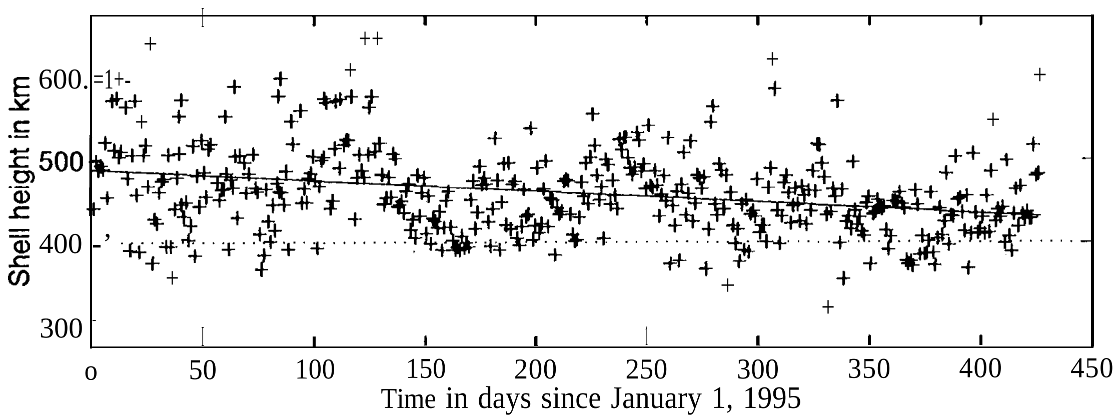

Figure 8. Daily estimates of a common shell height.

Correlation With Solar and Geomagnetic Indices

We may now correlate our TEC coefficient series with solar and geomagnetic indices like *Sunspot number*, *solar radio flux number*, *Kp index*, *Ap index*, etc. This has not been done in detail yet, but we may summarize that

(i) the dominant double peak within the time span analyzed (see Figures 2 and 9a) is recognizable in solar and geomagnetic parameter series as well (see Figures 9b to 9e),

(ii) the times of increasing or decreasing *mean* TEC are highly correlated with the times where the solar activity level changes (see Figures 9b and 9c), .

(iii) when performing a spectral analysis the evolution of the mean TEC snows a prominent period of 25 to 30 days which comes from the differential rotation of the Sun, and

(iv) our RMS indicator (see Figure 7) representing the stochastic behaviour of the ionosphere seems to be well correlated with the A p index which characterizes the activity of the geomagnetic field.

Finally the GPS-derived mean TEC E_0 and four solar and geomagnetic parameters obtained from the National Geophysical Data Center, Boulder, Colorado, USA are compared in Figure 9.

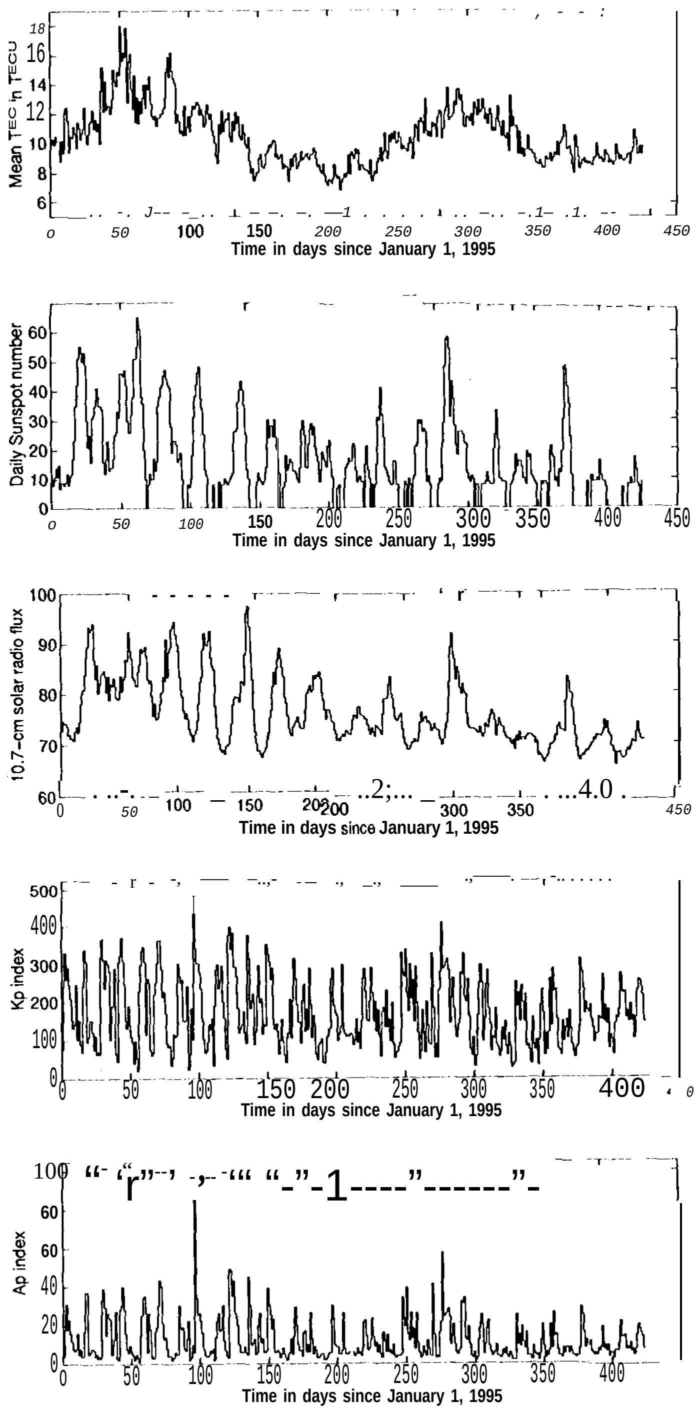

Figure 9. (a) Mean TEC derived by CODE, (b) daily Sunspot number, (c) Ottawa 10.7-cm solar radio flux (in solar flux units), (d) Kp index, and (e) Ap index.

CONCLUSIONS AND OUTLOOK

The global IGS core network of permanently tracking clual-frequency GPS receivers provides a unique opportunity to *continuously* monitor the Vertical Total Electron Content, on a global scale. A first long time series of TEC parameters indicates that *absolute* TEC determination is possible even when applying *interferometric* processing techniques. The CODE Analysis Center of the IGS shows that the production of Global Ionosphere Maps (GIMs) in an *automatic* mode is possible even under Anti-Spoofing (AS) conditions. *No* restrictions concerning receiver types or satellites have to be observed in this approach. If we support the global QIF ambiguity resolution using our one-day G lMs, the number of resolved ambiguity parameters is significantly higher. Since January 1, 1996 85 % instead of 75 % of the ambiguity parameters are resolved.

GIM files containing the global TEC information in an internal data format are available via the anonymous FTP server of the CODE processing center starting with January 1,1995. *Regional* ionosphere maps for Europe routinely generated since December 1995 are available on special request. If there is an interest in *rapid* GIMs, we might consider to establish such a service as part of our *rapid* orbit service. These GIMs (with less contributing stations) could be made available with a delay of about 12 hours, only.

At present one may *not* speak of a high degree of consistency of ionosphere maps produced by several groups analyzing GPS data, therefore TEC comparisons within the IGS and other interested organizations are necessary. Spaceborne applications like e.g. altimetry experiments might be used to validate GPS-derived ionosphere maps, too. Another essential aspect for the future development is an interface between the IGS and the ionosphere research community. We foresee that with high probability the IGS will be heavily involved in the ionosphere research area.

Monitoring the spatial and temporal variability of the *stochastic* part of the ionosphere by analyzing the *time-derivative* of phase observations using similar methods as for the global TEC determination will be our focus in the near future.

REFERENCES

Beutler, G., I. Bauersima, W. Gurtner, M. Rothacher, 'l'. Schildknecht, 1988, *Atmospheric Refraction and Other Important Biases in GPS Carrier Phase Observations*, Monograph 12, School of Surveying, University of New South Wales, Australia.

Beutler, G., I. Bauersima, S. Botton, W. Gurtner, M. Rothacher, 'l'. Schildknecht, 1989, Accuracy and biases in the geodetic application of the Global Positioning System, *Manuscripta Geodaetica*, Vol. 14, No. 1, pp. 2835.

Beutler, G., I. 1. Mueller, R. Neilan, 1994, The International GPS Service for Geodynamics (IGS): Development and Start of Official Service on 1 January 1994, *Bulletin Géodésique*, Vol. 68, No. 1, pp. 43-51.

Georgiadiou, Y. and A. Kleusberg, 1988, on the effect of ionospheric delay on geodetic relative GPS positioning, *Manuscripta Geodactica*, Vol. 13, pp. 1--8.

Komjathy, A. and R. B. Langley, 1996, *The Effect of Shell Height on High Precision ionospheric Modelling Using GPS*, Paper presented at the IGS AC! Workshop, Silver Spring, MD, USA, March 19 21, 1996.

Lanyi, G. E. and 'T'. Roth, 1988, A comparison of mapped and measured total ionospheric electron content, using global positioning system and beacon satellite observations, *Radio Science,* Vol. 23, No. 4, pp. 483-492.

Mannucci, A. J., B. D. Wilson, D.-N. Yuan, 1994, Monitoring Ionospheric Total Electron Content Using the GPS Global Network and TOPEX/POSEIDON Altimeter Data, *Proceedings of the Beacon Satellite Symposium*, Aberystwyth, Wales, July 1994.

Mervart, L., G. Beutler, M. Rothacher, U. Wild, 1993, Ambiguity Resolution Strategies Using the Results of the international GPS Geodynamics Service (IGS), *Bulletin Géodésique*, Vol. 68, No. 1, pp. 2938.

Mervart, I,. and S. Schaer, 1994, *Quasi-Ionosph erc-Free (QIF) Ambiguity Resolution Strategy*, Internal report, Astronomical Institute, University of Berne, Switzerland.

Mcrvart, I,., 1995, Ambiguity Resolution Techniques in Geodetic and Geodynamic Applications of the Globall 'positioning System, *Geodätisch-geophysikalische Arbeiten in der Schweiz*, Band 53.

Rothacher, M., G. Beutler, E. Brockmann, W. Gurtner, I,. Mcrvart, S. Schaer, T. A. Springer, 1996, The *Bernese GPS Software Version 4.0: Documentation*, Astronomical Institute, (University of Berne, Switzerland (in preparation).

Rothacher, M., G. Beutler, E. Brockmann, I,. Mervart, S. Schaer, T. A. Springer, U. Wild, A. Wiget, C. Boucher, Il. Seeger, 1996, *Annual Report 1995 of the CODE Analysis Center of the IGS* (in preparation).

Schaer, S., 1994, *Stochastische Ionosphärenmodellierung beim Rapid Static Positioning mit GPS*, Diplomarbeit, Astronomisches Institut, Universität Bern.

Schaer, S., G. Beutler, 1,. Mcrvart, M. Rothacher, U. Wild, 1995, Global and Regional ionosphere Models Using the GPS Double Difference Phase Observable, Proceedings *of the 1995 IGS* Workshop, Potsdam, Germany, May 1517, 1995, pp. 77-92.

Wild, U., 1993, Ionosphere and Ambiguity Resolution, *Proceedings of the 1993 IGS Workshop*, March 25-26, 1993, Berne, Switzerland, pp. 361-369.

Wild, U., 1994, ionosphere and Satellite Systems: Permanent GPS Tracking Data for Modelling and Monitoring, *Geodätisch-geophysikalische Arbeiten in der Schweiz*, Band 48.

Wilson, B. D. and A. J. Mannucci, 1993, *Instrumental Biases in Ionospheric measurements Derived from GPS Data*, Paper presented at 10N G I'S 93, Salt Like City, September 22-24, 1993.

The Effect of Shell Height on High Precision Ionospheric Modelling Using GPS

A. Komjathy and R.B. Langley
Both at: Geodetic Research Laboratory, Department of Geodesy and Geomatics Engineering
University of New Brunswick, P.O. Box 4400, Fredericton, N.B. E3B 5A3 Canada
Phone: 1-506-453-4698, Fax: 1-506-453-4943, email: w43y@unb.ca, lang@unb.ca

ABSTRACT

The dispersive nature of the ionosphere makes it possible to measure its total electron content (TEC) using dual-frequency Navstar Global Positioning System (GPS) observations collected by permanent networks of GPS receivers. One such network is that of the International GPS Service for Geodynamics (IGS). UNB has participated in an ionospheric experiment along with other ionospheric research groups under the auspices of the IGS and European Space Agency's European Space Operations Centre (ESA/ESOC). A 5 week long period of dual-frequency GPS measurements collected by IGS stations was designated as a test data set for the different research groups to analyse and produce TEC values and satellite-receiver differential delays. One of the primary goals of the experiment was to analyse the effect of geomagnetic disturbances on the ionospheric products. We have used dual-frequency GPS pseudorange and carrier phase observations from six European stations in the IGS network to derive regional TEC values and satellite-receiver differential delays.

In an earlier study we concluded that after processing data from 6 European stations collected over a 7 day period (the first 7 days of the ionospheric experiment organized by ESA/ESOC), we were able to follow highly varying ionospheric conditions associated with geomagnetic disturbances. We investigated the effect of using different elevation cutoff angles and ionospheric shell heights on the TEC estimates and satellite-receiver differential delays. These results pertaining to GPS week 823 have been presented earlier [Komjathy and Langley, 1996]. In our current research, we used 21 days' worth of data in a continuation of the study mentioned earlier with a more rigorous approach for ionospheric shell height determination which has been derived from the International Reference Ionosphere 1990 (IRI90) [Bilitza, 1990]. We looked at the effect of using ionospheric shell heights fixed at a commonly used altitude (400 km) on the TEC and differential delay estimates. We found differences in the differential delays between the two approaches of up to the 0.3 ns ($\approx$ 1 total electron content unit – TECU) level and differences in the TEC estimates up to the 1 TECU ($\approx$ 0.16 m delay on L1) level. We also compared our differential delay estimates with those obtained by other research groups participating in the experiment. We found agreement in the differential delays between three analysis centers at the 1 ns level.

INTRODUCTION

The electromagnetic signals from the GPS satellites must travel through the earth's ionosphere on their way to GPS receivers on or near the earth's surface. Whereas these effects may be considered a nuisance by most GPS users, they will provide the ionospheric community with an opportunity to use GPS as a tool to better understand the plasma surrounding the earth. Dual-frequency GPS observations can be used to eliminate almost all of the ionosphere's effect. To correct data from a single-frequency GPS receiver for the ionospheric effect, it is possible to use empirical models. We arc conducting an on-going study to assess the accuracy and efficacy of such models.

We dceided to include the new IRI90 model [Bilitza, 1990] in our ionospheric research after Newby [1992] investigated the International Reference Ionosphere 1986 (IRI86) model's performance. Earlier we used Faraday rotation data as "ground-truth" with which wc compared the vertical ionospheric range error corrections predicted by the Broadcast model of the GPS navigation message [Klobuchar, 1986] and the IRI90 model. For low solar activity, mid-latitude conditions we concluded that based on the comparison between the Broadcast and IRI90 models, both for day-time and night-time periods, the IRI90 model appeared to be more accurate than the Broadcast model [Komjathy et al., 1995a ; 1995b]. Since data from the GOES geostationary satellites that would provide the Faraday rotation measurements for use as "ground-truth" is no longer readily available, we have decided to use dual-frequency pseudorange and carrier phase GPS measurements to infer ionospheric TEC.

Early studies used single station observations to estimate the line-of-sight pseudo-TEC which is the sum of the satellite-receiver differential delays and the actual line-of-sight TEC (e.g., Lanyi and Roth [1988], Coco et al. [1991]). Recently the ionospheric community started applying multi-site fitting techniques to produce global and/or regional ionospheric maps with more accurate TEC and differential delay estimates. These ionospheric maps and differential delays are becoming freely accessible on the Internet. As an ionospheric observable, most research groups use a "phase-levelling" technique in which the integer ambiguity afflicted differences of the L1 and L2 (L1 -L2) carrier phase measurements are adjusted by a constant value determined for each phase-connected arc of data using precise pseudorange measurements. This technique is widely used to estimate ionospheric model parameters as well as satellite-receiver differential delays (see, e.g., Gao et al. [1994], Sardon et al. [1994], Wilson and Mannucci [1994], and Runge et al. [1995]). It is also feasible to use double-differenced L1 -L2 carrier-phase observations to estimate global or regional ionospheric models [Schaer et al. 1995]. The advantage of this latter technique is that by using the double-differenced ionospheric observable, one does not have to estimate the satellite-receiver differential delays as they are difference away – although some of the resolution of the ionospheric signal is eliminated during the process. A technique used by Bishop et al. [1995] infers TEC and satellite-receiver differential delays by requiring maximum agreement between ionospheric measurements when the observed paths of two satellites cross.

ESTIMATION STRATEGY

The estimation strategy we used is described in Komjathy and Langley [1996] in detail. In this section, wc will briefly summarize the basic principles of our technique to help explain the recent improvements wc made to the algorithm. We model the ionospheric measurements from a GPS receiver with the commonly used single-layer ionospheric model using the observation equation:

$$I_r^s(t_k) = M(e_r^s)\cdot\left[a_{0,r}(t_k) + a_{1,r}(t_k)\cdot d\lambda_r^s + a_{2,r}(t_k)\cdot d\varphi_r^s\right] + b_r + b^s$$

where

$I_r^s(t_k)$ is the L] -L2 phase measurement at epoch t_k made by receiver r observing satellites,

$M(e_r^s)$ is the thin-shell elevation angle mapping function projecting the line-of-sight measurement to the vertical with e_r^s being the elevation angle of satellites viewed by receiver r at the subionospheric point – the intersection of the ray path of a signal propagating from the satellite to the receiver with a thin spherical shell (see, e.g., Schaer et al. [1995]),

$a_{0,r}, a_{1,r}, a_{2,r}$ are the parameters for spatial linear approximation of TEC to be estimated per station assuming a first-order Gauss-Markov stochastic process [Gail et al. 1993],

$d\lambda_r^s = \lambda_r^s - \lambda_0$ is the difference between a subionospheric point and the mean longitude of the sun,

$d\varphi_r^s = \varphi_r^s - \varphi_r$ is the difference between the geomagnetic latitude of the subionospheric point and the geomagnetic latitude of the station, and

b,, b' refer to the receiver and satellite differential delay respectively.

The three parameters $a_{0,r}, a_{1,r}, a_{2,r}$ in the above equation are estimated for each station using a Kalman filter approach. The prediction and update equations for the state estimation are described by e.g., Schwarz [1987], Coster et al. [1992] and van der Wal [1995]. Due to the highly varying ionospheric conditions during the observation window processed, we allowed the model to follow a relatively high 1 TECU per 2 minutes change in the total electron content which resulted in the process noise variance rate of change being 0.008 $TECU^2$ / second characterizing the uncertainties of the dynamic ionospheric model. For the variance of the measurement noise, we used 1 $TECU^2$ - the assumed uniform uncertainty in the observations.

We estimated the combined satellite-receiver differential delays for station Madrid. In a network solution, additional differential delay parameters for the rest of the stations have to be estimated based on the fact that the other receivers have different differential delays. Therefore, for each stat ion other than stat ion Madrid, an additional differential delay parameter was estimated which is the difference between the receiver differential delay between a station in the network and station Madrid. This technique is described by e.g., Sardon et al. [1994].

We chose a solar-geomagnetic reference frame based on sun-fixed longitude and geomagnetic latitude since the main reason for the ionosphere's existence is the interaction of ionizing radiation (principally from solar ultraviolet and x-ray emissions) with the earth's atmosphere and magnetic field [Langley, 1996]. Furthermore, the ionosphere varies much more slowly in sun-fixed reference frame than in an earth-fixed one. The use of such a reference frame results in more accurate ionospheric delay estimates when using Kalman-filter updating [Mannucci et al., 1995].

A parameter that affects the TEC estimation is the assumed height of the ionospheric shell which plays a role in computing the coordinates of the subionospheric points. It is also an input parameter of the $M(e_r^s)$ mapping function (see equation). At this stage we use a simple $1/\cos(90^0 - e_r^s)$ mapping function. Later on, we plan on looking at other mapping functions that would reduce mapping function errors for low elevation angle satellites. The single-layer ionospheric model assumes that the vertical TEC can be approximated by a thin spherical shell which is located at a specified height above the earth's surface. This altitude is often assumed to correspond to the maximum electron density of the ionosphere, Furthermore, it is usually assumed that the ionospheric shell height has no temporal or geographical variation and therefore it is set to a constant value regardless of the time or location of interest. In Komjathy and Langley [1996], we looked at the effect of different fixed ionospheric shell heights of 300, 350, and 400 km and also included variable heights computed by the IRI90 model using F2 layer peak heights. We found that at the 2 TECU level, the ionospheric estimates using these specified heights agree depending on geographic location and time of the day. We also found that using different elevation cutoff angles (1 5°, 20°, and 25°) had an impact on TEC estimates at the 2 TECU level. These results should be considered only valid for the low solar activity conditions under which the estimates were made.

After the promising results of using the IRI90 model for ionospheric shell height determination, we decided to carry on with this investigation. In our current study, we use the IRI90 model to compute even more accurate ionospheric shell heights by integrating the predicted electron densities through the six subregions of the IRI90 profile. Ionospheric shell height predictions were obtained upon reaching 50 percent of the predicted total electron content during the numerical integration procedure using a step size of 1 km. We computed the predicted total electron content up to an altitude of 1000 km (see Figure 1), consequently, plasmaspheric electron content has not been considered at this stage but its effect should be less than about 50 percent of the night-time total electron content near sunspot minimum [Davies, 1990]. The omission of the plasmaspheric electron content has an effect primarily on the night-time TEC predictions at the 2 TECU level. We believe that this method provides an even more rigorous approach compared to what has been described in Komjathy and Langley [1996]. Note in Figure 1 that the predicted ionospheric shell height is always slightly above the height of the F2 layer peak electron density since the topside region of the ionosphere contains more electrons than the bottomside. The predicted ionospheric shell heights are used as input into our software for estimating TEC maps as well as satellite-receiver differential delays.

THE DATA SET

Along with several other research groups, we participated in an experiment to assess the capabilities of GPS data to provide TEC values. Organized under the auspices of the International GPS Service for Geodynamics (IGS) and the Orbit Attitude Division of the European Space Agency's European Space Operations Centre (ESA/ESOC), the experiment involves the processing and analysis of a 5 week long data set of dual-frequency GPS data from the stations of the IGS network (GPS weeks 823 through 827). We have analysed the GPS data sets from 6 of the European IGS stations. The stations are Madrid, Grasse, Matera, Brussels, Wettzell, and Onsala and are identified on the map in Figure 2. The differences in geomagnetic latitudes of stations Madrid, Grasse, and Matera are less then 5 degrees, and 3.3 degrees in the case of stations Brussels and Wettzell. Therefore, we can identify three distinct latitude regions in our test network (1. Madrid, Grasse, Matera; 2. Brussels, Wettzell; 3. Onsala). All 6 stations use Allen Osborne Associates TurboRogue receivers.

We processed 21 days' worth of data from the 6 stations spanning the time period 15 October to 4 November 1995 (GPS weeks 823, 824, and 825) during which a geomagnetic disturbance occurred [NGDC, 1995]. The planetary equivalent amplitude of magnetic activity a_p suggests that the magnetic disturbance started on 18 October 1995 (day of year 291) and lasted for about 6 days until 23 October 1995 (day 296). The peak ($a_p = 111$) occurred on 19 October 1995. The magnetic disturbance on day 292 affected the diurnal variation of the total electron content. The effect of this disturbance on our TEC estimates has been discussed previously in Komjathy and Langley [1996]. In that study we found that on day 292, at stations Madrid, Grasse and Matera, the diurnal peak of TEC values increased considerably compared to diurnal peaks for the previous days. On the other hand, for stations Brussels, Wettzell and Onsala, the GPS-derived TEC estimates show diurnal peaks with smaller size than the ones on the previous days. Also, even though the magnetic disturbance started during European night-time, it only caused a TEC increase (stations Madrid, Grasse, Matera) and decrease (Brussels, Wettzell) on the following day around noon (day 292). The fact that we detected at some stations a TEC increase and at others a TEC decrease may suggest that the magnetic disturbance was moving equatorward which is a well known feature of such disturbances [Davies, 1990].

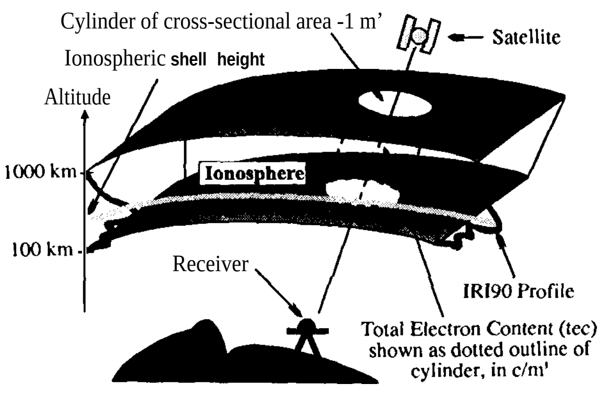

Figure 1. Illustration of ionospheric shell height determination.

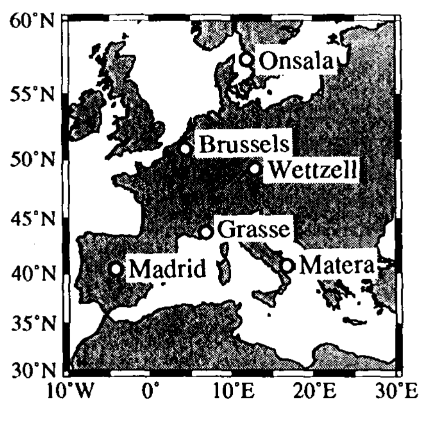

Figure 2. Locations of IGS stations used for data analysis.

RESULTS AND DISCUSSION

We used the PhasEdit version 2.0 automatic data editing program to detect bad points and cycle slips, repair cycle slips and adjust phase ambiguities using the undifferenced data. The program takes advantage of the high precision dual-frequency pseudorange measurements to adjust L1 and L2 phases by an integer number of cycles to agree with the pseudorange measurements [Freymueller, 1995]. Subsequently, a modified version of the University of New Brunswick's Differential Positioning Program (DIPOP) package was used to estimate ionospheric parameters and satellite-receiver differential delays using a Kalman filter algorithm.

For our investigation, we. used the IR190-derived ionospheric shell height predictions as input into our DIPOP-based processor. As a first step, we computed the IRI90 predicted total electron content by integrating the predicted electron densities along the IRI90 profile. A simplified version of the profile can be *seen* in Figure 3 (for an explanation of the symbols, see Hakegard [1995] or Bilitza [1990]). Secondly, we used these TEC predictions to integrate the electron densities along the profile again. This time, the goal was to determine the height at which 50 percent of the total electron content was reached. We did this for all six stations we used for data processing for the 21 days under investigation. As an example, we have plotted the predicted ionospheric shell heights for day 288 in Figure 4. We can clearly see a diurnal variation of the IRI90-derived ionospheric shell height. The shell height seems to peak at night-time values of about 400 km and goes down to day-time values typically at the 300 km level. Diurnal curves were plotted for all 6 stations for day 288. There are noticeable differences from station to station even under the current low solar activity conditions. The spatial variation of the ionospheric shell height in our regional network for GPS weeks 823 to 825 was between 10 and 30 km depending on the time of the day.

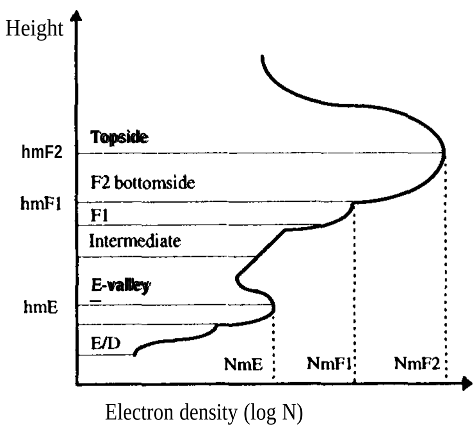

Figure 3. IRI90 profile (afterHakegard,[19951).

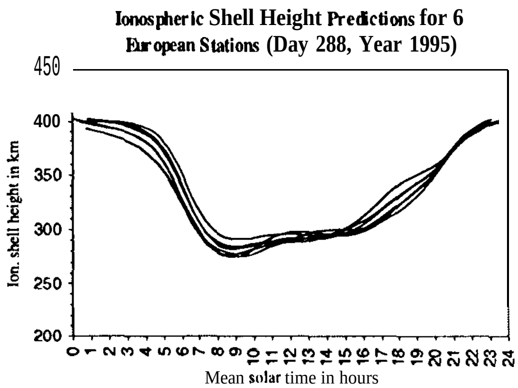

Figure 4. The diurnal variation of the ionospheric shell height.

For a better understanding of the magnitude range of varying ionospheric shell height, we computed the predicted ionospheric shell heights for high (year 1990), medium (year 1992) and low (year 1995) solar activity conditions. In Figure 5, we plotted the diurnal curves for the two stations that are furthest apart in our network: stations Madrid and Onsala. Each diurnal curve represents the conditions for the 15th day of one month of the year displaying not only the diurnal variation but also the seasonal variation of the ionospheric shell height. Note that the x axis is a category time axis on which 12 diurnal curves have been plotted one after the other each representing a "typical day" of a month. The "typical day" was arbitrarily chosen to be the 15th day of the month for illustration purposes. A small discontinuity y is visible between some of the curves at 24 hours reflecting month-to-month variations. During high solar activity conditions, the peak to peak variation of the diurnal curve is between 400 and 600 km, depending on season and geographic location of the station. During medium solar activity conditions, the variation is between 300 and 500 km. For low solar activity conditions this variation is between 300 and 400 km. As solar activity decreases, the dependency on geographic location, at least for our two European stations, becomes less significant. For high solar activity conditions, station Onsala (furthest north in the network) had the highest ionospheric shell heights. Also, during winter months the separation between shell heights predicted for stations Onsala and Madrid seems to be larger than for the rest of the year. For high solar activity conditions, the average ionospheric shell height is around 466 km; for medium solar activity conditions, 385 km; for low solar activity conditions, 335 km. It seems that the diurnal, seasonal, solar-cycle and spatial variations of the ionospheric shell heights are associated with the temporal and spatial variation of the F2 layer peak electron density,

Ionospheric Shell Height Predictions for Stations Madrid and Onsala

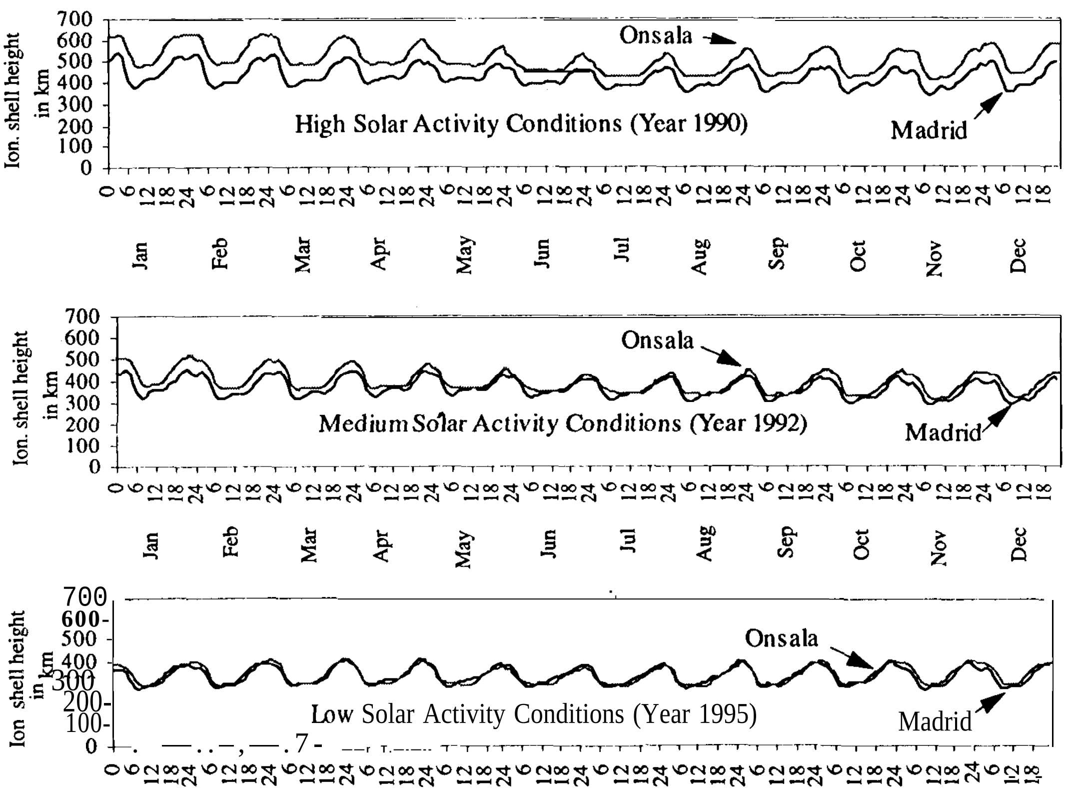

Figure 5. Ionospheric shell height predictions using the IRI90 model.

Using varying ionospheric shell heights as input into our model produces TEC and satellite-receiver differential delay estimates that are somewhat different from those obtained using a fixed ionospheric shell height. To determine the magnitude of the differences, we produced a set of TEC and differential delay estimates using both a commonly adopted fixed ionospheric shell height (400 km) and varying ionospheric shell heights predicted by the IRI90 model as described earlier. The entire 21 days' worth of data was used for this investigation. We difference the means (over 21 days) of the differential delay estimates for each satellite and station using the varying IRI90-predicted and 400 km ionospheric shell heights. The differences in differential delays can be seen in Figure 6. The differences are less than 0.3 ns with a mean of 0.14 ns and mean standard deviation of 0.13 ns. In Figure 6, the error bars represent the mean standard deviation of the UNB differential delay estimates. We also produced hourly TEC maps at a

1 degree by 1 degree grid spacing for the region displayed in Figure 2. We produced the TEC maps by evaluating at each grid node our expression for the spatial linear approximation of TEC described by the three parameters estimated for each IGS station. For evaluating the model at each grid node, we used the three estimated parameters from the nearest IGS station. In the future, we will modify this approach with an appropriate multi-station weighting scheme. We used both the varying and 400 km ionospheric shell heights to compute different sets of ionospheric maps. We difference the corresponding TEC values at each grid node that were computed for each hour of the 21 days under investigation. The differences are plotted in Figure 7. The histogram is based on 640,584 ((31 by 41 grid) times (24 hours) times (21 days)) TEC estimates. 53 percent of the differences fall into a bin that can bc characterized with a lower boundary of-0.5 TECU and upper boundary of O TECU. The mean of the differences is -0,34 TECU and its associated standard deviation is 0.58 TECU. Note that the TEC differences were formed by subtracting TEC values using a 400 km shell height from those using the IRI90-derived shell height TEC values.

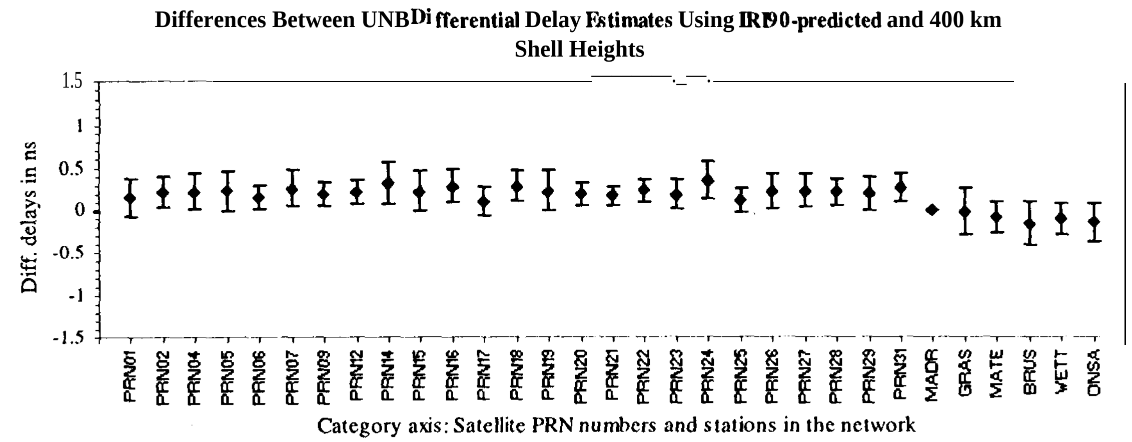

Figure 6. Comparison of satellite-receiver differential delay estimates between using IR190-derived and **400** km ionospheric shell heights.

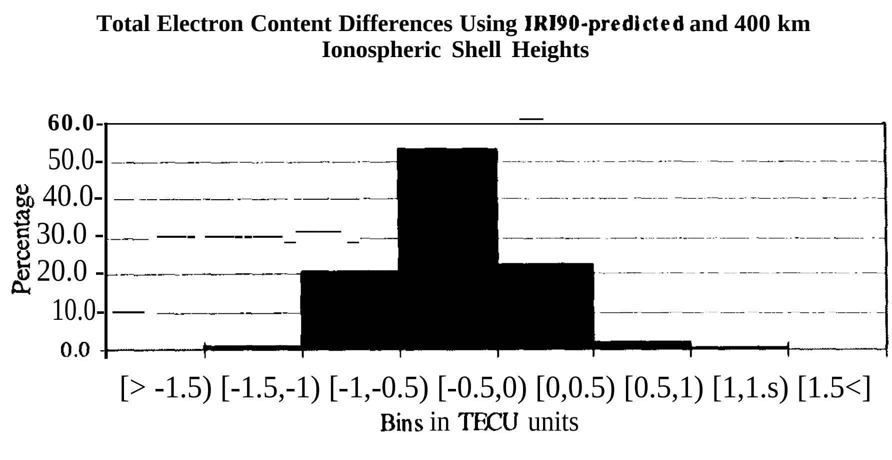

Figure 7. Comparison of TEC estimates between using IRI90-derived and 400 km ionospheric shell heights.

We conclude from this investigation that taking the temporal and spatial variation of the ionospheric shell height into account has an effect on the TEC estimates of up to 1 TECU, and 0.3 ns in the case of the differential delay estimates. These values will likely only hold for mid-latitude conditions at low solar activity levels. As we have seen earlier in Figure 5, during higher solar activity times, we can expect these differences to increase. The 1 TECU level differences are fairly small and may be within the error bars of the TEC estimates. Therefore, we decided not to compare our TEC estimates (maps) with those obtained by other research groups to try to determine the effects of using different values for the ionospheric shell height. Furthermore, the differences between ionospheric modelling methods used by different groups would make it difficult to draw conclusions on the specific effect of their selected ionospheric shell heights.

Instead, we computed the means and the standard deviations of our daily differential delays for all 21 days. We also obtained a set of differential delay estimates computed by two of the other participating members of the ionospheric experiment, namely, the Deutsche Forschungsanstalt fur Luft und Raumfahrt (DLR) Fernerkundungsstation, Neustrelitz, Germany and the European Space Agency's European Space Operation Centre (ESA/ESOC), Darmstadt, Germany. After computing the means and standard deviations of the differential delays obtained from DLR and ESOC for all 21 days, we computed the differences of the corresponding means. The differences among the 3 analysis centers' results are displayed in Figure 8.

Comparison of Differential Delay Differences Between Different Processing Centers for GPS Weeks 823 to 825 (UNB: Ion. Shell Height Predicted by IRI90)

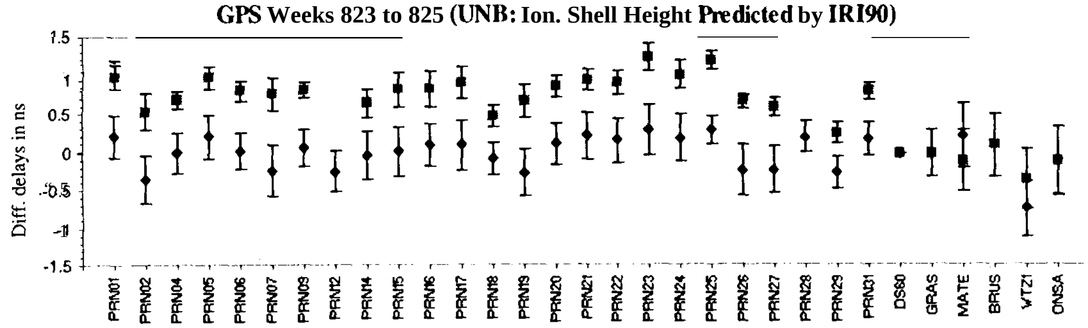

Category x axis: satellite PRN numbers and stations used for UN B processing

▪ UNB-DLR • UNB-ESOC

Comparison of Differential Delay Differences Between Different Processing Centers for GPS Weeks 823 to 825 (UNB: Ion. Shelf Height Fixed at 400 km)

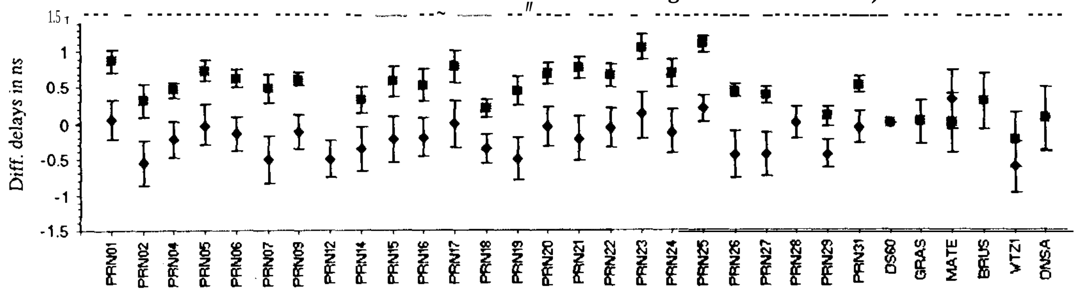

Category x axis: satellite PRN numbers and stations used for UNB processing

, UNB-DLR ♦ UNB-ESOC

Figure 8. Comparison of differential delay differences between processing centers.

The differences were formed as UNB minus DLR and UNB minus ESOC using both our IRI90-derived shell height results (upper panel) and our results using the 400 km shell height (lower panel). Note in Figure 8 that satellites PRN12 and PRN28 are not used by DLR and stations Grasse and Brussels are not processed by ESOC. The associated standard deviations of the differential delays about the means of the two other processing centers were also plotted. The standard deviations of the means of the UNB differential delays were plotted earlier in Figure 6 and have not been considered in computing the error bars in Figure 8. The differences of the differential delay estimates are at the 1 ns level for both shell height models (upper and lower panel). It is interesting to see that there is a clear bias between the DLR and ESOC satellite differential delays. A part of the bias can be explained by the fact that the ESOC algorithm uses 350 km for the ionospheric shell height whereas the DRL algorithm uses 400 km. As our investigation indicated in Figure 6, a 0.14 ns level bias can be expected between the differential delay differences using the IRI90-derived differential delays and the ones obtained using 400 km. However, a 1 ns level difference indicates that there are effects coming from other differences in the algorithms used by the processing centers. The fact that the UNB-ESOC differences do not seem to show a consistent bias might be explained by the fact that the mean of the IRI90-predicted diurnal variation of the ionospheric shell height is around 335 km under low solar activity conditions which is close to the 350 km height used by ESOC.

One of the potential error sources that may contribute significantly to the UNB error budget is the mapping function error. Since we use a simple secant mapping function at this stage, this could introduce unwanted errors at low elevation angles (say between 20 and 30 degrees). Throughout our processing, we used a 20 degree elevation cutoff angle. The very ability to do ionospheric modelling is based on the possibility of separating estimates of TEC from differential delays by using the elevation angle dependence of the TEC variation. Should this separation suffer from mapping function errors, a bias could be introduced into both the TEC and differential delay estimates.

It seems that using pre-defined values for ionospheric shell height has a scaling effect on the differential delay estimates. The results presented in Komjathy and Langley [1996] were also indicative of this. The lower the ionospheric shell height is set (arbitrarily or otherwise) from the “true” value, the higher the estimated differential delays will be. Furthermore, this effect seems to have an opposite sign in the case of the TEC estimates: The lower the ionospheric shell height is set from the “true” value, the lower TEC estimates can be expected. Using pre-defined fixed values for ionospheric shell height may lead to errors both in the satellite-receiver differential delays and the TEC estimates. This conclusion seems to be supported by the maximum 0.3 ns error in differential delay differences we found which corresponds to about 1 TECU. This also corresponds to the maximum TEC differences that were found to be at the 1 TECU level (see Figure 7). Using 400 km as a fixed ionospheric shell height during low solar activity conditions overestimates the day-time TEC by up to 1 TECU assuming that the IRI90-derived ionospheric shell height predictions are free of error. In the case of the satellite-receiver differential delays, using a fixed 400 km ionospheric shell height underestimates the differential delays by up to 0.3 ns under the same assumption. We believe these numbers would be even higher for higher solar activity conditions. An approximate value for the error we can expect by inappropriately setting the ionospheric shell height is about 0.5 TECU for every 50 km error in the height. This number corresponds to about 0.14 ns in the case of the differential delays. Also, these numbers could be different when modelling the ionosphere by fitting polynomials to the diurnal variation of TEC over a certain period of time. This procedure inherently averages over different ionospheric shell heights. This can also be a feasible explanation for our not detecting differences between the UNB and ESOC differential delay estimates.

CONCLUSIONS

The concept of accounting for the temporal and spatial variation of the ionospheric shell height using the IRI90 model has been described, We showed that on a small regional network of IGS stations, the predicted ionospheric shell height can vary with geographic location, time of day, season, and solar activity. After comparing our results with those obtained earlier using a fixed ionospheric shell height, we found differences in the differential delays of up to 0.3 ns. A similar study was conducted for the TEC estimates and we found that the estimates can be different by as much as 1 TECU when the temporal and spatial variation of the ionospheric shell height is not considered. We believe that these differences can be even larger during high solar activity conditions.

Furthermore, taking into account the temporal and spatial variation of the ionospheric shell height provides a more rigorous approach when estimating ionospheric model parameters along with satellite-receiver differential delays. By inappropriately setting the ionospheric shell height, we can expect a possible 0.5 TECU level error for every 50 km error in the shell height. For the differential delays, the equivalent error level is about 0.14 ns.

ACKNOWLEDGEMENTS

We greatly appreciate the assistance of Dieter Bilitza in providing us with an update of the IRI90 model. Funding from the University of New Brunswick and the Natural Sciences and Engineering Research Council of Canada is gratefully acknowledged. Without their help this research could not have been completed.

REFERENCES

Bilitza, D. (cd.) (1990). *international Reference ionosphere 1990.* National Space Science Center/World Data Center A for Rockets and Satellites, Lanham, MD. Report Number NSSDC/WDC-A-R&S 90-22.

Bishop, G. J., A.J. Mazzella, and E.A. Holland (1995). "Application of Score Techniques to Improve Ionospheric Observations". ION GPS-95, Proceedings of the 8th international Technical Meeting of the Satellite Division of The Institute of Navigation, Palm Springs, CA, 12-15 September, The Institute of Navigation, Alexandria, VA, pp. 1209-1218.

Coco, D. S., C.E. Coker, S.R. Dahlke, and J.R. Clynch (1991). "Variability of GPS Satellite Differential Group Delay Biases." IEEE Transactions on Aerospace Systems, Vol. 27, No. 6, pp. 93 1 -938.

Coster, A.J., E.M. Gaposchkin, and L.E. Thornton (1992). "Real-time Ionospheric Monitoring System Using GPS." Navigation: Journal of the Institute of Navigation. Vol. 39, No. 2, pp. 191-204.

Davies, K. (1990). *Ionospheric Radio.* Peter Peregrinus Ltd., London, United Kingdom.

Freymueller, J. (1995). Personal communication. Department of Geophysics, Stanford University, Stanford, CA, January.

Gail, W. B., B. Prag, D.S. Coco, and C. Coker (1993). "A Statistical Characterization of Local Mid-latitude Total Electron Content." Journal of Geophysical Research, Vol. 98, No. A9, pp. 15,717-15,727.

Gao, Y., P. Heroux, and J. Kouba (1994). "Estimation of GPS Receiver and Satellite L1/L2 Signal Delay Biases Using Data from CACS." KIS94, Proceedings of the International Symposium on Kinematic Systems in Geodesy, Geomatics, and Navigation, Banff, Alberta, 30 August -2 September, Department of Geomatics Engineering, The University of Calgary, Calgary, Alberta, pp. 109-117.

Hakegard, O.P. (1995). *A Regional Ionospheric Model for Real-time Predictions of the Total Electron Content in Wide Area Differential Satellite Navigation Systems.* Dr. Eng. Thesis, Norwegian Institute of Technology, Trondhcim, Rapport 429506.

Klobuchar, J.A. (1986), "Design and Characteristics of the GPS Ionospheric Time Delay Algorithm for Single-Frequency Users." *Proceedings of the PLANS-86 Conference,* Las Vegas, NV, 4-7 November, pp. 280-286.

Komjathy, A., R.B. Langley, and F. Vejražka (1995a). "A Comparison of Predicted and Measured Ionospheric Range Error Corrections." *EOS Transactions of the American Geophysical Union,* Vol. 76, No. 17, Spring Meeting Supplement, S87.

Komjathy, A., R.B. Langley, and F. Vejražka (1995b.J "Assessment of Two Methods to Provide Ionospheric Range Error Corrections for Single-frequency GPS Users." Presented at IUGG XXI General Assembly, Boulder, CO, 2-14 July 1995.

Komjathy, A. and R.B. Langley (1996). "An Assessment of Predicted and Measured Ionospheric Total Electron Content Using a Regional GPS Network." Presented at the ION National Technical Meeting, Santa Monica, CA, 22-24 January 1996.

Langley, R.B. (1996). "Propagation of the GPS Signals." in *GPS for Geodesy,* International School, Delft, The Netherlands, 26 March -1 April, 1995. Springer-Verlag, New York.

Lanyi, G.E. and T. Roth (1988). "A Comparison of Mapped and Measured Total Ionospheric Electron Content Using Global Positioning System and Beacon Satellite Observations", Radio Science, Vol. 23, No. 4, pp. 483-492.

Mannucci, A., B. Wilson, and D. Yuan (1995). "An Improved Ionospheric Correction Method for Wide-Area Augmentation Systems." 10N *GPS-95, Proceedings of the 8th International Technical Meeting of the Satellite Division of The Institute of Navigation,* Palm Springs, CA, 12-15 September, The Institute of Navigation, Alexandria, VA, pp. 1199-1208.

National Geophysical Data Center, NGDC (1995). Geomagnetic Database, ftp://www.ngdc.noaa.gov/STP/GEOMAGNET IC_DATA/INDICES/KP_AP/199.v 12, accessed January 1996.

Newby, S.P. (1992). *An Assessment of Empirical Models for the Prediction of the Transionospheric Propagation Delay of Radio Signals.* M. Sc.E. thesis, Department of Surveying Engineering Technical Report No. 160, University of New Brunswick, Fredericton, N. B., Canada.

Runge, T., U. Lindqwister, A. Mannucci, M. Reyes, B. Wilson, and D. Yuan (1995). "Generation of GPS Observable for Global Ionospheric Mapping." *EOS Transactions of the American Geophysical Union,* Vol. **76, No. 17,** Spring Meeting Supplement, S87.

Sardon, E., A. Rius, and N. Zarraoa (1994). "Estimation of the Transmitter and Receiver Differential Biases and the Ionospheric Total Electron Content from Global Positioning System Observations." Radio Science, Vol. 29, No. 3, pp. 577-586.

Schaer, S., G. Beutler, L. Mervart, and M. Rothacher (1995). "Global and Regional Ionosphere Models Using the GPS Double Difference Phase Observable." Presented at the 1995 IGS Workshop, Potsdam, Germany, 15-17 May.

Schwarz, K.P. (1987). "Kalman Filtering and Optimal Smoothing." *Papers for the CISM Adjustment and Analysis Seminars,* 2nd cd., The Canadian Institute of Surveying and Mapping, Ottawa, Ontario, Canada, pp. 230-264.

van der Wal, A. D. (1995). *Evaluation of Strategies for Estimating Residual Neutral-atmosphere Propagation Delay in High Precision Global Positioning System Data Analysis.* M.Sc.E thesis, Department of Geodesy and Geomatics Engineering Technical Report No. 177, University of Ncw Brunswick, Fredericton, N. B., Canada.

Wilson, B. and A. Mannucci (1994). "Extracting ionospheric Measurements from GPS in the Presence of Anti- spoofing." ION *GPS-94, Proceedings of the 7th International Technical Meeting of the Satellite Division of The Institute of Navigation,* Salt Lake City, UH, 20-23 September, The Institute of Navigation, Alexandria, VA, Vol. 2, pp. 1599-1608.

Verification of ESOC Ionosphere Modeling and Status of IGS Intercomparison Activity

J. Feltens [1], J.M. Dow [2], T.J. Martín-Mur [2], C. García Martinez [3], M.A. Bayona-Pérez [3]

1. EDS at Orbit Attitude Division, ESA, European Space Operations Centre, Robert-Bosch-Str. 5, D-64293 Darmstadt, Germany
2. ESOC
3. GMV at ESOC

Abstract

ESOC is planning to extend the use of IGS data also for ionospheric modeling. It is intended to provide ionospheric VTEC models and receiver/satellite differential delay values as new IGS products - besides orbits, earth orientation parameters and station coordinates. Different mathematical models were worked out to represent the ionosphere as single layer. ESOC-internally a short term analysis of these models indicated reliable performance.

In preparation of the IGS workshop in Silver Spring a comparison of ionosphere VTEC models originating from different Analysis Centers was organized. This comparison offers the opportunist y to verify the modeling & implementations of the participating AC'S.

ESOC will use the knowledge earned from this comparison, to define its final mathematical modeling and implement it in the Ionosphere Monitoring Facilit y (IONMON), which is under development at ESOC. Apart from the routine provision of ionospheric products to IGS, it is intended to use the ionosphere models for the support of other ESA-missons, e.g. ERS and ENVISAT.

1 INTRODUCTION

Since June 1992 ESOC participates as an Analysis Center at IGS. ESOC's activities within IGS include the routine provision of rapid and precise GPS orbits, earth orientation parameters, GPS satellite and station clock parameters, and ground station coordinates (SINEX), as well as GPS data tracking and retrieval from own ESOC tracking sites (currently, March 1996, these are: Kiruna, Kourou, Malindi, Maspalomas, Perth and Villafranca) on routine basis.

The transmission of navigation signals on two well defined frequencies is one of the basic characteristics of GPS. On the other hand, ionospheric effects, that are acting on satellite transmitted signals, are frequency-dependent. So, more or less as a by-product, the global dual-frequency GPS data, daily retrieved as part of ESOC's IGS activities, offer the opportunity to perform some kind of ionosphere monitoring to update ionosphere models using actual GPS data, and to provide these updated ionosphere models for other ESA missions to allow them to make ionospheric corrections on their own tracking data. This was the basic idea to concept and to establish an Ionosphere Monitoring Facility (IONMON) at ESOC.

The IONMON is currently under development, and a prototyping version is close to be operational. This prototyping version was used for an intercomparison of ionosphere products between ESOC and other Analysis Centers in preparation of the IGS workshop in Silver Spring in March 1996 (see also next chapter). The results of this comparison were used to verify the performance of nlathematical modeling in ESOC fits to TEC data. Once the final IONMON software is established, it will replace the prototyping version.

2 IONOSPHERE MODELS - A NEW PRODUCT OF IGS ?

The opportunity to exploit dual-frequency GPS data from IGS for ionosphere monitoring was also recognized by other members of the IGS, and following the IGS workshop in Potsdam in May 1995 it was suggested that a comparison of ionospheric products should be organized between the Analysis Centers.

Several of the Analysis Centers participating in the IGS (JPL, EMR, CODE), as well as some external processing centers (DLR Neustrelitz, University of New Brunswick (UNB) - these will in the following text be denoted as Analysis Centers too) have already experience with the evaluation of ionospheric parameters from dual-frequency GPS data and possess dedicated software. Others (ESOC) are currently implementing ionospheric modeling into their software, as was already mentioned in the above chapter.

In order to bring all the varying activities into one common direction of a routine provision of ionospheric information as a new product of the IGS, an intercomparison of ionosphere products originating from the different Analysis Centers was organized in preparation of the IGS workshop in Silver Spring in March 1996. The intent of this intercomparison was to find out:

- How ionosphere modeling is done at the different Analysis Centers, i.e. which mathematical models, which update rate, which geographical extent, etc.
- Which accuracies are currently obtained.

It is the intent of this paper to present the results of ESOC mathematical model verification in special (see above chapter) and to summarize the intercomparison between the different Analysis Centers in general.

3 MATHEMATICAL MODELS USED AT ESOC

Generally the IONMON offers so called single layer models to represent ionospheric VTEC, i.e. TEC observations are modeled as follows:

$$l + \varepsilon = Map \cdot VTEC + k_j + k^i \qquad (3.1)$$

where:

l	TEC observable,
ε	observation noise,
Map	mapping function projecting the observed TEC to tbe vertical,
VTEC	single layer model to represent the vertical TEC,

k_j receiver differential dela y,

k^i satellite differential delay.

The following general assumptions are made:

- Assumed height of ionospheric shell: $h_I = 350$ km.
- Mapping function: Either standard (see e.g. Mannucci et al, 1993), or the so called Q-factor mapping function (see Newby, 1992).
- Elevation cutoff is set equal to $el_{min} = 20^o$.
- Elevation-dependent weights are applied to favour high-elevation TEC observable and to prejudice low-elevation TEC observable:

$$W = e^{-a(1 - el/90^o)^{\beta}} \quad \text{with} \quad el = elevation, a = \beta = 2$$

- The reference frame used is aligned to the Sun's direction and to the geomagnetic pole. The algorithm of Biel (1990) is applied to transform from the geographic frame into the geomagnetic one.
- Fits of ionosphere models to TEC observation data are done in batch estimation mode.

Initially restricted to the above listed simple modeling, it is planned to extend the IONMON in successive versions for parameter updates in sequential estimation mode as well as to include more sophisticated models to represent the ionosphere's electron content, e.g. profiles and other physically based models, and evaluation of non-GPS and of satellite-to-satellite tracking data.

Depending on geographic extent, ESOC mathematical modeling can be classified into polynomial, spherical harmonic and Gauss-function fits, as described in the following sections.

3.1 Polynomials for Local VTEC representations

Polynomials (ref. R5) are fitted to TEC data which were collected at a certain ESA ground site to obtain a local VTEC model around that ground site in form of a higher-order surface. Fits are done in 6-hour time intervals, and the satellite/receiver differential delay values are constrained to 0.5 nanoseconds with respect to the values obtained from the nighttime fit (see Section 3.4). Polynomial development is linear in latitude and quadratic in local time (cubic for the equatorial ESA stations Kourou and Malindi).

3.2 Spherical Harmonics for Global/Regional VTEC Models

Degree and order $n,m = 8$ spherical harmonics (ref. R5) are fitted to regionally (e.g. Europe) and globally collected TEC data. The coefficients ale, a_{11} and b_{11}, which define the origin of the coordinate reference, are kept fixed with zero. Fits are done in 12-hour time intervals, and the satellite/receiver differential delay values are constrained to 0.5 nanoseconds with respect to the values obtained from the nighttime fit (see Section 3.4).

3.3 Gauss-Type Exponential Functions for Global VTEC Models

The method to model the global VTEC with Gauss-Type Exponential (GE) functions was worked out at ESOC, and is under testing now. It is out of the scope of this paper to present the GE-function theory, so only the very basic can be shown here: The VTEC of the above Equation (3.1) is represented by a GE-function single layer model as follows:

$$VTEC = \Xi + \mathcal{G} \cdot e^{-a_1 x - a_2 x^2 - a_3 x^3 - \ldots - a_{2n} x^{2n}} \cdot e^{-b_1 y - b_2 y^2 - b_3 y^3 - \ldots - b_{2m} y^{2m}} \cdot e^{-c_1 xy - c_2 x^2 y - c_3 x y^2 - \ldots - c_{l-k+2} x^{k-1} y - \ldots - c_l x y^{k-1}} \tag{3.2}$$

with

$$k = minimum(2n,\ 2m) \qquad l = k \cdot (k-1)/2$$

where:

VTEC	single layer VTEC, now represented by a GE-function,
x	independent variable; x is a function of local time,
Y	independent variable; y is a function of latitude,
Ξ	constant offset,
$\mathcal{G}$	amplitude,
a_i	x-coefficients,
b_j	y-coefficients,
c_q	mixed terms coefficients.

The constant offset Ξ, the amplitude $\mathcal{G}$ and the coefficients a_i, b_j, c_q are estimated as unknowns. The degree and order of GE-function development must always be an even one - therefore $2n$ and 2m in the above Equation (3.2). The number of mixed terms depends on the degree and order of develpoment. If k is the lower one of degree and order, the total number of mixed terms is given by $l = k \cdot (k-1)/2$. Local time and geomagnetic latitude are re-scaled into the x,y variables to get appropriate arguments for the GE-function. Unlike polynomials and spherical harmonics, GE-functions are not linear in their coefficients, i.e. initial values are required to establish linear observation equations. This problem can be overcome, when the GE-function is logarithmerized. Provided initial values for the constant offset Ξ and for the satellite/receiver differential delays are known, the observation equation (3. 1) can be setup in logarthmerized form, and a first iteration is made in logarithmic mode to get initial values for the amplitude $\mathcal{G}$ and the coefficients a_i, b_j, c_q. All successive iterations are then made in normal mode with linearized observation equations.

Ref. R6 presents the detailed description of the GE-function algorithm development from the first idea to the final formulae (i.e. detailed mathematics, partials, scaling of x,y, first iteration in logarithmic mode, etc.).

Global TEC data are fitted to GE-functions in 12-hour intervals. Degree of development, i.e. local time component, is $2n = 10$ and order, i.e. latitude component, is $2m = 6$. Including the constant offset, the amplitude and the mixed terms, a total of 33 GE-function parameters are estimated (plus unknown satellite/receiver differential delays). The satellite/receiver differential delay values are constrained to 0.5 nanoseconds with respect to the values obtained from the nighttime fit (see Section 3.4).

3.4 Differential Delay Estimation Procedure

For each day, i.e. in 24-hour intervals, satellite/receiver differential delay values are determined in a special fit into which only global nighttime TEC data enter. A degree $n = 4$ and order $m = 2$ spherical harmonic is used to model the nighttime VTEC. The coefficients a_{10}, a_{11} and b_{11}, which define the origin of the coordinate reference, are kept fixed with zero. No a priori constrains are applied to the satellite/receiver differential delay values, no elevation-dependent weights are applied to the TEC observable. The satellite/receiver differential delays obtained from this nighttime fit are then introduced as reference values into all the other fits for that a day and are constrained with 0.5 nanoseconds in these solutions (seethe above Sections 3.1 to 3.3).

4 COMPARISONS - RESULTS

Several Analysis Centers contributed ionospheric products for comparison over the GPSweeks 0823 to 0827: COD provided for these five weeks daily global VTEC maps in a 20.5 grid. DLR and UNB delivered for weeks 0823 to 0825 hourly regional VTEC maps for the european area in 1° grids and daily satellite/receiver differential delay values. ESOC provided for all five weeks global 12-hour VTEC maps in a 20.5 grid and 1° gridded local VTEC maps around the ESA ground sites Kiruna, Kourou, Madrid (instead of Villafranca), Maspalomas and Perth. ESOC's algorithms were described in the above Chapter 3. The mathematical approaches of COD, DLR and UNB can be found in (Schaer et al., 1995), (Engler et al., 1993), (Engler et al., 1995) and (Komjathy et al., 1996). Further methods of VTEC map computation are described in (Mannucci et al., 1993) and (Gao et al., 1994).

4.1 *VTEC Maps*

Five weeks of VTEC maps from four Analysis Centers are quite a lot amount of data to be compared and analyzed. To do this task efficiently, a certain scheme had to be worked out on how to make this intercomparison. The global VTEC maps of COD and ESOC were compared in 12-hour intervals. Comparison of - and with the regional VTEC maps of DLR and UNB and the local maps of ESOC was done in 6-hour intervals, i.e only the Oh, 6^h, 12h and 18^h maps of DLR and UNB were included into the comparison.

In the case that global 20.5 grid maps were compared with 1° grid regional and local maps, linear interpolation was used to calculate VTEC values from the global 20.5 grids in 1° intervals in the case of non-identical points.

Since the VTEC maps originating from the different Analysis Centers were referred to different reference epochs, rotations had to be made before the comparisons.

Concerning the local ESOC VTEC maps, only the results of the comparison with the Madrid maps were included in this paper.

In spite this comparison scheme reduced the number of possible combinations considerably, the remaining amount of VTEC map pairs to be compared was still too large to analyze all these comparisons by the inspection of plots. Additionally some statistics were appreciated. So a small program called **"vteccm"** was developed which performs a rapid comparison of two given VTEC maps and provides some general information on their agreement. To do this, **vteccm** calculates the differences between the two VTEC map files at all grid points. As already mentioned above, linear interpolation is used in non-identical grid points. Considering these differences as residuals, a residual VTEC map is obtained from which a mean offset between the two VTEC maps and a sigma with respect to this mean is calculated. In a next level the residual map is subdivided into 4 equally sized sub-parts, and for each part a sigma with respect to the overall mean is calculated. In the 3rd level the residual VTEC map is subdivided in 16 equally sized parts and the sigmas are computed, and so on. **vteccm** finally outputs:

. The minimum and the maximum residual obtained.

. The mean offset,

. The overall sigma at the **1st** level.

. 4 sigmas at the 2nd level.

16 sigmas at the 3rd level.

. . . . and so on.

The sigmas at the different levels are arranged in matrix form where their positions in the matrix correspond to the locations of their sub-parts in the residual VTEC map. So from analyzing the sigmas at the different levels one can directly see in which parts of the compared area the differences between the two VTEC maps are the largest. As an example Figure 4.1 presents a **vteccm** output. In the south-east the residuals are at largest.

AC1: aaa **AC2:** bbb

the area that was finally compared:

latmax = 70.0 **latmin** = 30.0

lonmin = -20.0 **lonmax** = 40.0

vtec1: min = 2.6 max = 11.5 (minimurn and maximum **value** of **1st VTEC** map)
vtec2: rnin = 2.1 max = 16.1 (minimum and maximum value of 2nd **VTEC** map)
rvtec: min = -4.6 max = 5.2 (minimurn and maximum value of the residual **VTEC** map)
xvtec: min = 2.6 max = 11.5 (minimum and maximum value of the interpolated VTEC map)

*** mean offset -0.26

sigmas at level 1

latitude/longitude range **considered** at level 1: **latmax** = 70.0 **latmin** = 30.0
lonmin = -20.0 **lonmax** = 40.0

0.145D+01

sigmas at level 2

latitude/longitude range considered at level 2 latmax = 70.0 latmin = 32.5
lonmin = -20.0 lonmax = 37.5

0.1 17D+01 0.513D+O0
0.111D+01 0.180D+01

sigmas at level 3

latitude/longitude range considered at level 3: latmax = 70.0 latmin = 32.5
lonmin = -20.0 lonmax = 37.5

0.106D+01 0.112D+01 0.651D+00 0.148D+00
0.126D+01 0.130D+01 0.554D+00 0.580D+O0
0.928D+00 0.810D+00 0.536D+O0 0.147D+01
0.185D+01 0.420D+00 O. 146D+01 0.298D+01

Figure 4.1: Example Output from the vteccm Program, all numbers are given in [TECU].

vteccm is invoked from a TCL for each VTEC map pair combination of one day, i.e. submission of this TCL once provided the vteccm comparison outputs of all VTEC map pair combinations for that day. The TCL was run for each day of the five weeks, and a quick look on maximum and minimum residuals, mean offset and 1st level sigma gave a fast overview. Only in critical cases - based on the vteccm output - closer consideration was done, i.e in cases of large offsets and/or sigmas. Also a general overview over the day-to-day agreement of certain VTEC map pair combinations was easily obtained.

Figures 4.2 a-k show the comparison results for all considered VTEC map pair combinations, based on the vteccm output. Each plot contains 3 curves: The upper curve shows (mean offset + σ), the middle curve shows (mean offset), and the lower curve shows (mean offset - σ), i.e. at days at which all three curves are close together the agreement between two VTEC maps with respect to the mean offset is good, and in cases of big distances between the curves the agreement is bad.

The following Sub-sections 4.1,1 to 4.1.7 summarize the results obtained for the different comparisons according to the defined scheme, together with some remarks.

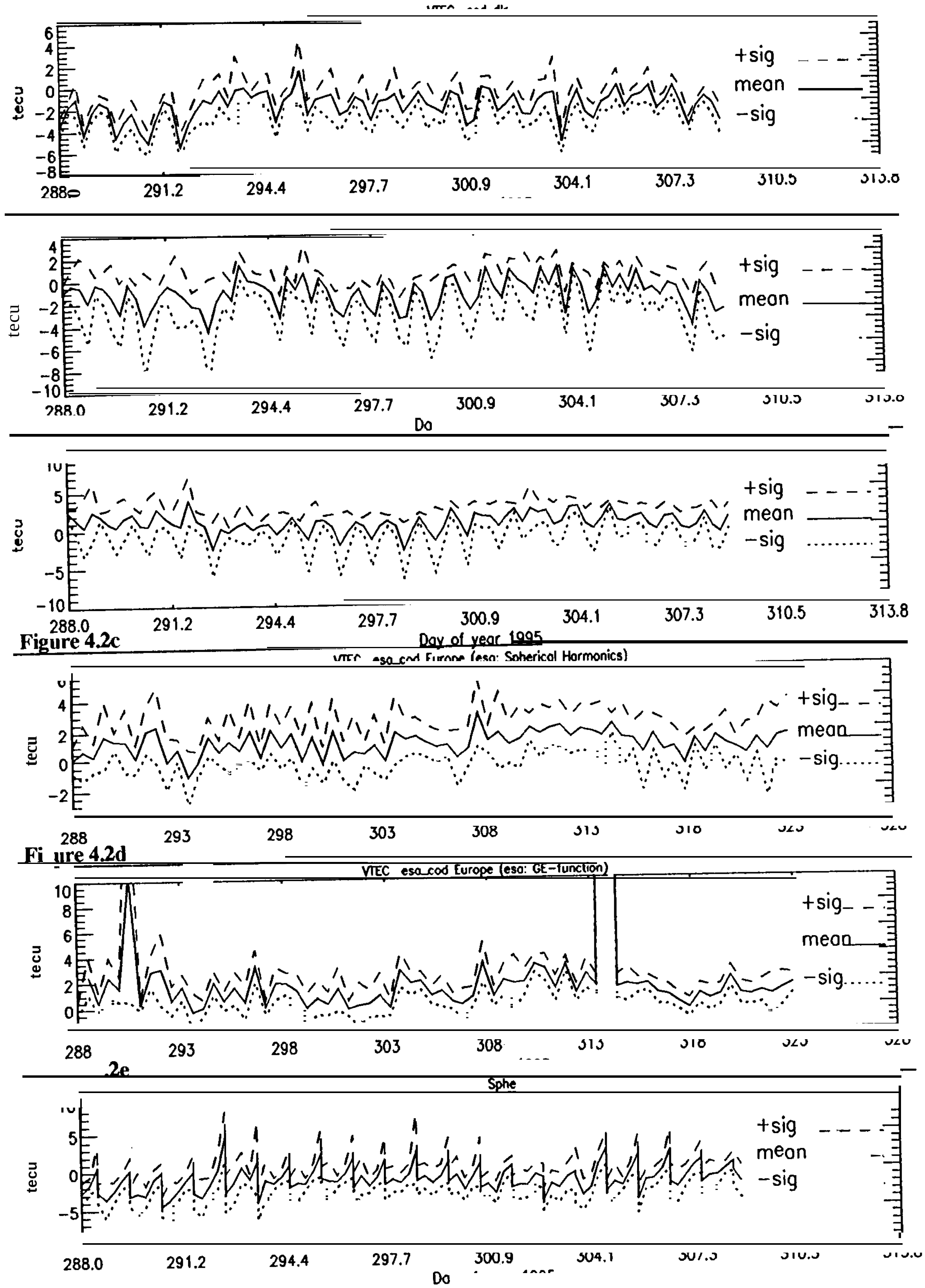

Figures 4.2 a-f: Results of VTEC Map Comparison.

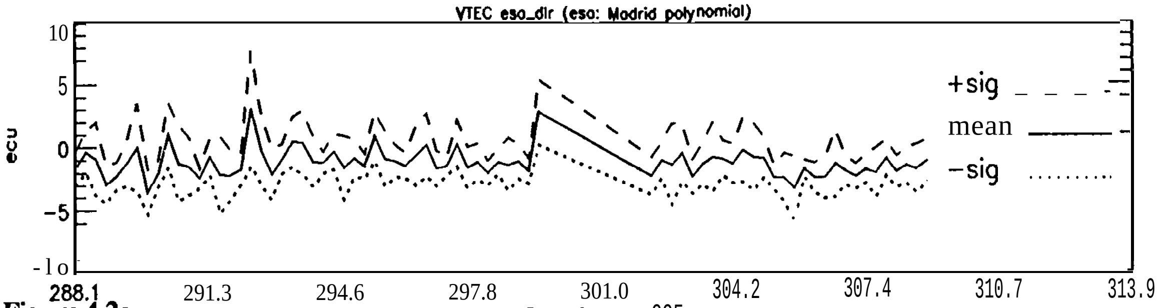

Figure 4.2g

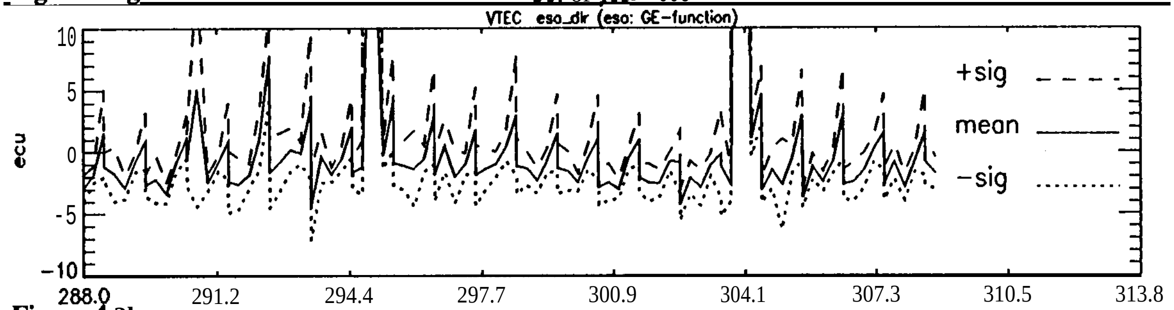

Figure 4.2h

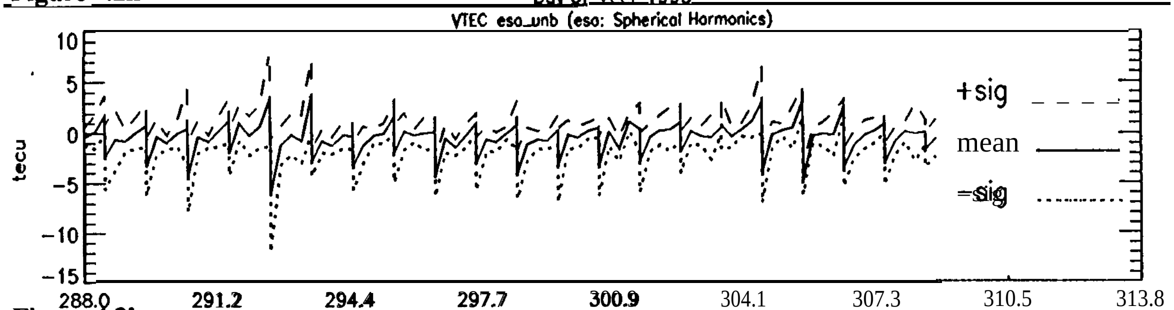

Figure 4.2i

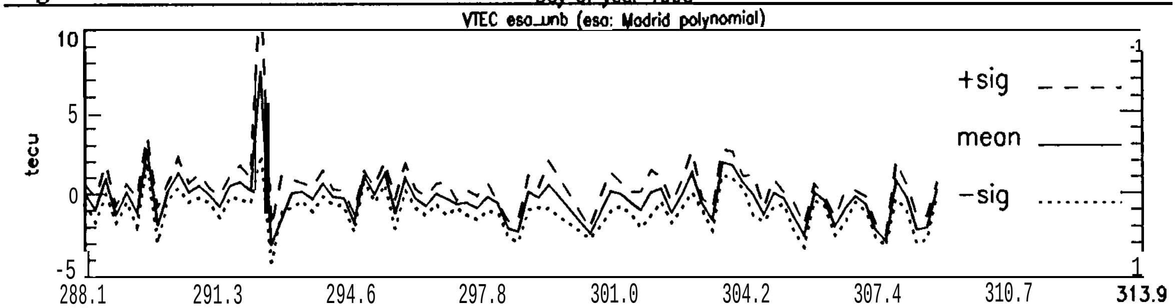

Figure 4.2j

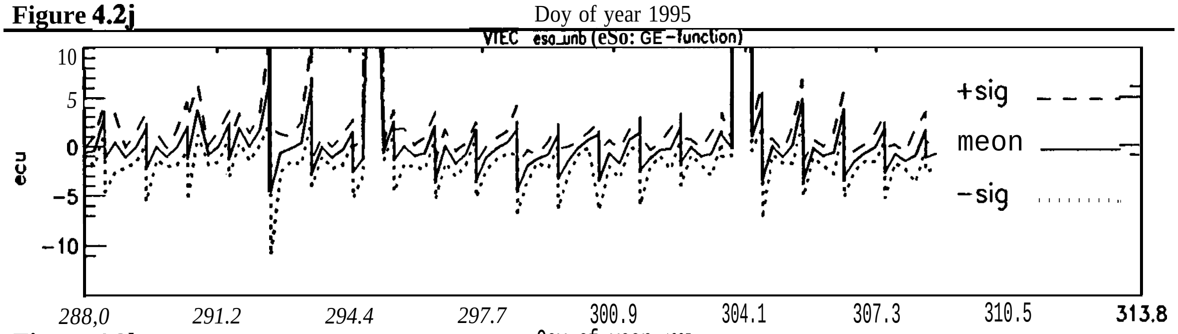

Figure 4.2k

Figures 4.2 g-k: Results of VTEC Map Comparison.

4.1.1 Comparison COD ⇔ DLR

An offset of 1-5 TECU, in the mean about 2 TECU, can be observed between the COD and the DLR VTEC maps. The offset is always negative. That means that the COD maps are systematically lying below the DLR maps. The sigmas with respect to the daily offsets vary between 1 to 1.5 TECU. A closer look to some days with larger offsets and sigmas showed that generally the agreement seems to be better in the middle of the compared area than at the borders. Figure 4.2a shows the variation of the mean offset and the sigmas over the weeks 0823-0825.

4.1.2 Comparison COD ⇔ UNB

Again an overall negative offset can be recognized, in the mean about -1.5 TECU, i.e. the COD VTEC maps are again lying systematically below the foreign maps -in this case the UNB ones. With respect to the daily mean offsets sigmas of 1-3 TECU can be seen. A closer look to some days with larger offsets and sigmas showed that generally the agreement seems to be best in the center and in the north-east corner of the compared area. Figure 4.2b shows the variation of the mean offset and the sigmas over the weeks 0823-0825.

4.1.3 Comparison DLR ⇔ UNB

No significant systematic offset can be observed between the DLR and the UNB VTEC maps. The daily offsets seem to vary around 1-3 TECU, and the sigmas are in the same order. A closer look to some days with larger offsets and sigmas showed that generally the agreement seems to be worst in the south-east corner of the compared area. Figure 4.2c shows the variation of the mean offset and the sigmas over the weeks 0823-0825.

4.1.4 Comparison ESOC ⇔ COD

Only the global ESOC spherical harmonic and GE-function models were compared with the COD VTEC maps.

Comparison with ESOC spherical harmonics: Comparison was done globally and restriced to the european area. Since especially on the southern hemisphere there are large gaps in station coverage (ESOC uses only Rogue stations in its processing), the spherical harmonics are bad determined in these zones. This leads to abnormal spherical harmonic behaviour in these areas, which can be seen in the VTEC plots in form of high hills and holes of same depth directly near the hills. As the global comparison with COD showed, the mean offsets between ESOC and COD VTEC maps are quite small - but the sigmas are large, up to 10 TEC, and up to 80 TECU in areas were no observation data had entered into the ESOC processing.

So only the comparison results over the region of Europe are presented here. In the european area an overall offset of about 1 TECU can be recognized between ESOC and COD VTEC maps. This offset is always positive, but since COD were now subtracted from the other Analysis Center's maps - in this case ESOC, this means that COD lies again below the foreign model. With respect to this overall offset daily offsets and sigmas seem to vary around 1-2 TECU each. A closer look to some days with larger offsets and sigmas showed that there seems to be a trend that in the north-west corner of the compared area the agreement is worst. Figure 4.2d shows the variation of the mean offset and the sigmas over the weeks 0823-0827.

Comparison with GE-functions: Concering station coverage, the GE-functions are affected similarly as the spherical harmonics, i.e. in areas with good station coverage the GE-functions are good too. Additionally GE-functions seem to be more vulnerable to bad receiver data. The Maspalomas station data, which was known to be problematic at that time, caused for instance every day an abnormal GE-function peak at high northern latitudes. Also the data of Kourou and the Seychelles was problematic. Further tests made as consequence of the comparison results have shown that, after these stations were excluded from GE-function processing, the high-latitude anomaly had disappeared or was at least drastically reduced. Also variations in the degree and order of GE-function development (e.g. $2n = 8$, $2m = 4$; $2n = 10$, $2m = 4$; $2n = 10$, $2m = 8$) caused the anomaly to disappear. Further tests will be necessary to find out an optimal way of GE-function processing.

Because of the problems pointed out above, only the comparison results of the GE-function maps with the COD models over the region of Europe are presented here. As with the spherical harmonics, an overall offset of about 1 TECU can be recognized. Again this overall offset is positive, which means that the COD maps seem to lie below the GE-function models. With respect to this overall offset, daily offset variations of 1-2 TECU can be seen and sigmas around 1 TECU. On doy 290 and 313 large outliers are present. These outliers were caused by the above mentioned problematic stations. Apart from these outliers the GE-functions seem to be a little bit closer to the COD models as the ESOC spherical harmonics. A closer look to some days with larger offsets and sigmas seem to indicate that the agreement is a little bit worse in the southern and sometimes in the western part of the compared area. Figure 4.2e shows the variation of the mean offset and the sigmas over the weeks 0823-0827,

4.1.5 Comparison ESOC $\Leftrightarrow$ DLR

Comparison with ESOC spherical harmonics: Because the ESOC spherical harmonics are well feeded with observation data in the european area (see above Section 4. 1.4), the agreement with the DLR VTEC models is quite good. An overall mean offset of about -1 to -2 TECU seems to be present, which means that the ESOC models lie systematically below the DLR models. Around that overall offset variations and sigmas of about 3 TECU can be seen, Since the 12h DLR models were compared with the 6^h and the 18h ESOC spherical harmonic models (both rotated to 12h), peaks appear every day at 12h. A closer look to some days with larger offsets and sigmas showed that the worst agreement seems to be at the southern border of the compared area. Figure 4.2f shows the variation of the mean offset and the sigmas over the weeks 0823-0825.

comparison with ESOC local polynomials for Madrid: Also the Madrid local polynomial models seem to show an overall offset of about 1 TECU below the DLR maps and around that overall offset variations and sigmas about 1-3 TECU. Around doy 300 there was a data gap. A closer look to some days with larger offsets and sigmas showed that the worst agreement seems to be in the north-west and sometimes in the south-east corner of the compared area. Figure 4.2g shows the variation of the mean offset and the sigmas over the weeks 0823-0825.

Comparison with GE-functions: As was pointed out in the above Section 4.1.4, the GE-functions had problems in the high northern latitudes. However, the european area, in which the GE-functions were compared with the DLR VTEC maps, is far enough in the south, so that the agreement was in most cases good. Only on some days, especially on cloys 295 and 304, the high latitude anomaly propagated so far southward, that it was felt in the comparison. Except from these outliers, mean offsets up to 3 TECU are present without an overall offset. The sigmas around the mean offsets range between 1-3 TECU. Again the 12h DLR maps were compared with the 6^h and the 18h ESOC models (both rotated to 12^h). A closer look to some days with larger offsets and sigmas showed the worst agreement in the north (for the reasons stated above) and sometimes in the south-east. Figure 4.2h shows the variation of the mean offset and the sigmas over the weeks 0823-0825.

4.1.6 Comparison ESOC ⇔ UNB

Comparison with ESOC spherical harmonics: As with the DLR models, the agreement with UNB over the european area is good. An overall offset of -1 TECU seems to be present, i.e. the ESOC maps are lying below the UNB maps. Around that overall offset the daily mean offsets and sigmas seem to vary about 2 TECU. From doy 294 on the variations become smaller but increase again at doy 304. Since the 12^h UNB models were compared with the 6^h and the 18^h ESOC spherical harmonic models (both rotated to 12h), peaks appear every day at 12h. A closer look to some days with larger offsets and sigmas showed the worst agreement to be in the north-west and in the south-east corner of the compared area. Figure 4. 2i shows the variation of the mean offset and the sigmas over the weeks 0823-0825.

Comparison with ESOC local polynomials for Madrid: Madrid local polynomial models and UNB VTEC maps show very close agreement of O-1 TECU in the daily mean offsets as well as in the sigmas. Only on doy 292 there is a significant outlier; on this day a large geomagnetic field disturbance occured. A closer look to some days with larger offsets and sigmas showed the worst agreement to be in the north-west and in the south-east corner of the compared area. This north-west/ south-east effect was also present in the 9-hour comparison for doy 292, together with a whole sigma level higher as usual. Figure 4.2j shows the variation of the mean offset and the sigmas over the weeks 0823-0825.

comparison with GE-functions: Generally the agreement between GE-functions and UNB VTEC maps is about 1-3 TECU in the mean offsets and sigmas of 1 TECU around these offsets. Because of the problems stated in the above Section 4.1.4, the GE-functions showed sometimes abnormal behaviour in the high northern latitudes. Here this can be seen in form of outliers, especially on cloys 295 and 304. Again the 12^h UNB maps were compared with the 6^h and the 18^h ESOC models (both rotated to 12h). A closer look to some days with larger offsets and sigmas showed, that, apart from casual discrepancies in the north, worst agreement was found in the south-east part of the compared area. Figure 4.2k shows the variation of the mean offset and the sigmas over the weeks 0823-0825.

4.1.7 Comparison of ESOC Local with Global Models

As a representative of the five ESA ground sites for which local polynomial models were fitted to at ESOC, only the results for Madrid were presented in the previous sections. To the agreement of the polynomial maps for Kiruna, Kourou, Maspalomas and Perth with the ESOC spherical harmonic and GE-function models some short remarks only:

- Generally good agreement was observed with the Kiruna, Madrid and Perth polynomials: O-3 TECU mean offsets (1-6 TECU offsets at Perth with the spherical harmonics) and sigmas of 1-3 TECU with respect to these offsets.
- In the case of Kourou and Maspalomas the agreement was significantly worse. Especially from Maspalomas it is well known, that there were considerable receiver problems at the time for which the intercomparison was done. In particular during the week 0826 the Maspalomas data was bad, and in week 0827 Maspalomas provided tracking data only for one and a half day. Quite often unrealistic polynomials were obtained for both stations, Kourou and Maspalomas.
- Generally the GE-functions seem to be closer to the polynomial models than the spherical harmonics.

4.2 *Differential Delays*

Comparison of differential delays was done between results provided by DLR, UNB and ESOC. The UNB differential delay files contain differential delay values for all satellites and 6 ground stations. DLR provided values for all satellites, except PRN 12 and PRN28, and for 16 ground stations. And ESOC determined values for all satellites and 64 ground stations.

The day-to-day variation in the values of all 3 series is in most cases within the 0.5 nanosecond limit. Especially the DLR and ESOC differential delay series seem to indicate a generally higher day-to-day scatter for the stations than for the satellites. Typical examples are Arequipa and Fortaleza. - There are of course also a lot of stations which show the same lower order of scatter as the satellites. The ESOC differential delay files show additionally a clear increase of sigmas of the mean values by a factor 2-3 for GPSweeks 0824-0827 with respect to week 0823. This can especially be seen at the satellites.

A comparison between the three series seem to indicate an offset of the DLR series of about 1 nanosecond with respect to the ESOC series, and the UNB series seems to be close to the ESOC results. This was also confirmed by A. Komjathy (private communication). ESOC uses 350 km as ionospheric shell height while DLR and UNB are using 400 km. So ESOC repeated the differential delay estimation for week 0823 also with 400 km shell height. However, no variances of more than 0.2 nanoseconds with respect to the 350 km solution for that week could be observed. A. Komjathy and R.B. Langley (1996) made similar calculations with the same result. Obviously the difference in shell height cannot explain this 1 nanosecond offset. The reason for this offset might come from differences in the algorithms used and/or from the different sets of ground stations used. Additionally DLR rejects the satellites PRN 12 and PRN28 in its solution. Figure 4.3 compares the DLR, UNB and ESOC series exemplarily for 2 stations and 4 satellites.

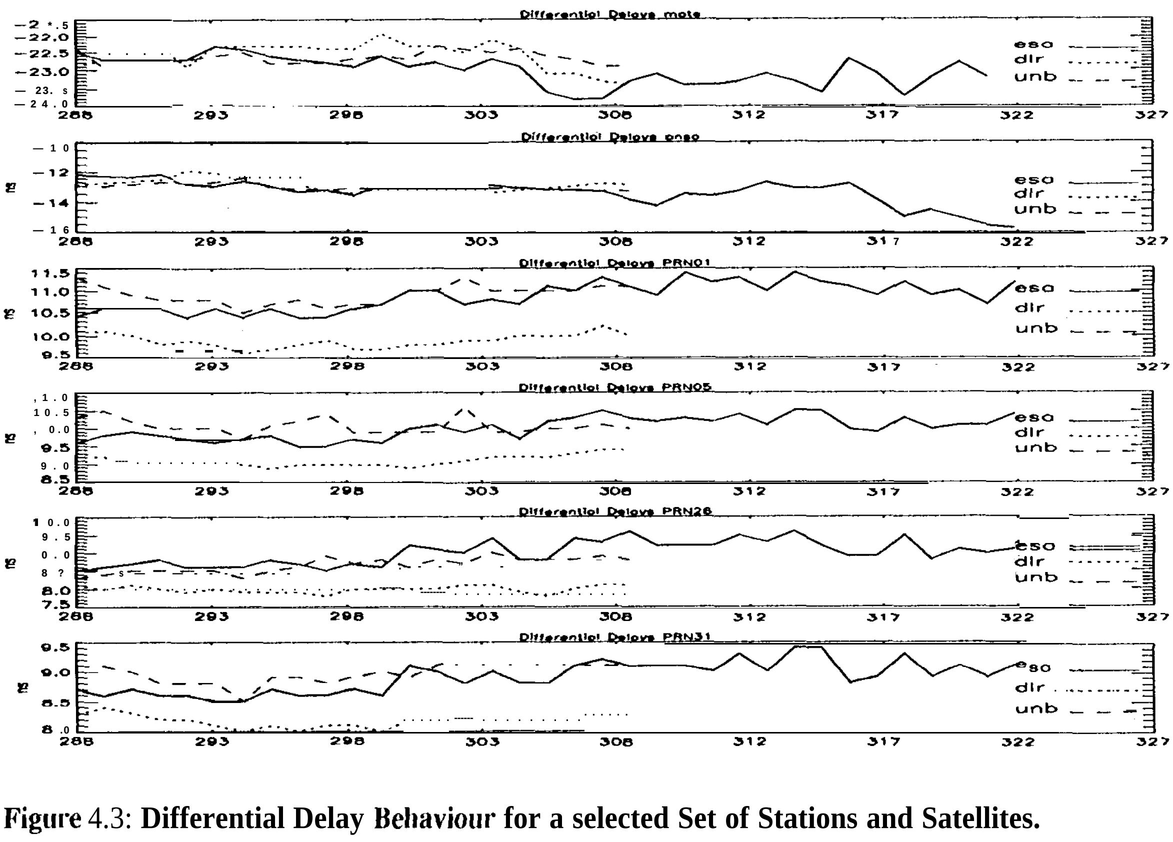

Figure 4.3: Differential Delay Behaviour for a selected Set of Stations and Satellites.

5 CONCLUSIONS

With regard to include ionosphere data into the IGS product list, an intercomparison of ionosphere products provided by different Analysis Centers was organized in preparation of the IGS workshop in Silver Spring in March 1996. Four Analysis Centers contributed to this comparison with own results.

In areas with tracking data of sufficient density the different VTEC models seem to show a general agreement of 5 TECU and better, normally about 3 TECU. For the differential delay values agreement within 1 nanosecond was achieved. In summary the intercomparison results look encouraging to do further steps into the direction of a routine provision of ionosphere maps as new part of IGS.

ESOC used the comparison as opportunity to verify its own mathematical modeling. The following weak points were identified from the analysis of the intercomparison results:

- The ground station net used by ESOC must be densified around the equator and at the southern hemisphere - gaps in station coverage have caused abnormal behaviour of global fits in weakly observed areas.

- Bad receiver data must be identified in a preprocessing step, since it had seriously affected the solutions.

- More testing is necessary to overcome the above mentioned problems and to achieve robust modeling.

Based on the knowledge earned from the intercomparison, the next steps into the direction of IGS must be undertaken now - relevant aspects are pointed out in ref. R4.

Beyond its IGS activities ESOC is also interested to use GPS-derived ionosphere maps to correct ERS-2 and other ESA satellite data.

Acknowledgments

The authors wish to express their acknowledgments to the Analysis Centers for their readyness to contribute to the intercomparison with own results and fruitful discussions. Thanks also to A. Komjathy and R.B. Langley for setting up the GPS-IONO mailing list at the University of New Brunswick which was very helpful for fast exchange of information and discussion.

6 REFERENCES

R 1. Biel, H.A. von (1990): ‘The geomagnetic time and position of a terrestrial station.’ Journal of Atmospheric and Terrestrial Physics, Vol. 52, No. 9, pages 687-694, 1990.

R2. Engler, E., N. Jakowski, A. Jungstand and D. Klähn (1993): ‘First experiences in TEC monitoring and modelling at the DLR Remote Sensing Station Neustrelitz.’ Proceedings of the

GPS/Ionosphere Workshop Modelling the Ionosphere for GPS Applications, DLR/DFD, Fernerkundungsstation Neustrelitz, Germany, September 29-30, 1993, pages 122-125.

R3. Engler, E., E. Sardón and and D. Klähn (1995): 'Real Time Estimation of Ionospheric Delays'. Proceedings of the ION GPS-95, 8th International Technical Meeting of The Satellite Divison of The Institute of Navigation, Palm Springs, California, U. S.A., September 12-15, 1995.

R4. Feltens, J. (1996): 'Ionosphere Models - A New Product of IGS ?', IGS Position Paper, Proceedings of the IGS Analysis Center Workshop, Silver Spring, MD, U. S.A., March 19-21, 1996.

R5. Feltens, J. (1995a): 'GPS TDAF Ionosphere Monitoring Facility, Mathematical Model Developments'. GTDAF-TN-08 1ss 1/- 11 Sep-95 (ES OC-internal document).

R6. Feltens, J. (1995 b): 'GPS TDAF Ionosphere Monitoring Facility, Examination of the Applicability of Gauss-Type Exponential Functions to Ionospheric Modeling'.GTDAF-TN-091ss l/- 11 Sep-95 (ESOC-internal document).

R7. Gao, Y., P. Heroux and J. Kouba (1994): 'Estimation of GPS Receiver and Satellite L1/L2 Signal Delay Biases Using Data from CACS'. Proceedings of the International S ymposium on Kinematic Systems in Geodesy (KIS94), Geomatics and Navigation, Banff, Canada, August 30- September 2, 1994, pages 109-117.

R8. Komjathy, A. and R.B. Langley (1996): 'An Assessment of Predicted and Measured Ionospheric Total Electron Content Using a Regional GPS Network'. Proceedings of the ION GPS-96, 9th International Technical Meeting of The Satellite Divison of The Institute of Navigation, Santa Monica, California, U. S. A., January 22-24, 1996.

R9. Mannucci, A.J., B.D. Wilson and C.D. Edwards (1993): 'A New Method for Monitoring the Earth's Ionospheric Total Electron Content Using the GPS Global Network'. Proceedings of the ION GPS-93, 6th International Technical Meeting of The Satellite Divison of The Institute of Navigation, Salt Lake City, Utah, U. S. A., September 22-24, 1993, Vol. II, pages 1323-1332.

R 10. Newby, S.P. (1992): 'An Assessment of Empirical Models for the Prediction of the Transionospheric Propagation Delay of Radio Signals'. University of New Brunswick, Dept. of Surveying and Engineering, Canada, Technical Report No. 160, August 1992.

R11. Schaer, S., G, Beutler, L. Mervart, M. Rothacher and U. Wild (1995): 'Global and Regional Ionosphere Models Using the GPS Double Difference Phase Observable'. Paper presented at the 1995 IGS Workshop, Potsdam, Germany, May 15-17, 1995.

Comparison of GPS/IGS-derived TEC data with parameters measured by independent ionospheric probing techniques

N. Jakowski and E. Sard6n
DLR e.V., Fernerkundungsstation Neustrelitz,
Kalkhorstweg 53, Germany

Abstract
In order to evaluate TEC-data products derived from numerous GPS/IGS stations, comparisons are made with ionospheric parameters deduced from independent ionospheric measurements. The study includes data obtained from bottomside and topside vertical ionospheric sounding, NNSS radio beacon measurements and incoherent scatter radar probing (EISCAT). The results indicate general physical agreement between the GPS/IGS derived TEC data and the other ionospheric parameters. Furthermore a comparison is made between the GPS-based TEC obtained by different groups using different estimation techniques for the location of the ionosonde station Juliusruh (54.6°N; 13.3°E) during a selected time interval in October, 1995. For the same period, a reference is made to the ionospheric electron content up to 1000 km height deduced from the updated IRI90 model.

1. Introduction

The GPS receiving technique provides a unique possibility to monitor the ionospheric electron content on regional and global scales (Coco, 1991; Wilson et al., 1995, Zarraoa and Sard6n, 1996). The derived total electron content (TEC) is an important parameter which , on one hand, characterizes the first order ionospheric propagation error in space-based radio navigations ystems and, on the other hand, provides valuable information about the behaviour of the ionosphere/plasmasphere systems.

Since TEC estimations based on dual frequency GPS data require an accurate in-flight-calibration of the differential instrumental delays of the satellites and receivers, the derived TEC data are as accurate as these calibrations have been made. Although different algorithms were developed by different groups to derive the instrumental biases and/or TEC, all these methods utilize simplifying assumptions about the ionospheric behaviour. The accuracy of the corresponding algorithms can be checked by controlling the internal consistency of the derived data products (internal check) and by comparing the data products with equivalent data obtained by independent ionospheric measurements (external check). So independent ionospheric probing techniques such as vertical sounding, incoherent scatter radar, radio beacon measurements provided by satellite systems such as NNSS, PRARE or DORIS or two frequency satellite altimeters can be used to validate the derived TEC data and/or to get a comprehensive insight into ionospheric processes (Jakowski, 1995).

In the following section TEC mapping results obtained in DLR Neustrelitz by using the European IGS network of GPS receivers (e.g. Zumberge et al., 1994) are compared with simultaneously measured ionospheric parameters derived from non-GPS techniques. The used algorithms to derive TEC-maps from GPS measurements are described elsewhere (Sardón et. al., 1994, Jakowski and Jungstand, 1994). In particular the analysis includes also comparative studies of TEC mapping made at different centres such as CODE, ESOC, University of New Brunswick and DLR Neustrelitz for October 1995. The GPS-based TEC derived by these groups is also compared with the IRI90 model updated by ionosonde data.

2. Comparison with ionospheric data obtained by independent measurements

2.1 Vertical sounding

Vertical sounding stations provide valuable information about the peak electron density NmF2 and the height hmF2 of the F2 layer. Combining the peak electron density $NmF2 = 0.0124 \cdot (foF2)^2$ with the derived vertical TEC, the equivalent slab thickness τ of the electron density profile can be derived by applying $\tau = TEC / NmF2$.
The equivalent slab thickness τ is a measure of the width of the electron density profile and ranges in most cases between 200 and 500 km. Due to the enhanced night-time loss of plasma in the bottomside ionosphere, the higher τ values occur generally during night-times. Although foF2 and TEC have different physical meanings, the diurnal variation of both parameters should be well correlated.
This is shown in Fig. 1 where hourly foF2 data measured by the vertical sounding station Juliusruh (54.6° N; 13.3° E) are plotted against the diurnal behaviour of the corresponding vertical TEC data derived from the regional TEC map.
The diurnal variations of both these parameters are closely correlated thus indicating a reliable TEC estimation algorithm in general. The absolute level of TEC can be checked by computing the equivalent slab thickness values τ.

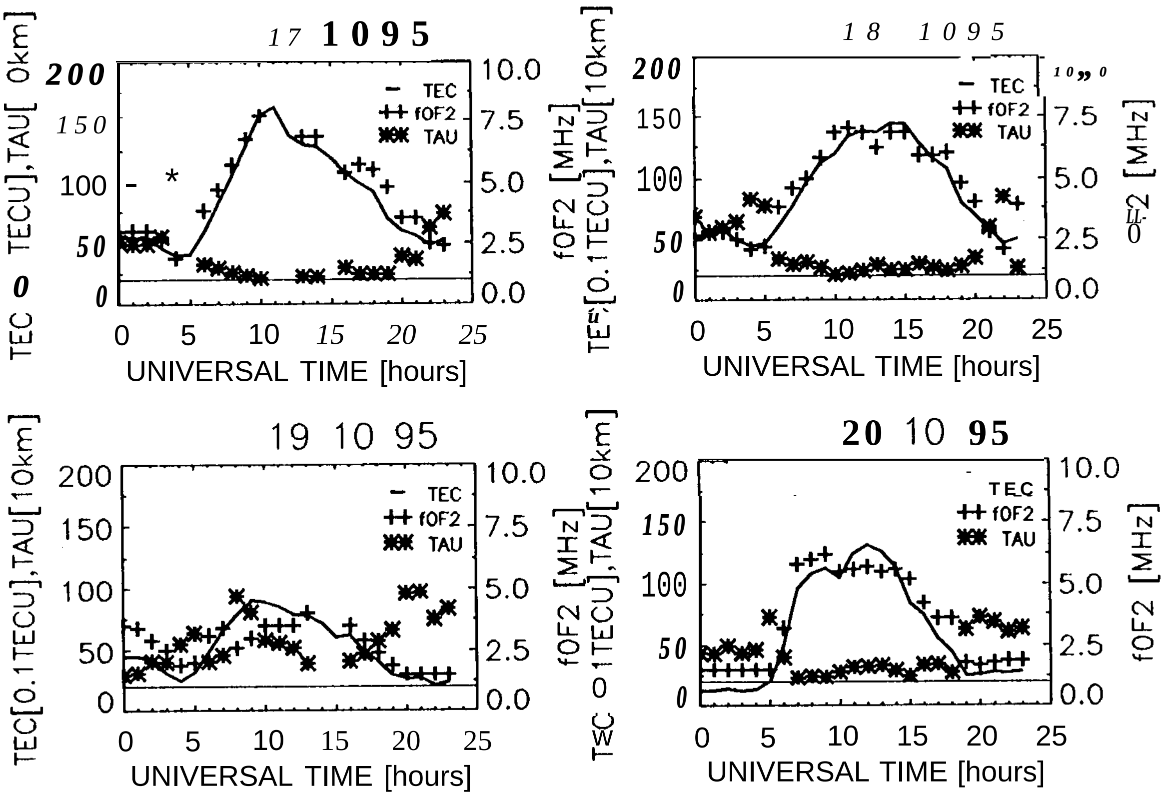

Figure 1
Comparison of GPS derived TEC data with foF2 data measured by the ionosonde station Juliusruh for some days in October 1995. The 200 km slab thickness level is marked by a thin line.

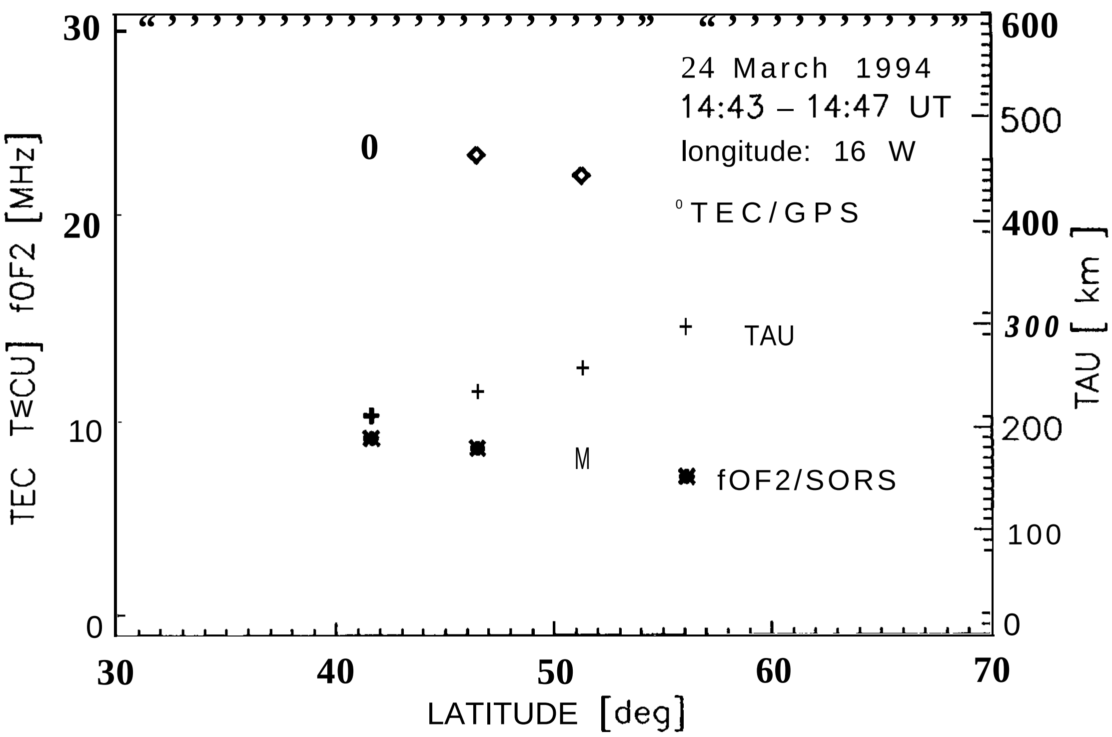

Figure 2
Comparison ofGPS derived TEC data with foF2 measured by topside vertical sounding. The F2 layer critical frequency foF2 was measured onboard the Russian CORONAS satellite by the SORS topside sounder during a satellite pass on March 24, 1994 over Europe.

The results indicate an absolute TEC level accuracy in the order of <3 TECU. Reducing the night-time TEC values by 3 TECU the resulting slab thickness τ is still acceptable. A further lowering of TEC values would provide, however, physically unreasonable low τ values at night.

It should be underlined that especially topside sounder measurements onboard low orbiting satellites can provide valuable information about the peak electron density along the satellite trace. Such an example is given in Fig. 2 where foF2 data measured onboard the Russian CORONAS satellite are compared with the corresponding TEC values of the map along the satellite trace. Again the derived equivalent slab thickness values behave quite “normal” during the satellite pass.

The measured foF2 and hmF2 data can also be used to update ionospheric models such as the International Reference Ionosphere (IRI). A subsequent integration of the vertical electron density profile up to 1000 km height provides the Ionospheric Electron Content IEC or N_I which differs from the total electron content N_T up to GPS heights by the plasmaspheric contribution Np according to $N_T = N_I + N_p$.

Due to permanent changing geometric relationships between satellite-receiver links, in particular with respect to the geomagnetic field lines, the plasmaspheric contribution will change from satellite to satellite. But nevertheless, an average plasmaspheric electron content in the order of 1...3 TECU should be taken into account over the whole day even under low solar activity conditions (e.g. Soicher, 1976). Fig. 3 illustrates a comparison of TEC data derived from GPS/IGS measurements for the ionosphere over Juliusruh with the diurnal variation of the IEC derived from IRI90 electron density profiles updated by the ionosonde (IS) data. By the way, it is clearly shown that the non-updated IRI90 model underestimates the observations by more than 50% thus indicating that also well qualified models such as IRI90 fail in describing TEC under geomagnetically disturbed conditions. The correlation between GPS derived TEC data (GPS/IGS) and the IEC data (IS) is quite good. The remaining difference in the order of 1...3 TECU during the night-time could be explained by the plasmaspheric contribution Np. However, since IRI90 represents only an average behaviour and the internal measuring accuracy of TEC estimations is in the same order as the plasmaspheric content, one should be careful in deriving conclusions about the plasmaspheric content based on such comparisons. A more detailed discussion of this subject is given in section 3.

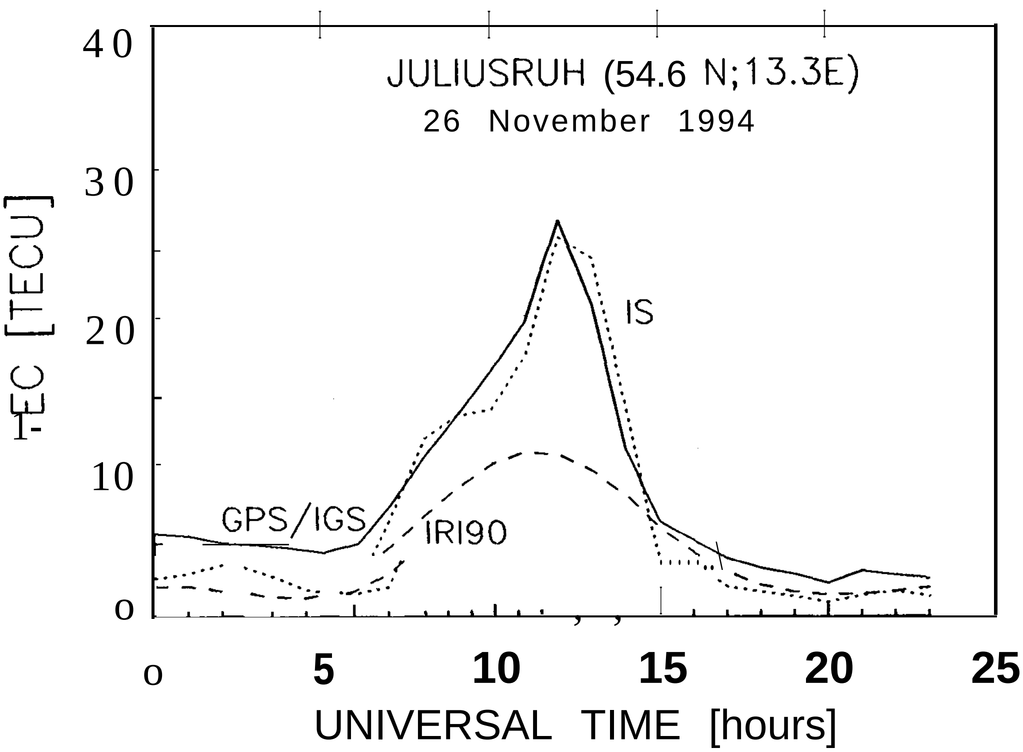

Figure 3
Comparison of GPS derived TEC data (GPS/IGS) with the height integrated electron density profiles computed from the IRI90 model based on CCIR tables (IRI90) and measured vertical sounding data (IS).

2.2 NNSS data

The Navy Navigational Satellite System (NNSS) transmits a pair of coherent carrier frequencies on 150/400 MHz. Such sensitive differential Doppler measurements can provide meridional TEC profiles with a high spatial resolution up to about 10 km. Comparing NNSS with GPS derived TEC data, conclusions about the spatial resolution of the produced TEC maps can be derived. Because the absolute calibration of NNSS data would produce new problems to discuss, we confine our attention only to the relative TEC variations when comparing the corresponding TEC data. As Fig. 4 demonstrates, the occurrence of Traveling Ionospheric Disturbances (TID 's) with wavelengths in the order of a few hundred kilometers is well documented in the NNSS data. Due to a number of different reasons such small effects are

commonly not reproduced in the GPS derived TEC data. Considering only the corresponding GPS carrier phase data, TID´s should also be observable along the GPS trace, but the interference of the ray path movement through the ionosphere with TID propagation makes their analysis difficult.
It should be underlined that on the other hand large scale phenomena such as the mid-latitude electron density trough are well documented. Although the spatial resolution of NNSS measurements cannot be reached by GPS data, the trough phenomena is well pronounced in the produced maps especially in conjunction with ionospheric storms (e.g. Jakowski, 1995).

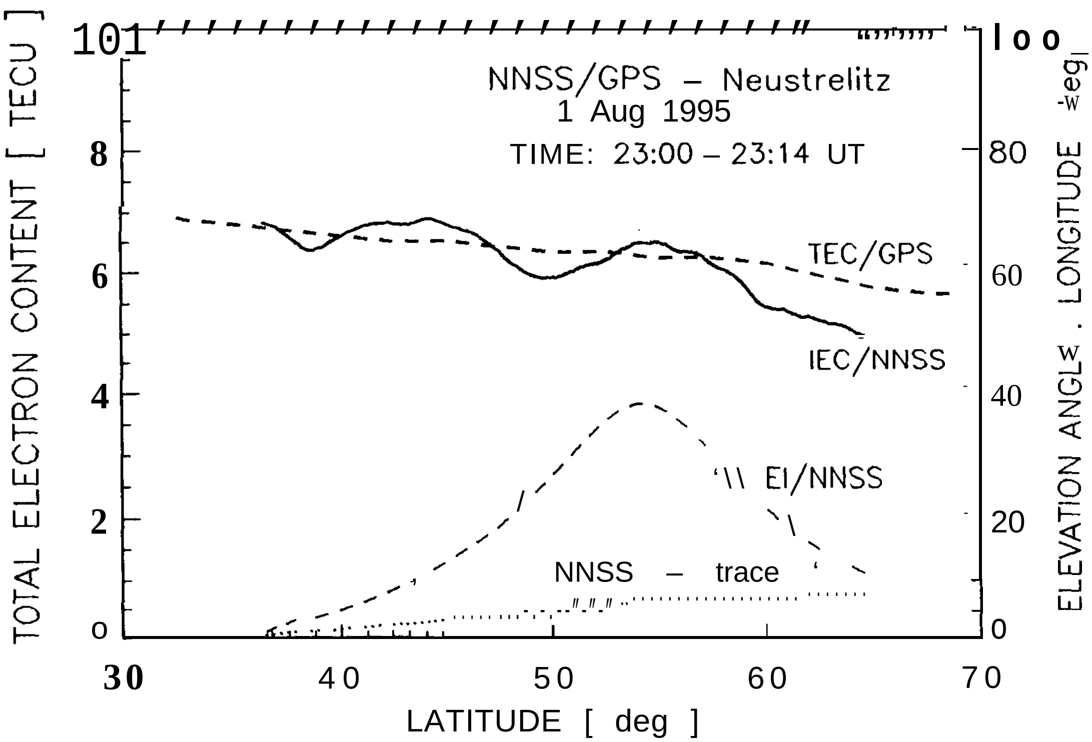

Figure 4
Illustration of a TID observed by NNSS differential Doppler measurements on August 1.1995.
The corresponding GPS derived TEC data smooth over-tie TID variation.

2.3 EISCAT data

Incoherent scatter radar measurements provide a number of different ionospheric parameters for complex studies of the ionosphere, So the Common Programme Three (CP-3) of the European Incoherent SCATter facility (EISCAT) in Tromsø measures the electron density along different lines between 62°N and 78°N during 30 min north-south scans. Due to the overlapping region with our routine TEC map a comparison with height integrated CP-3 electron density profiles in the height range 150-500 km is possible. The results obtained on February 4, 1995 are documented in Fig. 5. The difference between EISCAT and GPS derived electron content data should be related to the topside ionosphere/plasmasphere contribution.
Since the plasmaspheric content and its behaviour is not well known, such studies could improve our knowledge about plasmasphere-ionosphere relationships especially in high latitudes.

The GPS/IGS based TEC data are deduced from subsequent TEC maps available every 10 minutes in such a way that the angular distance between EISCAT and GPS measuring points is less than 5 degrees. To have more reliable data, several subsequent EISCAT scans were used during the given time interval resulting in more than one electron content value at the fixed latitude points. It is interesting to note that the difference between EISCAT and GPS/IGS derived electron content data decreases significantly with increasing latitude. This could be due to a reduced contribution of the plasmaspheric content expected at high latitudes. It can be seen that a further reduction of the GPS/IGS derived TEC data by more than 1 TECU would lead to unreasonable low values for the topside and plasmaspheric contribution.

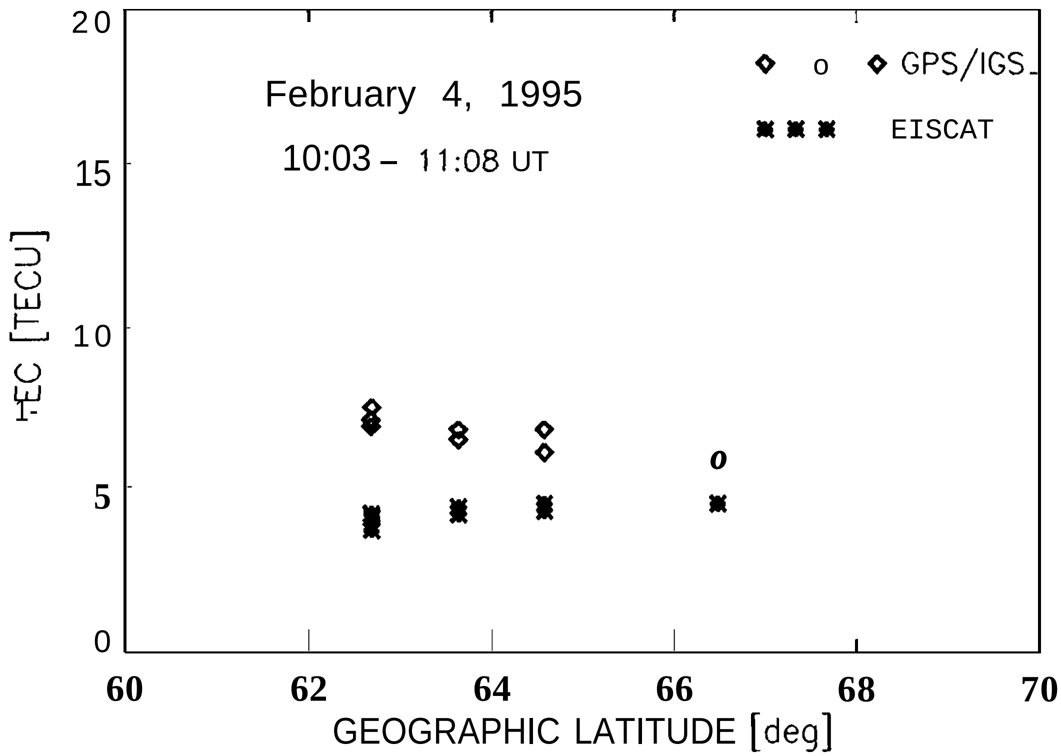

Figure 5
Comparison of electron content data derived from GPS and EISCAT CT-3 measurements on February 4.1995. The EISCAT IEC data correspond with the integral of the vertical electron density profile in the altitude range of about 150...500 km height.

3 Comparison of vertical TEC data derived by different GPS-based methods and the IRI90 model

In order to compare GPS/IGS TEC data products generated by several groups in a more effective way, a common reference is made to the IEC data derived from height integrated IRI90 electron density profiles up to 1000 km height. To give more realistic results the IRI90 model is updated by hourly ionosonde measurements at Juliusruh as described in section 2.1. Therefore the TEC data products are referred to this location.
As GPS-derived TEC values we use the grid maps estimated by the CODE IGS analysis center (cod), ESOC (esa), the University of New Brunswick (unb) and DLR-Neustrelitz (dir). The CODE and ESOC groups have computed global TEC maps once per day (at 12 UT) and twice per day (at 6UT and 18UT), respectively, whereas the other two groups provide hourly maps

for the European region. From these maps we have computed the vertical TEC over Juliusruh every hour using the data from the four grid points surrounding the zenith of the ionosonde station as the base for a spatial linear interpolation scheme. To construct hourly TEC values from the daily map of CODE the close longitude-time relationship was used. The ESOC data were processed in the same way, but taking into account a weighted mean of both maps at different hours.

In Fig.6 the different vertical TEC data over Juliusruh are presented for 12 days. For days 19 and 26 of October there were no ionosonde data available, for the other days also some hourly data were rejected. We have also computed the hourly differences between each GPS-based method and the values given by IRI. Fig. 7 presents the average of these differences through the 15th to the31st of October and Fig.8 shows the corresponding RMS deviations.

As it can be seen in most of the figures, the DLR-TEC values are, in general, larger than the other GPS-based values, but closer to the IRI-values during day-time. The night-time DLR-TEC values are most of the times about 2-3 TECU larger than the rest. On the other hand, the CODE-TEC values are almost always smaller than the rest, both during day and night. For the ES OC-TEC values a discrepancy between consecutive days can be seen, so the last value of the day is about 2 TECU larger than the first one of the next day. From the 15th of October to the 4th of November, the daytime values of DLR and UNB agree very well for 12 days, but for the rest there are maximum differences of 2-4 TECU.

In principle we expect the IRI-IEC values to be smaller than the GPS-derived TEC data, due to the missing plasmaspheric contribution. As already discussed in section 2.1, the difference between corresponding IEC and TEC data is the plasmaspheric content Np which should be in the order of 1...3 TECU. Due to the higher absolute variability of TEC data at day-time only the night-time data should be considered when discussing the plasmaspheric content.

Fig. 7 indicates a rather stable difference between IEC and TEC-DLR during the night-time. This would agree with the rather stable plasmaspheric electron content. The other stations provide differences which are too low to be interpreted as the plasmaspheric content when taking the IRI90 model as a reference.

4. Summary and Conclusions

The validation of GPS derived TEC maps by independent ionospheric measurements is still an important task to have more knowledge about the absolute and relative accuracy of TEC data products. A variety of ionospheric probing techniques may be used for such comparative studies. In each case additional assumptions have to be made in order to make the different parameters comparable. Since the validation of TEC data by other ionospheric techniques is somewhat complicated, different measuring techniques should be used. The results obtained in this study indicate general physical agreement between the GPS/IGS derived TEC data products at DLR and other ionospheric parameters. Attention should be paid to such comparative studies which provide physically unusual conclusions. This gives the possibility to adjust derived TEC data and/or to get more knowledge about the validity of assumptions or models related to the ionospheric/plasmaspheric behaviour. In the same sense the intercomparison of the results obtained by different mapping techniques is very helpful in examining the different strategies and algorithms to evaluate TEC.

When comparing GPS-based TEC derived by different groups with updated IRI90 model, we find a better consistency in the results of DLR-Neustrelitz. The maximum differences in the GPS-based TEC of the various groups are in the order of 2..4 TECU.

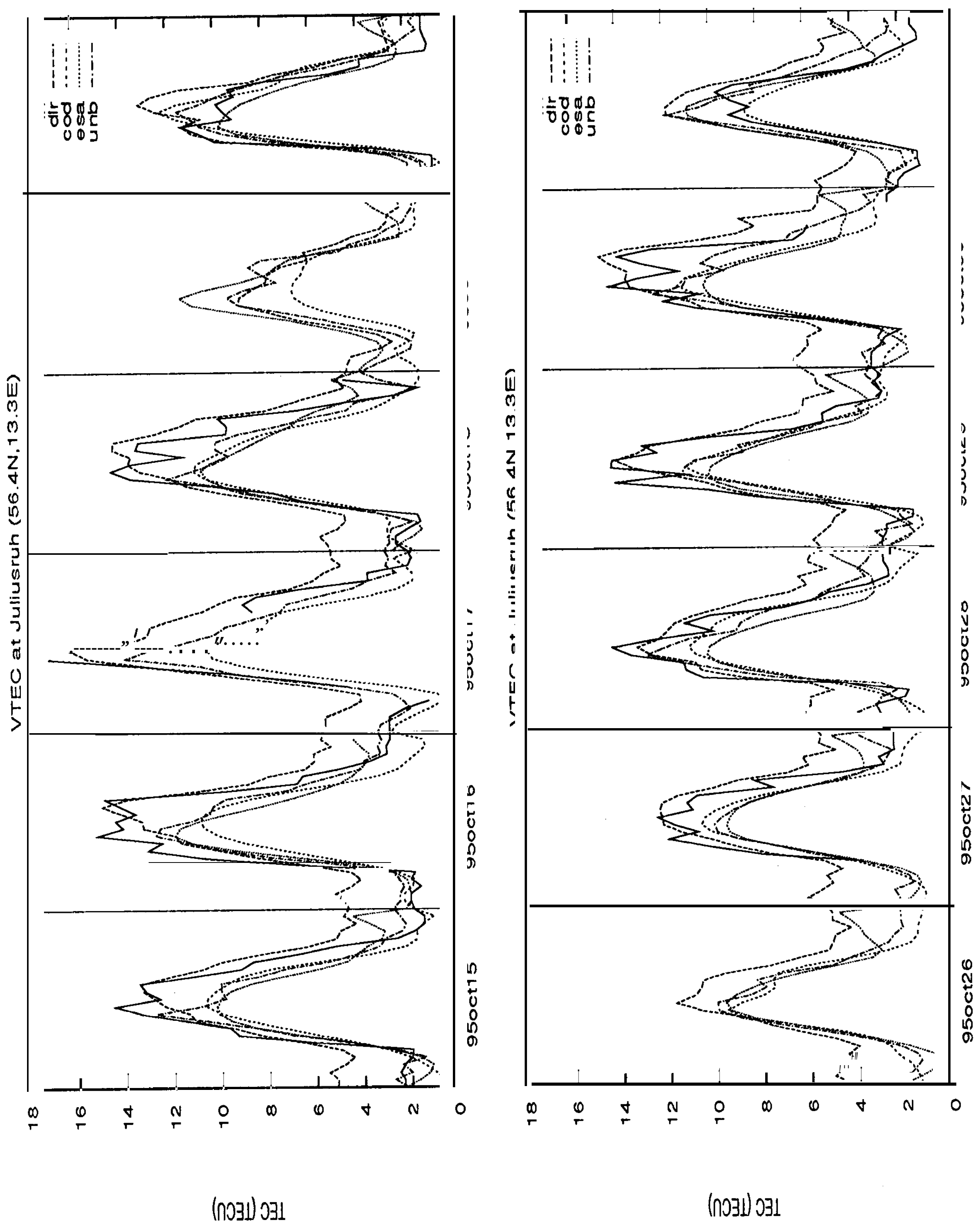

Figure 6
Vertical TEC computed for **Juliusruh** using the **IRI90** model and the **TEC** maps provided by several groups using GPS data.

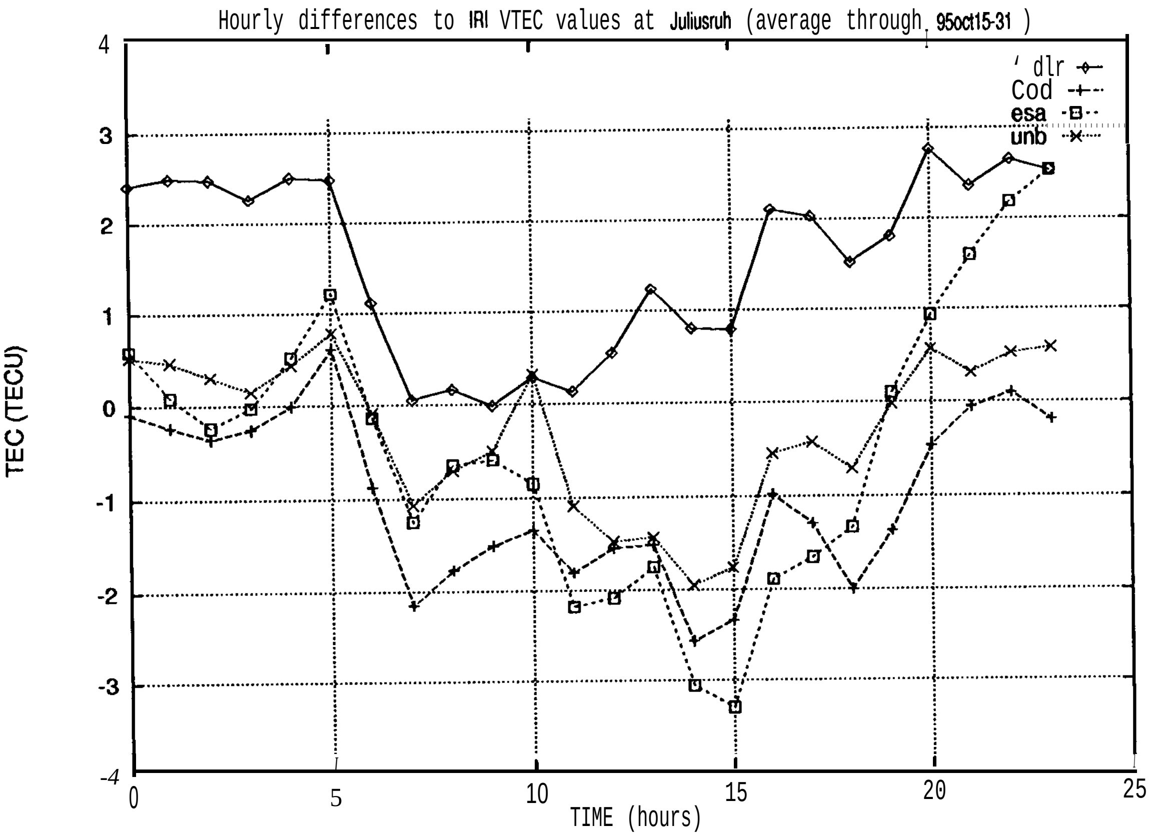

Figure 7
Hourly differences to IRI VTEC value at Juliusruh for the different groups.

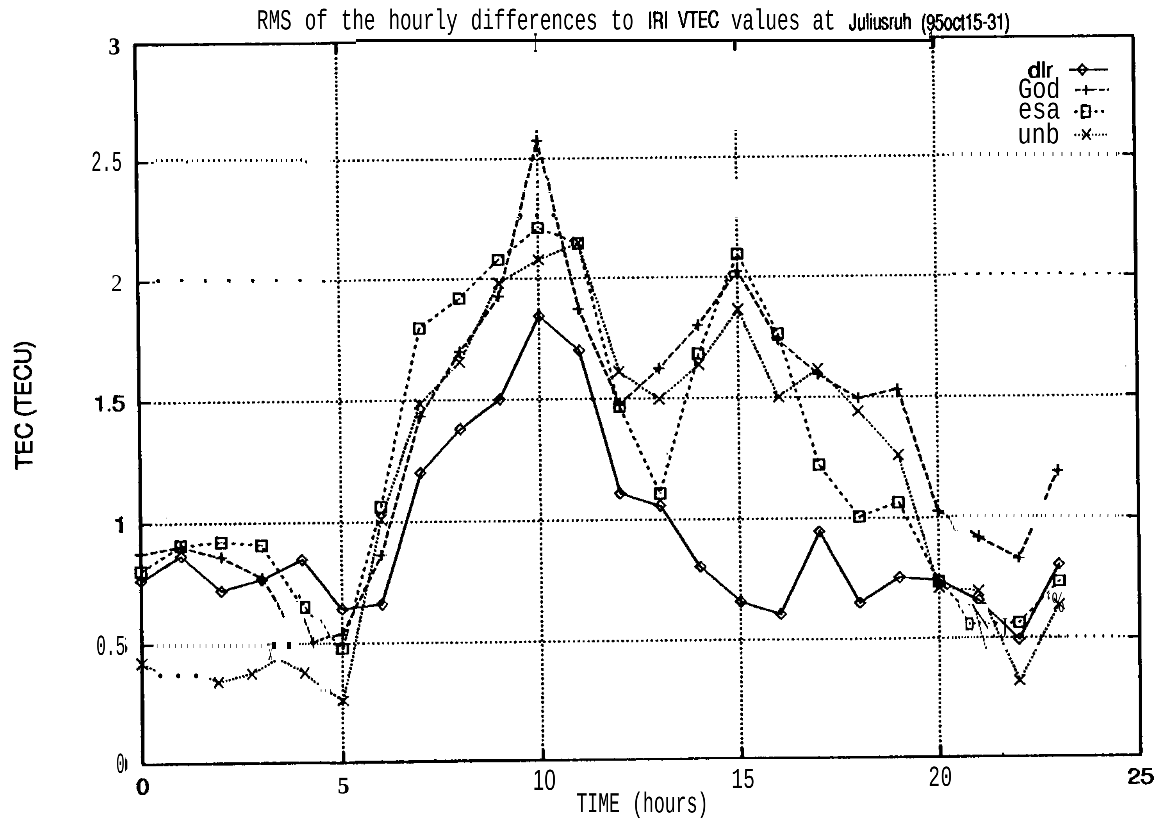

Figure 8
RMS of the hourly differences to IRI VTEC values at Juliusruh for the different groups.

Acknowledgments
The authors express their deep thanks to the colleagues of the IGS community and especially the groups involved in these comparisons who made available high quality GPS data sets and TEC data products, Respectively,
We thank also J. Mielich, J. Weiß and I. Prutensky for providing ionosonde data and K. Schlegel for providing EISCAT data.
We are also grateful to D. Adrian for her help in preparing the manuscript.
The research was supported by the German Agency of Space Activities (DARA) under contract 50Y19202.

References

Coco, D., GPS-Satellites of Opportunity for Ionospheric Monitoring, GPS world, 47-50, October 1991.

Jakowski N. and A. Jungstand, Modeling the Regional Ionosphere by Using GPS Observations, Proc. Int., Beacon Sat. Symp. (Ed,: L. Kersley), University of Wales, Aberystwyth, 11-15 July 1994, pp 366-369.

N. Jakowski, Ionospheric Research and Future Contributions of the IGS Network, paper presented at the IGS-workshop, Potsdam, 15.-17.05.1995.

Sard6n. E., A. Rius, and N. Zarraoa, Estimation of the receiver differential biases and the ionospheric total electron content from Global Positioning System observations, Radio Science, 29,577-586,1994.

Soicher, H., Diurnal, Day-to-Day, and Seasonal Variability of NF, NT and Np at Fort Monmouth, New Jersey, Proc. Int. Beacon Sat. Symp. (Ed.: M. Mendillo), Boston 1-4 June, 1976,pp231-243.

Wilson B .D., A. J. Manucci, and Ch. D. Edwards, Subdaily northern hemisphere ionospheric maps using an extensive network of GPS receivers, Radio Science 30,639-648, 1995.

Zarraoa, N., E. Sard6n, Test of GPS for permanent ionospheric TEC monitoring at high latitudes, Ann. Geophys. 14, 11-19, 1996.

Zumberge, J., R. Neilan, G. Beutler, and W. Gurtner, The International GPS-Service for Geodynamics-Benefits to Users., Proc. ION GPS-94, Salt Lake City, September 20-23.1994.

APPENDIX 1

SINEX - Solution (Software/technique) INdependent Exchange Format
Version 1.00 (June 30, 1996)

INTRODUCTION

The SINEX acronym was suggested by Blewitt et al. (1994) and the first versions, 0.04, 0.05 and 1.00 evolved from the work and contributions of the SINEX Working Group (WG) chaired by G. Blewitt. The other SINEX WG numbers consisted of Claude Boucher, Yehuda Bock, Jeff Freymueller, Gerd Gendt, Werner Gurtner, Mike Heflin and Jan Kouba. Also contributions of Z. Altamimi, T. Herring, Phil Davies, Remi Ferland, David Hutchison and other IGS AC colleagues are noted and acknowledged here, in particular all the ACs submitting and using SINEX(0.05) every week since mid 1995, as a part of the IGS ITRF densification pilot project.

SINEX was designed to be modular and general enough to handle GPS as well as other techniques. In particular the information on hardware (receiver, antenna), occupancy and various correspondence between hardware, solution and input files can be preserved, which is essential for any serious analysis and interpretation of GPS results. It preserves input/output compatibility so that output SINEX files can be used (latter on) as input into subsequent computation/solutions. It also provides complete information on apriori information so that it can be removed whenever required, making it unnecessary to submit or distribute multiple (SINEX) solution files, e.g. constrained and unconstrained (free) solution files.

CHANGES FROM VERSION 0.05 TO 1.00

The version 0.05 has undergone some "finetuning"as the result of the IGS ITRF densification pilot project but it is yet to be proof tested by other techniques. More specifically the following is a summary of the changes and enhancementts from the previous version 0.05 to the new version 1.00:

1) Backward compatibility with the version 0.05 is assuredmy the version #, which MUST be coded on the first line.

2) Strictly fixed format, all fields are now specified and described in details in the Appendix I. In most cases the format fields are the same as in the version 0.05 with some notable exceptions. For crucial fields such as SOLUTION/ESTIMATE and SOLUTION/MATRIX a generous field length of 21 is specified which should be sufficient for up to 16 significant digits; furthermore the field lengths for receiver and antenna types in the SITE/RECEIVER and SITE/ANTENNA blocks were increased from 16 to 20 chars to make them compatible with RINEX. Also strict adherence to IGS receiver/antenna code names is now required (see the Appendix III for the list of the IGS receiver/antenna standard names).

3) The version 1.00 accommodates the CORR matrix type in a different fashion, namely when the CORR matrix type is used in the SOLUTION/MATRIX blocks it is now required that standard deviations (STDs) are coded on the main diagonal, in place of 1.000's. This way the STDS in the CORR matrix could be given to the full precision and they take precedent over any STDs in the SOLUTION/ESTIMATE & SOLUTION/APRIORI blocks which may not be given to a sufficient precision. The other matrix form (e.g. COVA) is still valid and acceptable.

4) A new (mandatory for IGS) block (SOLUTION/STATISTICS) is introduced for needed solution statistics (see the example below)

```
+SOLUTION/STATISTICS
*_STATISTICAL PARAMETER________ __VALUE (S)___________
 VARIANCE FACTOR                0.9260149874E-02
 NUMBER OF OBSERVATIONS         811865
 NUMBER OF UNKNOWNS             22142
 SAMPLING INTERVAL (SECONDS)     120
-SOLUTION/STATISTICS
```

Other possible headings/entries might include e.g.:
SQUARE SUM RESIDUALS (VTPV)
NUMBEROF DEGREES OF FREEDOM , etc.

5) Additional standardized parameter code names were introduced to accommodate some specific users, more parameter codes may be introduced as the need arises. For future applications and to ease interpretation, the parameter code fields have been increased from four to six chars in all the relevant (SOLUTION) blocks, with sane minor changes in the format fields to accommodate this change. It is suggested that the current (four chars) codes used by IGS (STAX, STAY, STAZ, VELY, VELY, VELZ, LOD, UT, XPO, YPO) are retained for compatibility/continuity reasons and that any new ones take the advantage of the six chars field. E.g. for the orbit parameters the following code names could be suggested:

```
SAT X PR01   X state of PRN 01
SAT-Y  PR01  Y  "  "
SAI-Z  PR01  Z  "  "

SAT_VX PR01  Vx    ". "
.

SAT_RP PR01 Rp scale of PRN 01
SAT_GX PR01   Gx    "   "
SAT_GZ  PR01   Gz  "   "
SATYBI PR01   Gy  bias  "

TROTOT ALGO  Tropo delay (wet + dry) at ALGO
TRODRY ALGO  Tropo delay (dry)
TROWET ALGO  Tropo delay (wet)
```

etc.

Note: The use of SV rather PR could be considered here, as it is more meaningful, but since the GPS users are accustomed to PRN's (and PRNs are used in sp3) we may not have any other choice. Considering that "P" is used by IERS as the technique code forGPS, it may not be (i.e. "PR") such a bad choice. Other satellite system would then have to be assigned unique code of two chars.

6) The version 1.00 discontinues the practice of using separate OCC_ and SOLN codes in the SITE and SOLUTION blocks, respectively, as it serves no useful purpose. Further more it is suggested to use the SOLN codes for the SITE blocks as well (i.e. SITE/ECCENTRICITY, ./RECEIVER; ./ANTENNA and ./DATA). Inmost cases for the individual AC SINEXes, the SOIN codes should then be coded with the default characters "-" which could mean that "this

record applies to all estimates" (note SITE+PT+SOLN defines a unique estimate, SITE+PT is equivalent to DOMES (DOMEX) and uniquely identifies a geodetic mark). What is exactly meant should be clear from the examples below:

```
+SITE/ANTENNA
*Code PT SOLN T _Data Start_ __Data End_  _antenna type_       _S/N_
* lines removed
 GOID  A ---- P  92:180:00000 95:304:79200 DORNE MARGOLIN R        95
 GOLD  A---- P  95:304:79200 00:000:00000 DORNE MARGOLIN T      -----
* etc.
*    (NOTE: above ANTENNA TYPE FIELD = 20chars)
```

```
+SITE/ECCENTRICITY
*Code PT SOLN T _Data Start_ __Data End_ type _ ARP-benchmark (m)_______
* lines removed
 GOLD A---- P 92:180:00000 95:304:79200 UNE    .0000    .0000    .0000
 GOLD A---- P 95:304:79200 00:000:00000 UNE    .0025    .0000    .0000
* etc.
* NOTE: Continuity of multiple entry of a site must be adhered, i.e. the
*    end epoch of the first ( must be coded) =< the start epoch of the second
*    entry .
.
```

This would allow only one (e.g. SOLN=1) for GOLD in the ESTIMATE blocks. on the other hand if one prefers two SOLNs (e.g. 1 & 2) for GOLD in the ESTIMATE blocks, e.g. before and after an antenna change, then the same (e.g. 1 & 2) SOLN must be used in all GOLD entries in the SITE blocks as well. Conversely when two solutions (SOLN 1, 2) are introduced for some reasons other than instrum?nt/antenna change (e.g. as a result a coseismic change, with the sank? rec/antenna/eccentricity) then, only one entry in the SITE blocks with the default character codes ("-") in the SOLN filed need to be coded *or* alternatively two identical entries with 1 and 2 in the SOLN field could be used (except, of course, for the start and end epochs which must be continuous and non overlapping). This considerably enhances the SINEX effectiveness.

SINEX SYNTAX

SINE)(is an ASCII file with lines of 80chars or less. It consists of a number of blocks which are mutually referenced (related) through station codes/names, epochs and/or index counters. Some blocks consist of descriptive lines (starting in Col.2) and/or fixed format fields with numerous headers and descriptive annotations.

The first line is MANDATORY and must start with "%" in col 1, and contains information abut the agency, file identification, solution spans, techniques, type of solution, etc. (for more details see the Appendix I or II). The last line ends with "%ENDSNX".

The SINEX format consists of a number BLOCKS which start with "+" in the first col. followed by a standardized block labels, and each block ends with "-" and the block label. Each block data starts in the column 2 or higher. Blocks can be in any order, provided that they start with (+) and end with (-) block labels. The first header line and most blocks are related through epochs or time stamps in the following format:

YY: DOY: SECOD YY-year; DOY- day of year; SECOD -see of day;
E.g. the epoch 95:120:86399 denotes April 30, 1995 (23:59 :59UT). The epochs 00:00:00000 are allowed in all blocks (except the first header line) and default into the start or end epochs of the first header line which must always be coded. This is particularly useful for some blocks, such as the ones related to hardware, occupancy, which should be centrally archived by IGSCB with 00:00:00000 as the end (current) epochs, and which should be readily usable by ACs for SINEX and other analysis/processing as official (authoritative) IGS information.

COMMENT lines starts with "*" in Col. 1 and can be anywhere within or outside a block, though for the clarity sake, beginning and ends of blocks are preferable. For increased portability, the floating number exponent of "E" should be used rather than "D" or "d" which is not recognized by some compiler/installations. Fields not coded should be filled with "-" characters to allow efficient row and column format readings.

The most important blocks are the SOLUTION blocks. They are in fixed format and have been adopted and used by IERS (ISEF1) submission format as well. (For more information on the format, see the Appendix I). Only two SOLUTION blocks (SOLUTION/ESTIMATE and SOLUTION/MATRIX_ESTIMATE) are MANDATORY and must be coded. They contain complete solutions (apriori + solution vector) and the corresponding standard deviations, and the corresponding matrix. Although various matrix forms are allowed in SINEX (as specified by a matrix type code), triangular correlation matrix (e.g. SOLUTION/MATRIX_ ESTIMATE L CORR) is preferred and recommended for IGS sinoe it is easier to visualize. Important but not mandatory (though RECOMMENDED for IGS purposes) are the next two blocks, i.e. the SOLUTION/APRIORI and SOLUTION/MATRIX_APRIORI. The scale of estimated and apriori standard deviations can, in principle, be arbitrary (note even apriori scaling is arbitrary, depending on the observation weighting). However, both estimated and apriori standard deviations (and the corresponding matrices) MUST use the same scaling (i.e. variance) factor. Otherwise the apriori information cannot be rigorously removed to form free solutions (e.g. normal matrices). Scaling between different SINEX solutions is beyond the SINEX format and must be dealt with at the combination/analysis stage.

REFERENCES

Blewitt, G., Y. Bock and J. Kouba: "Constraining the IGS Polyhedron by Distributed Processing", workshop proceedings : Densification of ITRF through Regional GPS Networks, held at JPL, Nov 30-Dec 2, 1994, pp. 21-37.

A P P E N D I X   I

S I N E X

V E R S I O N   1 . 0 0

D E T A I L   F O R M A T   D E S C R I P T I O N

1. Introduction

This document describes the Software INdependent EXchange (SINEX) format. The need for such a format grew out of the increasing need to exchange station coordinates information. It started in early 1995 by an effort from a number of IGS participants. The format has quickly evolved beyond the original objectives. The information is organized by blocks. The format is designed to be easily extended as need may arise.

2. Data Structure

Each SINEX line has at most 80 ASCII characters.
The SINEX file is subdivided in groups of data called blocks. Each block is enclosed by a header and trailer line. Each block has a fixed format. The blocks contain information on the file, its input, the sites and the solution. All elements within a line are defined. A character field without information will have "-"s within its field and a missing numerical element will have a value of 0 within its field. *This* lets the SINEX file to be accessible "column-wise" as well as "line-wise". Character fields shouldbe left hand justified whenever applicable.

The first character of each line identify the type of information that the line contains. Five characters are reserved. They have the following meaning when they are at the beginning of a line, they identify:

Character	Definition
"%"	Header and trailer line,
"*"	Comment line within the header and trailer line,
"+"	Title at the start of a block
"-"	Title at the end of a block
" "	Data line within a block

No other character is allowed at the beginning of a line.

A SINEX file must start with a Header line and ends with a footer line.

The following blocks are defined:

FILE/REFERENCE
FILE/COMMENT
INPUT/HISTORY
INPUT/FILES
INPUT/ACKNOWLEDGEMENTS
SITE/ID
SITE/DATA
SITE/RECEIVER
SITE/ANTENNA
SITE/GPS_PHASE_CENTER
SITE/ECCENTRICITY
SOLUTION/EPOCH
SOLUTION/STATISTICS
SOLUTION/ESTIMATE
SOLUTION/APRIORI
SOLUTION/MATRIX_ESTIMATE {p} {type}
SOLUTION/MATRIX_APRIORI {p} {type}

where: {p} L or U
{type} CORR or COVA or INFO or SRIF

These block titles are immediately preceded by a "+" or a "-" as they mark the beginning or the end of a block. The block titles must be in capital letters. After a block has started(+) it must be ended(-) before another

Field	Description	Format
Time	YY:DDD:SSSSS. "UKY" YY = last 2 digits of the year, if YY <= 50 implies 21-* century, if YY > 50 implies 20-th century, DDD = 3-digit day in year, SSSSS = 5-digit seconds in day.	12.2, 1H:,I3.3, 1H:,I5.5
Constraint Code	Single digit indicating the constraints: 0-fixed/tight constraints, 1-significant constraints, 2-unconstrained.	A1
Parameter Type	Type of parameter. List of allowed parameters: STAX - station X coordinate, m STAY - station Y coordinate, m STAZ - station Z coordinate, m VELX - station X velocity, m/y VELY - station Y velocity, m/y VELZ - station Z velocity, m/y LOD - length of day, ms UT - delta time UT1-UTC, ms XPO - X polar mot ion, mas YPO - Y polar motion. mas XPOR - X polar mot ion rate, ma/d YPOR - Y polar mot ion rate, ma/d SAT__X - Satellite X coord., m SAT__Y - Satellite Y word., m SAT__Z - Satellite Z coord., m SAT_VX -Satellite X velocit y, m/s SAT_VY - Satellite Y velocity, m/s SAT_VZ - Satellite Z velocity, m/s SAT_RP - Radiation pressure, SAT_GX - GX scale, SAT_GZ- GZ scale, SATYBI - GY bias, " m/s2 TROTOT - wet + dry Tropo delay m TRODRY - dry Tropo delay m TROWET - wet Tropo delay m	A6
Site Code	- For stations: Call sign for a site. (It should be consistent with IGS convention) . - For satellites: Use "PRXX" where XX is the PRN number.	A4
Point Code	A two character code identifying physical monument within a site. Typically has a code A, but could vary if the site has more than one monument.	A2
Solution ID	Character identif ying the solution given for a point at a site. "---" applies to all.	A4
Observation Code.	A single character indicating the technique (s) used to arrive at the solutions obtained in this SINEX file. It should be consistent with the IERS convention. This character code may be: C-Combined techniques used. D-DORIS, L-SLR, M-LLR, P-GPS, R-VIM.	A1

block can begin. The general structure is as follow:

```
%=SNX ........... (Header line)----------!
..............                           |
+(BLOCK TITLE)-------------|             |
 ............              |             |
 ............              |             |
 ............                            |
-(BLOCK TITLE)------------- |            |
..............                           |
+(BLOCK TITLE) -------------I            |
 ............              |             |
 ............              |             |
 ............                            |
-(BLOCK TITLE)------------ |             |
.............                            |
%ENDSNX          (Trailer line)---------|
```

Most fields within a SINEX line are separated by a single space. In the following sections, each SINEX line is definedby its field name, a general description and the (FORTRAN) format.

The comment line (not to be confused with the FILE/COMMENT Block) can be written anywhere within the header and the footer line is defined as:

COMMENT DATA LINE		
Field	Description	Format
Comment	Any general comment relevant to the SINEX file.	1H*,A79
		80

For example, the use of "*" in the first column can be used to effectively hide information from the software without deleting it from the file.

Some fields are found in several blocks. To keep the description short, they are described in detail here, and will be referred to in the sections with additional information added when necessary. The fields defined below will be referenced to by putting them within square brackets [] when encountered in the following sections.

3. Header Line (Mandatory)

Description

The **Header line** must be the **first** line in a **SINEX file.**

Contents:

HEADER LINE		
Field	Description	Format
First Character	Single character '%' in column #1. No other character than '%' is allowed.	A1
Second Character	Single charatter '=' in n column?. Indicates '*resultant*' solution. No other character than '=' is allowed.	A1
Document Type	Three characters 'SNX' in columns 3 to 5. Indicates that this is a SINEX document .	A3
Format Version	Four digits indicating the version of SINEX format used. '1.00' for this version.	1X, F4 .2
File Agency Code	Identify the agency creating the file.	lX, A3
[Time]	Creation time of this SINEX file.	1X, I2.2, 1H:,I3.3, 1H:,I5.5
[Agency Code]	Identify thhe agency providing the data in the SINEX file	1X,A3
[Time]	start time of the data used in the SINEX solution Value 00:000:00000 should be avoided.	1X,I2.2, 1H:,I3.3, 1H:,I5.5
[Tim]	End time of the data used in the SINEX solution Value 00: 000:00000 should be avoided.	1X,I2.2, 1H:,I3.3, 1H:,I5.5
[Observation Code]	Technique(s) used to generate the SINEX solution	lX, Al
Number of Estimates	Number of parameters estimated in this SINEX file. Mandatory field.	1X,I5.5
[Constraint call?]	Single charatter indicating the const raint in the SINEX solution. Mandatory field.	lx, Al
Solution contents	Solution types contained *in* this SINEX file. Each character in this field may be one of the following: X - Station Coordinates, V - station Velocities, o - Orbits, E - Earth Rotation Parameters T - Troposphere BLANK	5(IX, Al)

i 77

Relationship with other blocks:

This line is duplicated as the resultant line of the INPUT/HISTORY Block with the exoeption of its first character.

4. **FILE/REFERENCE** Block (Mandatory for IGS)

Description:

This block provides information on the Organization, point of contact, the software and hardware involved in the creation of the file.

Contents:

FILE REFERENCE DATA LINE

Field	Description	Format
Information Type	Describes the type of information present in the next field. May take on the following values: 'DESCRIPTION' - Organizations) gathering/altering the file contents. 'OUTPUT' - Description of the file contents. 'CONTACT' - Address of the relevant contact. e-mail 'SOFTWARE' - Software used to generate the file. 'HARDWARE' - Computer hardware on which above software was run. 'INPUT' - Brief description of the input used to generate this solution. Any of the above fields maybe and in any order.	1X,A18
Information	Relevant information for the type indicated by the previous field.	lX, A60
		80

5. **FILE/COMMENT** Block **(Optional)**

Description:

This Block can be used to provide general comments about the SINEX data file.

Contents:

FILE COMMENT DATA LINE		
Field	Description	Format
Cement	Any general comment providing relevant information about the SINEX file.	1X, A79
		80

6. INPUT/HISTORY Block (Recommended)

Description:

This block provides information about the source of the information used to create the current SINEX file.

Contents:

INPUT HISTORY DATA LINE		
Field	Description	Format
File Code	Only one of the following characters is permitted: '+' - This character indicates that the information that follows identify an input solution contributing to this SINEX file. '=' - This character indicates that the information that follows identify the output solution file.	1X, A1
Document Type	Three characters 'SNX' in columns 3 to 5. Indicates that this is a SINEX document.	A3
Format Version	Four digits indicating the version of SINEX format used. '1.00' for this version.	1X, F4.2
[Agency Code]	Identify the agency creating the file.	1X,A3
[Time]	Creation time of this SINEX file.	1X,I2.2, 1H:,I3.3, 1H:,I5.5
[Agency Code]	Identify the agency providing the data in the SINEX file.	1X,A3
[Time]	Start time of the data used in the SINEX solution.	1X,I2.2, 1H:,I3.3, 1H:,I5.5
[Time]	End time of the data used in the SINEX solution.	1X,I2.2, 1H:,I3.3, 1H:,I5.5
[Observation Technique]	Technique(s) used to generate the SINEX solution.	1X,A1
Number of Estimates	Number of parameters estimated in this SINEX file.	1X, I5.5
[Constraint cab]	Single digit indicating the constraint in the SINEX solution.	1X, A1
solution Contents	Solution types contained in this SINEX file. Each character in this field may be one of the following: X - Station Coordinates, V - Station Velocities, O - Orbits, E - Earth Rotation Parameters T - Troposphere BLANK	6(1X, A1)
		79

Comment:

The fiml data line "=" describes the current SINEX file and match the Header line with the exception of the first character.

7. INPUT/FILES Block (Optional)

Description:

This block identify the input files and allow for a short comment to be added to describe those files.

Contents:

INPUT FILES DATA LINE

Field	Description	Format
[Agency Code]	Agency creating the solution ales- cribed in this data line.	lX, A3
[Time]	Time of creation of the input SINEX solution	1X,12.2, 1H:,I3.3, 1H:,I5.5,
File Name	Name of the file containing the solution described in the current data line.	1X,A29
File Description	General description of the file referredto on this data line.	1X,A32
		80

Comments:

There must be exactly one INPUT/FILES data line for every INPUT/HISTORY data line. The final data line must describe this current SINEX file.

8. INPUT/ACKNOWLEDGEMENTS Block (Optional)

Description:

This block defines the agency codes contributing to the SINEX file.

Contents:

INPUT ACKNOWLEDGMENTS DATA LINE

Field	Description	Format
[Agency Code]	Agency(ies) contributing to this SINEX file.	lX, A3
Agency Description	Description of agency code.	1X,A75
		80

9. SITE/ID Block (Mandatory)

Description:

This block provides general information for each site containing estimated parameters.

Contents:

SITE ID DATA LINE

Field	Description	Format
[Site Code]	Call sign for a site.	1X, A4
[Point Code]	Physical monument used at a site	lx, A2
Unique Monument Identification	Unique alpha-numeric monument identification. For ITRF purposes, it is a nine character DOMES/DOMEX number (five/six digits, followed by the single letter 'M' or 'S', followed by four/three digits)	1X, A9
[Observation Code]	Observation technique(s) used.	lx, Al
Station Description	Free-format description of the site, typically the town and/or country.	1X,A22
Approximate Longitude	Approximate longitude of the site in degrees(W/+), minutes and seconds.	1X, 13, 1X, 12, 1X,F4.1
Approximate Latitude	Approximate latitude of the site indegrees(NS/+-), minutes and seconds.	1X, 13, 1X, 12, 1X,F4.1
Approximate Height	Approximate height of the site in meters.	1X,F7.1
		75

10. SITE/DATA Block (Optional)

Description:

This block gives the relationship between the estimated station parameters in the SINEX file and in the input files.

Contents:

SITE DATA LINE		
Field	Description	Format
[Site Code]	Site Code for solved station coordinates.	1X, A4
[Point Code]	Point Code for solved station coordinates.	1X, A2
[Solution ID]	Solution number to which the input in this data line is referred to.	1X, A4
[Site Code]	Site Code fran an input SINEX file	1X, A4
[Point Code]	Point code from an input SINEX file.	1X, A2
[Solution ID]	Solution Number for a Site/Point from an input SINEX file.	1X, A4
[Observation Code]	Observation Code for a Site/point/Solution Number from an input SINEX file.	1X, A1
[Time]	Tim of start of data for the input SINEX file.	1X,I2.2, 1H:,I3.3, 1H:,I5.5
[Time]	Tim of end of data for the input SINEX file.	1X,I2.2, 1H:,I3.3, 1H:,I5.5
[Agency Code]	Creation Agency Code for the input SINEX file.	1X,A3
[Time]	Creation time for the input SINEX file.	1X,I2.2, 1H:,I3.3, 1H:,I5.5

71

11. SITE/RECEIVER Block (Mandatory for IGS)

Description:

List the *receiver* used at each site during the observation period of interest.

Contents:

SITE RECEIVER DATA LINE		
Field	Description	Format
[Site Code]	Site code for which sane parameters are estimated.	1X, A4
[Point Code]	Point Code at a site for which some parameters are estimated.	lX, A2
[Solution ID]	Solution Number at a Site/Point code for which some parameters are estimated.	1X, A4
[Observation code]	Identification of the observation technique used.	lx, Al
[Time]	Time since the receiver has been operating at the Site/Point. Value 00:000:00000 indicates that the receiver has been operating at least since the "File Epoch Start Tire".	1X,12.2, 1H:,I3.3, 1H:,I5.5
[Time]	Time until the receiver is operated at a Site/Point. Value 00:000:00000 indicates that the receiver has been operating at least until the "File Epoch End *Time*".	1X,12.2, 1H:,I3.3, 1H:,I5.5
Receiver Type	Receiver Name & model. (See Appendix III for IGS Standard receiver names)	1X,A20
Receiver Serial Number	Serial number of the receiver. Takes on value '-----' if unknown.	lX, AS
Receiver Firmware	Firmware used by this receiver during the epoch specified above. Takes on value '----------- -----' if unknown.	1X,A11
		80

12. SITE/ANTENNA Block (Mandatory for IGS)

Description:

List of antennas used at each site used in the SINEX file.

Contents:

SITE ANTENNA DATA LINE		
Field	Description	Format
[Site Code]	Site code for which some parameters are estimated.	1X, A4
[Point Code]	Point Cede at a site for which some parameters are estimated.	lX, A2
[Solution ID]	Solution Number at a Site/Point code for which some parameters are estimated.	1X, A4
[Observation code]	Identification of the observation technique used.	lx, Al
[Time]	Tim? since the antema has been installed at the Site/Point. Value 00:000:00000 indicates that the antenna has been installed at least since the "File Epoch Start Time".	1X,12.2, 1H:,I3.3, 1H:,I5.5
[Time]	Time until the antenna is installed at a Site/Point. Value 00:000:00000 indicates that the antenna has been installed at least until the "File Epoch End Time".	1X,12.2, 1H:,I3.3, 1H:,I5.5
Antenna Type	Antema name & model. (see Appendix III for IGS Standard antenna names)	lx, A20
Antenna Serial Number	Serial number of the antenna. Takes on value '-----' if unknown.	lx, AS
		68

13. SITE/GPS_PHASE_CENTER Block (Mandatory for IGS)

Description:

List of GPS phase centers offset for all antennas described in the Site Antema block. The offset is given from the Antema Reference Point (ARP) to the L1 and L2 phase centers respectively. For IGS purposes see the IGS Central Bureau Information System for ARPs and antema phase center offsets: directory: igscb/station/general ; files: antenna.gra and rcv_ant.tab

Contents:

GPS PHASE CENTER DATA LINE

Field	Description	Format
Antenna Type	Antema name & model. (See Appendix III for IGS Standard antenna names)	lx, A20
Antenna Serial Number	Serial number of the antenna. Takes on value '-----' if unknown.	lx, A5
L1 Phase Center Up offset	Up(+) offset from the ARP to the L1 phase center in meters.	1X,F6.4
L1 Phase Center North Offset	North(+) offset from the ARP to the L1 phase center in meters.	1X,F6.4
L1 Phase Center East Offset	East(+) offset from the ARP to the L1 phase center in meters.	1X,F6.4
L2 Phase Center Up Offset	Up(+) offset from the ARP to the L2 phase center in meters.	1X,F6.4
L2 Phase Center North Offset	North(+) offset from the ARP to the L2 phase center in inters.	1X,F6.4
L2 Phase Center East Offset	East(+) offset franthe ARP to the L2 phase center in meters.	1X,F6.4
Antenna Calibration model	Name of the antenna model used in the correction of the observations for phase center variations.	lx, Alo
		80

14. SITE/ECCENTRICITY Block (Mandatory for IGS)

Description:

List of antenna eccentricities from the Marker to the Antenna Reference Point (ARP). For IGS purposes see the IGS Central Bureau Information System for antema eccentricities:
directory: igscb/station/tie; files: localtie.tab and localtie.chg

Contents:

SITE ECCENTRICITY DATA LINE		
Field	Description	Format
[Site Cede]	Site code for which some parameters are estimated.	1X,A4
[Point Code]	Point Code at a site for which some parameters are estimated.	1X, A2
[Solution ID]	Solution ID at a Site/Point code for which some parameters are estimated.	1X, A4
[Observation Cede]	Identification of the Observation technique used.	1X, A1
[Time]	Tine since the antenna has been installed at the Site/Point, Value 00:000:00000 indicates that the antenna has been installed at least since the "File Epoch Start Time".	1X, I2.2, 1H:,I3.3, 1H:,I5.5
[Time]	Time until the antenna is installed at a Site/Point. Value 00:002:00000 indicates that the antenna has been installed at least until the "File Epoch End Time".	1X, I2.2, 1H:,I3.3, 1H:,I5.5
Eccentricity Reference system	Reference system used to describe vector distance from monument benchmark to the antenna reference pint: 'UNE' - Local reference system Up, North, East. 'XYZ' - Cartesian Reference System x, Y, z. All units are in meters,	1X, A3
Up / X Eccentricity	Up / X offset from the marker to the Antenna referernce point (ARP).	1X, F8.4
North / Y Eccentricity	North/Y offset fran the marker to the Antenna reference point (ARP).	1X, F8.4
EaSt/Z Eccentricity	East/Z offset from the marker to the Antenna reference point (ARP).	1X, F8.4
		72

15. SOLUTION/EPOCH Block (Mandatory)

Description:

List of solution epoch for each Site Code/Point Code/Solution Nunber/Observation Code (SPNO) combination.

Contents:

SOLUTION EPOCHS DATA LINE		
Field	Description	Format
[Site Code]	Site code for which some parameters are estimated.	1X, A4
[Point Code]	Point Code at a site for which some parameters are estimated.	lx, A2
[Solution IDI	Solution Number at a Site/Point code for which some parameters are estimated.	1X,A4
[Observation code]	Identification of the observation technique used.	lx, A1
[Tim]	Start time for which the solution identified (SPNO) has observational	1X,12.2, 1H:,I3.3, 1H:,I5.5
[Time]	End time for which the solution identified (SPNO) has observationsl	1X,12.2, 1H:,I3.3, 1H:,I5.5
[Time]	Mean time of the observations for which the solution (SPNO) is derived.	1X,12.2, 1H:,I3.3, 1H:,I5.5
		54

16. SOLUTICN/STATISTICS Block (Optional)

Description:

List of solution epoch for each Site Code/Point Code/Solution Number/Observation Code (SPNO) combination.

Contents:

SOLUTION STATISTICS LINE

Field	Description	Format
Information Type	Describes the type of information present in the next field. May take on the following values: 'NUMBER OF OBSERVATIONS' #of observations used in the adjustment. 'NUMBER OF UNKNOWNS' # of unknowns solved in the adjustment. 'SAMPLING INTERVAL (SECONDS)' Interval in seconds between successive observations. 'SQUARE SUMOF RESIDUALS (VTPV)' Sum of squares of residuals. (V'PV); V-resid. vector; P- weight matrix 'PHASE MEASUREMENTS SIGMA' Sigma used for the phase measurements. 'CODE MEASUREMENTS SIGMA' Sigma used for the code (pseudo-range) measurements. 'NUMBER OF DEGREES OF FREEDOM' # of observations minus the # of unknowns (df) 'VARIANCE FACTOR' Sum of squares of residuals divided by the degrees of freedom (V'PV/df). Equivalent to Chi-squared/df. Any of the above fields maybe present and in any order.	1X, A30
Information	Relevant information for the type indicated by the previous field.	1X,F22.15
		54

17. SOLUTION/ESTIMATE Block (Mandatory)

Description:

Estimated parameters.

Contents:

SOLUTION ESTIMATE DATA LINE

Field	Description	Format
Estimated Parameters Index	Index of estimated parameters. values from 1 to the number of parameters.	1X, I5
[Parameter Type]	Identification of the type of parameter.	1X, A6
[Site Code]	Site code for which some parameters are estimated.	1X,A4
[Point Code]	Point Code at a site for which some parameters are estimated.	1X, A2
[Solution ID]	Solution ID at a Site/Point code for which some parameters are estimated.	1X, A4
[Time]	Epoch at which the estimated parameter is valid.	1X,I2.2, 1H:,I3.3, 1H:,I5.5
Parameter Units	Units used for the estimates and sigmas. Typical units are: m (meters), ms (milliseconds), mas (mini-arc-seconds) .	1X, A4
[Constraint Code]	Constraint applied to the parameter.	1X,A1
Parameter Estimate	Estimated value of the parameter.	1X,E21.15
Parameter Standard Deviation	Estimated standard deviation for the parameter.	1X,E11.6
		80

18, SOLUTION/APRIORI Block (Recommended/Mandatory)

Description:

Apriori information for estimated parameters. This block is mandatory if significant constraints have been applied to the estimated parameters in SOLUTION/ESTIMATE Block.

Contents:

SOLUTION ESTIMATE DATA LINE

Field	Description	Format
Apriori Parameters Index	Index of apriori parameters. values from 1 to the number of parameters.	1X, I5
[Parameter Type]	Identification of the type of parameter. Typical id's are:	1X, A6
[Site Code]	Site code with apriori parameter estimate.	1X, A4
[Point Code]	Point Code with apriori parameter estimate.	1X,A2
[Solution ID]	Solution ID at a Site/Point code with apriori parameter estimate.	1X,A4
[Time]	Epoch at which the apriori parameter is valid.	1X,I2.2, 1H:,I3.3, 1H:,I5.5
Parameter Units	Units used for the aprioris and sigmas. Typical units are: m (meters), ms (milliseconds), mas (mini-arc-seconds).	1X, A4
[Constraint Code]	Constraint applied to the parameter.	1X, A1
Parameter Apriori	Apriori value of the parameter.	1X,E21.15
Parameter Standard Deviation	Apriori standard deviation for the parameter.	1X,E11.6
		80

19. SOLUTION/MATRIX_ESTIMATE Block (Mandatory)

Description:

The Estimate Matrix can be stored in an Upper or Lower triangular form. Only the Upper or Lower portion needs to be stored because the matrix is always symmet rical.
The matrix contents can be:
CORR - Correlation Matrix
COVA - Covariance Matrix
INFO - Information Matrix (of Normals)
SRIF - Square Root Information Filter Matrix
The distinction between the form and its contents is given by the title block which must take one of the following form:

SOLUTION/MATRIX_ESTIMATE L CORR
SOLUTION/MATRIX_ESTIMATE U CORR
SOLUTION/MATRIX_ESTIMATE L COVA
SOLUTION/MATRIX_ESTIMATE U COVA
SOLUTION/MATRIX_ESTIMATE L INFO
SOLUTION/MATRIX_ESTIMATE U INFO
SOLUTION/MATRIX_ESTIMATE L SRIF
SOLUTION/MATRIX_ESTIMATE U SRIF

Contents:

SOLUTION MATRIX ESTIMATE DATA LINE

Field	Description	Format
Matrix Estimate Row Number	Row index for the Matrix Estimate. It must match the parameter index in the SOLUTION/ESTIMATE block for the same parameter.	1X, I5
Matrix Estimate Column Number	Column index for the Matrix Estimate. It must match the parameter index in the SOLUTION/ESTIMATE block for the same parameter.	1X, I5
First Matrix Estimate Element	Matrix element at the location (Row Number , Column Number).	1X,E21.14
Second Matrix Estimate Element	Matrix element at the location (Row Number , Column Number + 1).	1X,E21.14
Third Matrix Estimate Element	Matrix element at the location (Row Number , Column Number + 2).	1X,E21.14
		78

Comment:

The Matrix Estimate Row/Column Number correspond to the Estimated Parameters Index in the SOLUTION/ESTIMATE block. If the CORR matrix is used, standard deviations must be stored in the diagonal elements.

Missing elements in the matrix are assumed to be zero (0); consequently, zero elements may be omitted.

NOTE: The same scale (variance) factor MUST be used for both MATRIX_ESTIMATE and MATRIX_APRIORI, as well as for the standard deviations in the ESTIMATE and APRIORI Blocks.

20. SOLUTION/MATRIX_APRIORI Block (Recommended/Mandatory)

Description:

The Apriori Matrix can be stored in an Upper or Lower triangular form. Only the Upper or Lower portion needs to be stored because the matrix is always symmetrical. Mandatory if any significant constraint have been applied to the SOLUTION/ESTIMATE .
The matrix contents can be:
CORR - Correlation Matrix
COVA - Covariance Matrix
INFO - Information Matrix (of Normals)
SRIF - Square Root Information Filter Martix
The distinction between the form and its contents is given by the title block which must take one of the following form:

SOLUTION/MATRIX_APRIORI L CORR
SOLUTION/MATRIX_APRIORI U CORR
SOLUTION/MATRIX_APRIORI L COVA
SOLUTION/MATRIX_APRIORI U COVA
SOLUTION/MATRIX_APRIORI L INFO
SOLUTION/MATRIX_APRIORI U INFO
SOLUTION/MATRIX_APRIORI L SRIF
SOLUTION/MATRIX_APRIORI U SRIF

Contents:

SOLUTION MATRIX APRIORI DATA LINE

Field	Description	Format
Matrix Apriori Row Number	Row index for the Matrix Apriori. It must match the parameter index in the SOLUTION/APRIORI block for the same parameter.	1X, I5
Matrix Apriori Column Number	Column index for the Matrix Estimate. It must match the parameter index in the SOLUTION/APRIORI block for the same parameter.	1X, I5
First Matrix Estimate Element	Matrix element at the location (Row Number , Column Number) .	1X, E21.16
Second Matrix Estimate Element	Matrix element at the location (Row Number , Column Number + 1) .	1X, E21.16
Third Matrix Estimate Element	Matrix element at the location (Row Number, Column Number + 2) .	1X, E21.16
		78

Comment :

The Matrix Apriori Row/Column Number correspond to the Apriori Parameters Index in the SOLUTION/APRIORI block. If the apriori constraint matrix is diagonal and no loss of significant digits occurs by using the Parameter Standard Deviation in the SOLUTION/APRIORI block, then, this block becomes redundant. If the CORR matrix is used, Standard deviations must be stored in the diagonal elements. Missing elements in the matrix are assumed to be zero (0); consequently, zero elements may be omitted.

NOTE: The sank? scale (variance) factor MUST be used for both MATRIX_ESTIMATE and MATRIX_APRIORI, as well as for the standard deviations in the ESTIMATE and APRIORI Blocks.

21. **Footer** Line **(Mandatory)**

Description:

Marks the end of the SINEX file.

Contents:

FOOTER LINE		
Field	Description	Format
End of SINEX	The seven characters %ENDSNX at the beginning of the last line I mark the end of the SINEX file. Mandatory line.	A7
		7

APPENDIX II

Annotated (real) SINEX sample
(EMR07987.SNX annotated by Philip Davis of NCL (Newcastle AAC))

```
%=SNX 1.00 NRC 95:123:55260 NRC 95:113:00000 95:120:00000 P 00117 lXE
*-------------------------------------------------------------------------------
*
*  This is an annotated SINEX example, based on the first submission from
*  NRC. It has been amended and extended by NCL to illustrate the full
*  SINEX 1.00 format. Long blocks have keen truncated.
*

*   The following convention is followed for start and end date:
*     A start date of 00:000:00000 represents "since the beginning"
*     An end date of 00:000:00000 represents "up to now"
*  * *WARNING: NO overlapping epochs allowed, i.e. epochs referring to the
*  ***            same site must be continuous       *****
*
*       Constraints code S are determined as follows:
*       (Note this is Only SUGGESTION, common sense should be used here)
*       ratio   = ( apriori std. dev. ) / ( estimated std. dev. )
*
*                        ratio   < sqrt( 2 )      wde S = 0 (fixed/constrained)
*       sqrt( 2 ) =<     ratio   < 10             codes= 1 (significant constr.)
*              10  =<    ratio                    code S = 2 (loose or unconstr. )
*
*    WARNING: This has not yet been standardizedby IGS.
*
*
*
*  EOP parameter types:
*               SINEX   Units
*               XPo     mas      (mini-arc  seconds)     pole x
*               YPO     mas      (mini-arc  seconds)          y
*               XPOR    ma/s     (mini-arc seconds/s) pole x rate
*               YPOR    ma/s     (mini-arc seconds/s)       y rate
*               UT      ms       (mini-seconds)          UT1-UTC
*               LOD     ms       (mini-seconds)          Length of day
*
*       They are put at the end of the APRIORI and ESTIMATE blocks such they
*       can be removed easily.
*
*   In floating-point fields, the E symbol should be used for exponent -
*    other symbols (such as D) are not interpreted correctly by some
*    software (e.g. the ANSI C 1/0 library).
*
*   Fields should not be left blank if data is not applicable or
*    unavailable. These fields should be filled with a data-not-given
*    character '-' is used here. This enables the file to be read either
*    by column positions of fields, or by tokenising lines by whitespace.
*
* Block order should be kept consistent to aid readability. The format
* allows any blocks to be omitted, though obviously some are essential for
* solution submission, and the inclusion of all blocks is enwuraged.
*
* Note the relational problem annotated in SITE/ANTENNA.
```

```
* The first and last lines begin '%'. only '%', '*', '+', '-' and ' ' are
* allowed in the first column, meaning 'begin/end SINEX', 'comment',
* 'start block', 'end block' and 'data line' respectively.
*
* Header line explanation:
*
* '='                      Solution operator code. '=' means 'resultant' and is the
*                          only legal cede in a header line. See INPUT/HISTORY
*                          notes.
* 'SNX'                    This is a SINEX document. Other formats may use similar
*                          headers.
* '1.00'                   SINEX version number. MUST be coded. It is used for
*                          backward compatibility whenever required.
* 'NRC 95:122:67080'       The SINEX reference for this file. SINEX files are
*                          referred to by the three-character agency code, and a
*                          creation time-stamp in yy:ddd:sssss format. Agency codes
*                          should have entries in INPUT/ACKNOWLEDGEMENTS.
* 'NRC 95:113:00000
*       95:120:00000' The agency responsible for the data, and the overall
*                          data time span. 'COM' means multiple agencies.
* 'P'                      Technique code. 'P' (GPS) 'L' (SLR) 'R' (VLBI)
*                          'C' (multiple) and 'M' (LLR) are allowed.
* 00117                    This solution estimates 117 parameters.
* 1                        Constraint code. '2' (unconstrained), 'l' (significant
*                          constraints), '0' (fixed/tight constraints) are allowed.
* X E                      This solution includes coordinates and EOP. 'X', 'E'
*                          and 'V' (velocities) 'O' (orbits) are allowed.
*                          (Additional codes may be defined here)
*-------------------------------------------------------------------------------
*        1         2         3         4         5         6         7         8
*234567890123456789012345678901234567890123456789012345678901234567890123456789 0
*-------------------------------------------------------------------------------
+FILE/REFERENCE
* This block always contains the following six records
*info_type_________ info________________________________________________________
 DESCRIPTION        Natural Resources Canada / Geodetic Surveys, altered by NCL
 OUTPUT             NRCan 1995 weekly solution.
 CONTACT            ferland@gdim.geod .emr.ca
 SOFTWARE           combine v0.01
 HARDWARE           HP 750
 INPUT              NRCan daily solution
-FILE/REFERENCE
*-------------------------------------------------------------------------------
+FILE/COMMENT
* This is a free-format block for notes and comments. Substantial remarks
* should go in here, not in * lines.
*
 NB This is not an original NRC document.
 This is an example SINEX document with truncated blocks. Do not process.
-FILE/COMMENT
*-------------------------------------------------------------------------------
+INPUT/HISTORY
* Each input solution used to create this solution is listed here. A series
* of + lines give inputs to a combination - the = code is used for the
* resultant. The format is identical to the header line. The last line should
* always refer to this solution, i.e. match the header line.
```

```
*O_FM VERAGY TIME_STAMP __DAT DATA_START__ DATA_END     T PARAM C TYPE________
 +SNX 0.04 NRC 95:123 :52328 NRC 95:113:00000 95:114:00000 P 00081 2 X E
 +SNX O.O4 NRC 95:123:52590 NRC 95:114:00000 95:115:00000 P 00082 2 X E
 +SNX 0.04 NRC 95:123:52881 NRC 95:115:00000 95:116:00000 P 00082 2 X E
 +SNX 0.04 NRC 95:123:53091 NRC 95:116:00000 95:117:00000 P 00076 2 X E
 +SNX 0.04 NRC 95:123:53365 NRC 95:117:00000 95:118:00000 P 00073 2 X E
 +SNX 0.04 NRC 95:123:53646 NRC 95:118:00000 95:119:00000 P 00079 2 X E
 +SNX 0.04 NRC 95:123:53962 NRC 95:119:00000 95:120:00000 P 00082 2 X E
* ITRF93 ssc/ssv for the 13 ITRF stations in the line below
 +SNX 0.04 NRC 95:121:59613 NRC 95:116:00000 95:117:00000 P 00078 0 XV
 =SNX 1.00 NRC 95:123:55260 NRC 95:113:00000 95:120:OOOOOP 00117 1 XE
-INPUT/HISTORY
*-------------------------------------------------------------------------------
+INPUT/FILES
* Every SINEX file referenced in INPUT/HISTORY should have a filename entered
* here. The last line of this block is always the name of the current file.
* Path names should be given meaningful aliases to keep them short!
*
*AGY TIME_STAMP__ FILE_NAME_____________________ DESCRIPTION____________________
 NRC 95:123:52328 1995/w_798/EMR07980.snx        NRC Daily solution
 NRC 95:123:52590 1995/w_798/EMR07981.snx        NRC Daily solution
 NRC 95:123:52881 1995/w_798/EMR07982.snx        NRC Daily solution
 NRC 95:123:53091 1995/w_798/EMR07983.snx        NRC Daily solution
 NRC 95:123:53365 1995/w_798/EMR07984.snx        NRC Daily solution
 NRC 95:123:53646 1995/w_798/EMR07985.snx        NRC Daily solution
 NRC 95:123:53962 1995/w_798/EMR07986.snx        NRC Daily solution
 NRC 95:121:59613 stacomb_SINEX/950426_apr.snx ITRF93 for 13 stations
 NRC 95:123:55260 stacomb_SINEX/EMR07987.snx     Week 798 combination
-INPUT/FILES
*-------------------------------------------------------------------------------
+INPUT/ACKNOWLEDGMENTS
* Each agency three-character code used in any other block is explained here.
*
*AGY DESCRIPTION________________________________________________________________
 NRC Natural Resources Canada, Geodetic surveys
 NCL Newcastle AAC, University of Newcastle upon Tyne, England.
-INPUT/ACKNOWLEDGMENTS
*-------------------------------------------------------------------------------
+SITE/ID
* Each physical monument is known in SINEX by a four-character site code*
*   (standardised) andan alphabetic point code (arbitrary). Each CODE+PT is
*   equivalent to an IERS DOMES (or DOMEX) code. Each monument estimated in the
*   solution has an entry in this block. Unknown DOMES (DOMEX) codes are
*   represented as M or S following the IERS convention.
*
*CODE PT DOMES     T _STATION_DESCRIPTION___ APPROX_LON_ APPROX_LAT   APP_H_
 ALBH A40129MO03 P Albert Head, Canada       2363045.2  482323.?  31.0
 ALGO A 401O4MOO2 P Algonquin Park, Canada 281 55 43.1 45 57 20.9  200.0
 AREQ A42202MO05P Arequipa, Peru           288 30 26.0 -16 27 55.9 2488.0
 DAV1 A 6601OMOO1 P Davis, Antarctica       77 5821.5 -68 34 38.4    96.0
 DRAO A 401O5MOO2 P Dan. RAdio Obs.,Canada 240 22 30.1 49 19 21.5  541.0
 FAIR A 40408M001 P Fairbanks, U.S.A.      212 30 2.8 64 58 40.9   319.0
 FORT A 41602M001 P Fortaleza, Brazil      321 34 27.8 -3 52 38.9   19.0
 GOLD B 40405S031 P Goldstone, U.S.A.      243 638.8 35 25 30.6    986.0
 GUAM A 50501M002 P Dedego, Guam           144 52 6.2 13 35 21.4   206.0
 KIT3 A 12334M001 P Kitab, Uzbekistan       6653 7.6 39 8 5.2     622.0
 KOKB A 40424MO04 P Kokee Park,Haw.,U.S.A. 200 20 6.3 22 7 34.6   1167.0
 KOSG A 13504MO03 P Kootwijk, Netherlands    5 4834.8 52 10 42.4    96.0
```

```
*CODE PT DOMES     T _STATION_DESCRIPTION    APPROX_LON_ APPROX_LAT_ _APP_H_
 MADR A 13407S012 P Madrid, Spain           355 45 1.3 40 25 45.0   829.0
 MCM4 A 66001M003 P McMurdo, Antarctica     166 40 31.2 -77 50 55.2   -1.0
 NRC1 A      M    P NRC, Ottawa, Canada     284 22 30.0 45 27 15.0    82.0
 KERG A 91201M002 P Kerguelen Is.            70 15 19.9 -49 21 5.3    73.0
 RCM5 A40499S018 P Richmond, Flor. U.S.A. 279 36 57.9 25 36 49.7   -15.0
 SANT A 41705M003 P Santiago, Chile         289 1953.2 -33 9 1.1    723.0
 SCHE A      M    P Schefferville, Canada   293 0   .0 55 0 .0      200.0
 STJO A 4010IM001 P St-John's, Canada       307 1920.2 47 35 42.9   152.0
 TIDB A 50103M108 P Tidbinbilla, Australia 148 58 48.0 -35 23 57.2  665.0
 TROM A 10302M003 P Tromso, Norway           18 5618.0 6939 45.9    132.0
 TSK8 A 21730S005 P Tuskuba, Japan          140 5 15.0 36 620.4      67.0
 WETT A 14201M009 P Wettzell, Germany        12 52 44.1 49 8 39.3   666.0
 YAR1 A 50107M004 P Yaragadee, Australia    115 2049.2 -29 2 47.7   241.0
 YELL A 40127M003 P Yellowknife, Canada     245 31 9.5 62 28 51.3   180.0
 TAIW A 23601M001 P Taipei, Taiwan          121 32 11.6 25 1 16.8    44.0
 HART A 30302M002 P Hartebeesthoek, S. A.    27 4228.0-25 53 13.6 1555.0
 CHUR A      M    P Churchill, Canada       266 0   .0 59 0 .0         .0
 WILL A      M    P Williams Lake, Canada   237 4955.9 52 14 12.9 1097.0
-SITE/ID
*-----------------------------------------------------------------------
+SITE/DATA
* This block contains information on the source of each station.
* Since point and solution codes are
* arbitrary, the station name (SITE+PT+SOLN codes) may be different in the
* input solution - both are given here. Stations which are estimated in
* multiple input files have several lines here.
* The information here is fictional, to illustrate the format.
* Each station is defined in SOLUTION/EPOCHS, and each file (AGY+TIME_STAMP_)
* appears in INPUT/FILES.
*
*SOLUTION     INPUT________
*SITE PT SOLN SITE PT SOLN T DATA_START__ DATA_END____ AGY TIME_STAMP__
 ALBH A    1 ALBH B    1 P 95:113:00000 95:120:00000 NRC 95:123:52328
 ALBH A    1 ALBH A    1 P 95:113:00000 95:120:00000 NRC 95:123:52590
* etc.
 ALGO A    1 ALGO A    1 P 95:113:00000 95:120:00000 NRC 95:123:52328
* etc.
-SITE/DATA
*--------------- ------------------------------------------------------------
+SITE/RECEIVER
* Here each station (SITE+PT+SOLN codes) has receiver details attached. If
* receivers change during the data span for that station, multiple lines are
* used here. These data spans must fit within the overall station span
* (given in SOLUTION/EPOCHS) and should cover the entire span for each station
* and should not overlap.
*
* Note unknown fields are filled with - characters. No field is left blank.
*           ***new to version 1.00***
* The default characters ("----" in the SOLN field means that the information
* refers to all SOLN codes falling in between the start and end epochs.
*
*SITE PT SOLN T DATA_START__ DATA_END____ DESCRIPTION_________ S/N__ FIRMWARE___
 ALBH A    1 P 95:012:67680 00:000:00000 ROGUE SNR-8000        292 3.0.32.2
 ALGO A    1 P 94:355:00000 00:000:00000 ROGUE SNR-8000       T226 3.0.32.2
 AREQ A    1 P 94:032:00000 00:000:00000 ROGUE SNR-8000       T253 2.8.32.1x
 DAV1 A    1 P 94:192:00000 00:000:00000 ROGUE SNR-8100       C119 2.8.1.1
 DRAO A    1 P 95:102:61530 00:000:00000 ROGUE SNR-8000        347 3.0.32.3
```

```
*SITE PT SOLN T DATA_START__ DATA_END____ DESCRIPTION_________ S/N__ FIRMWARE
 FAIR A    1 P 94:125:00000 00:000:00000 ROGUE SNR-8          099 7.8
 FORT A    1 P 93:133:00000 00:000:00000 ROGUE SNR-8000      T119 2.8
 GOLD B    1 P 94:034:00000 00:000:00000 ROGUE SNR-8         ----- 7.6
 GUAM A    1 P 95:020:00000 00:000:00000 ROGUE SNR-8000       36Q 3.0
 KIT3 A    1 P 94:274:00000 00:000:00000 ROGUE SNR-8000      T191 2.8.32.1x
 KERG A    1 P 94:320:00000 00:000:00000 ROGUE SNR-8C        CR306 7.8
 KOKB A    1 P 94:125:00000 00:000:00000 ROGUE SNR-8           10 7.8
 KOSG A    1 P 94:327:00000 00:000:00000 ROWE SNR-8           117 7.8
 MADR A    1 P 94:035:00000 00:000:00000 ROGUE SNR-8         ----- 7.6
 MCM4 A    1 P 95:025:00000 00:000:00000 ROGUE SNR-8000       275 3.0
 NRCl A    1 P 93:001:0000000:000:00000 ROGUE SNR-8000       ----- -----------
 RCM5 A    1 P 95:009:00000 00:000:00000 ROGUE SNR-8000      T160 3.0.32.2
 SANT A    1 P 94:131:00000 00:000:00000 ROGUE SNR-8           95 7.8
 SCHE A    1 P 95:103:00240 00:000:00000 ROGUE SNR-8000       164 3.0.32.2
 STJO A    1 P 95:061:54000 00:000:00000 ROGUE SNR-8000       161 3.3.32.2
 TIDB A    1 P 94:041:00000 00:000:00000 ROGUE SNR-8            3 7.6
 TROM A    1 P 92:259:00000 00:000:00000 ROGUE SNR-8         ----- 4.0
 TSKB A    1 P 93:349:00000 00:000:00000 ROGUE SNR-8000       102 2.8
 WETT A    1 P 91:203:00000 00:000:00000 ROGUE SNR-800        200 7.3
 YARl A    1 P 94:138:00000 00:000:00000 ROGUE SNR-8            9 7.8
 YELLA     1 P 94:131:53520 00:000:00000 ROGUE SNR-8000      T302 2.8.32.1
 TAIW A    1 P 93:293:00000 00:000:00000 ROGUE SNR-8000       201 7.0
 HART A    1 P 91:001:00000 00:000:00000 ROGUE SNR-8          114 7.3
 CHUR A    1 P 94:103:72240 00:000:00000 ROGUE SNR-8000       305 3.0.32.1
 WILL A    1 P 93:279:68580 00:000:00000 ROGUE SNR-8000       165 -----------
-SITE/RECEIVER
*------------------------------------------------------------------------------
+SITE/ANTENNA
*
* Here each station (SITE+PT+SOLN codes) has antema details attached. If
* antennae change during the data span for that station, multiple lines are
* used here. These data spans must fit within the overall station span
* (given in SOLUTION/EPOCHS) and should cover the entire span for each station
* and should not overlap.
*
* Note unknown fields filled with '-' characters. No field is left blank.
*          ***new to version 1.00***
* The default characters ("----" in the SOLN field means that the information
* refers to all SOLN codes falling in between start and end epoch.
*
*SITE PT SOLN T DATA_START__DATA_END____DESCRIPTION_________ S/N__
 ALBH A    1 P 95:011:80100 00:000:00000 DORNE MARGOLIN T      368
 ALGO A    1 P 94:047:69300 00:000:00000 DORNE MARGOLIN T      173
 AREQ A    1 P 94:032:00000 00:000:00000 DORNE MARGOLIN T      294
 DAV1 A    1 P 94:192:00000 00:000:00000 DORNE MARGOLIN T      277
 DRAO A    1 P 95:102:64260 00:000:00000 DORNE MARGOLIN T      172
 FAIR A    1 P 91:290:00000 00:000:00000 DORNE MARGOLIN R       96
 FORT A    1 P 93:133:00000 00:000:00000 DORNE MARGOLIN T      119
 GOLD B    1 P 92:180:00000 00:000:00000 DORNE MARGOLIN R       95
 GUAM A    1 P 95:020:00000 00:000:00000 DORNE MARGOLIN T      481
 KIT3 A    1 P 94:274:00000 00:000:00000 DORNE MARGOLIN T      362
 KERG A    1 P 94:320:00000 00:000:00000 DORNE MARGOLIN T      154
 KOKB A    1 P 91:106:00000 00:000:00000 DORNE MARGOLIN R       10
 KOSG A    1 P 91:001:00000 00:000:00000 DORNE MARGOLIN B      119
 MADR A    1 P 89:349:00000 00:000:00000 DORNE MARGOLIN R    -----
 MCM4 A    1 P 95:025:00000 00:000:00000 DORNE MARGOLIN T      363
 NRC1 A    1 P 93:001:00000 00:000:00000 DORNE MARGOLIN T    -----
```

```
*SITE PT SOLN T DATA_START_ DATA_END____ DESCRIPTION_________ S/N_
 RCM5  A    1 P 94:195:00000 00:000:00000 DORNE MARGOLIN T      148
 SANTA      1 P 92:035:00000 00:000:00000 DORNE MARGOLIN R       95
 SCHE  A    1 P 94:196:00420 00:000:00000 DORNE MARGOLIN T      386
 STJO  A    1 P 95:061:78960 00:000:00000 DORNE MARGOLIN T      171
 TIDB  A    1 P 92:033:00000 00:000:00000 DORNE MARGOLIN R        2
 TROM  A    1 P 92:259:00000 00:000:00000 DORNE MARGOLIN B    -----
 TSKB  A    1 P 94:227:00000 00:000:00000 DORNE MARGOLIN T      105
 WETT  A    1 P 91:203:00000 00:000:00000 DORNE MARGOLIN B      113
 YAR1  A    1 P 90:337:00000 00:000:00000 DORNE MARGOLIN R        3
 YELL  A    1 P 94:075:72000 00:000:00000 DORNE MARGOLIN T      273
 TAIW  A    1 P 90:335:00000 00:000:00000 DORNE MARGOLIN B      118
 HART  A    1 P 95:026:00000 00:000:00000 DORNE MARGOLIN T    -----
 CHUR  A    1 P 94:103:72240 00:000:00000 DORNE MARGOLIN T      387
 WILL  A    1 P 93:279:68580 00:000:00000 DORNE MARGOLIN T    -----
-SITE/ANTENNA
*-------------------------------------------------------------------------------
+SITE/GPS_PHASE_CENTER
*
* Here each antenna (DESCRIPTION + S/N fields) listed in SITE/ANTENNA has phase
* center details attached.
*
* Note unknown fields filled with - characters. No field is left blank.
*
*                           UP     NORTH_ EAST__ UP____ NORTH_ EAST_
*DESCRIPTION_________ S/N  L1->ARP(m)__________ __L2->ARP(m)________ AZ EL
 DORNE MARGOLIN B     -----  .0780  .0000  .0000  .0960  .0000  .0000   None
 DORNE MARGOLIN B       113  .0780  .0000  .0000  .0960  .0000  .0000   None
 DORNE MARGOLIN B       119  .0780  .0000  .0000  .0960  .0000  .0000   None
 DORNE MARGOLIN R     -----  .0780  .0000  .0000  .0960  .0000  .0000   None
 DORNE MARGOLIN R         2  .0780  .0000  .0000  .0960  .0000  .0000   None
 DORNE MARGOLIN R         3  .0780  .0000  .0000  .0960  .0000  .0000   None
 DORNE MARGOLIN R        10  .0780  .0000  .0000  .0960  .0000  .0000   None
 DORNE MARGOLIN R        95  .0780  .0000  .0000  .0960  .0000  .0000   None
 DORNE MARGOLIN R        96  .0780  .0000  .0000  .0960  .0000  .0000   None
 DORNE MARGOLIN T     -----  .1100  .0000  .0000  .1280  .0000  .0000   None
 DORNE MARGOLIN T       105  .1100  .0000  .0000  .1280  .0000  .0000   None
 DORNE MARGOLIN T       119  .1100  .0000  .0000  .1280  .0000  .0000   None
 DORNE MARGOLIN T       148  .1100  .0000  .0000  .1280  .0000  .0000   None
 DORNE MARGOLIN T       154  .1100  .0000  .0000  .1280  .0000  .0000   None
 DORNE MARGOLIN T       171  .1100  .0000  .0000  .1280  .0000  .0000   None
 DORNE MARGOLIN T       172  .1100  .0000  .0000  .1280  .0000  .0000   None
-SITE/GPS_PHASE_CENTER
*-------------------------------------------------------------------------------
+SITE/ECCENTRICITY
*
* Here each station (SITE+PT+SOLN codes) has eccentricity vectors attached. If
* these change during the data span for that station, multiple lines are
* used here. These data spans must fit within the overall station span
* (given in SOLUTION/EPOCHS), should cover the entire span for each station and
* must not overlap.
```

```
*                                                   UP______ NORTH   EAST
*SITE PT SOLN T DATA_START__ DATA_END_    AXE ARP->BENCHMARK(m)_________
 ALBH A    1 P 95: 011:80100 00:000:00000 UNE    .1000     .0000     .0000
 ALGO A    1 P 94:139:00000 00:000:00000 UNE     .1000     .0000     .0000
 AREQ A    1 P 94:088:00000 00:000:00000 UNE     .0610     .0000     .0000
 DAV1 A    1 P 94:192:00000 00:000:00000 UNE     .0035     .0000     .0000
 DRAO A    1 P 95:102:64260 00:000:00000 UNE     .1000     .0000     .0000
 FAIR A    1 P 91:290:00000 00:000:00000 UNE     .1160     .0000     .0000
 FORT A    1 P 93:133:00000 00:000:00000 UNE     .6430     .0000     .0000
 GOLD B    1 P 92:180:00000 00:000:00000 UNE     .0000     .0000     .0000
 GUAM A    1 P 95:020:00000 00:000:00000 UNE     .0614     .0000     .0000
 KIT3 A    1 P 94:274:00000 00:000:00000 UNE     .0460     .0000     .0000
 KERG A    1 P 94:320:00000 00:000:00000 UNE     .4200     .0000     .0000
 KOKB A    1 P 91:106:00000 00:000:00000 UNE     .0930     .0000     .0000
 KOSG A    1 P 94:001:00000 00:000:00000 UNE     .1050     .0000     .0000
 MADR A    1 P 89:349:00000 00:000:00000 UNE     .0000     .0000     .0000
 MCM4 A    1 P 95:025:00000 00:000:00000 UNE     .1830     .0000     .0000
 NRC1 A    1 P 93:001:00000 00:000:00000 UNE     .0000     .0000     .0000
 RCM5 A    1 P 93:284:00000 00:000:00000 UNE     .0000     .0000     .0000
 SANT A    1 P 92:035:00000 00:000:00000 UNE     .0930     .0000     .0000
 SCHE A    1 P 94:196:00420 00:000:00000 UNE     .1000     .0000     .0000
 STJO A    1 P 95:057:48480 00:000:00000 UNE     .1000     .0000     .0000
 TIDB A    1 P 92:033:00000 00:000:00000 UNE     .0920     .0000     .0000
 TROM A    1 P 92:259:00000 00:000:00000 UNE    2.4734     .0000     .0000
 TSKB A    1 P 94:227:00000 00:000:00000 UNE     .0000     .0000     .0000
 WETT A    1 P 91:203:00000 00:000:00000 UNE     .0000     .0000     .0000
 YAR1 A    1 P 90:337:00000 00:000:00000 UNE     .0730     .0000     .0000
 YELL A    1 P 94:287:00900 00:000:00000 UNE     .1000     .0000     .0000
 TAIW A    1 P 90:335:00000 00:000:00000 UNE    1.7685     .0000     .0000
 HART A    1 P 91:001:00000 00:000:00000 UNE    9.7540     .0000     .0000
 CHUR A    1 P 94:103:72240 00:000:00000 UNE     .0000     .0000     .0000
 WILL A    1 P 93:279:68580 00:000:00000 UNE     .0010     .0000     .0000
-SITE/ECCENTRICITY
*-------------------------------------------------------------------------
+SOLUTION/EPOCHS
*
* This block is the logical starting-point for interpreting the file, since it
* defines the stations in the solution. A station is particular solution for
* a monument, referenced by SITE, PT and SOLN codes. Multiple integer solution
* codes may be used (arbitrarily) to give multiple solutions for a point in the
* same estimate - at different epochs, for instance.
*
* Each station invoked here should have one or more entries in each of
* SITE/RECEIVER, SITE/ANTENNA, SITE/DATA and SITE/ECCENTRICITY.
* The monument (SITE+PT) should be defined in SITE/ID.
*
*SITE PT SOLN T _DATA_START_ __DATA_END__ _MEAN_EPOCH_
 ALBH A    1 P 95:113:00000 95:120:00000 95:116:43200
 ALGO A    1 P 95:113:00000 95:120:00000 95:116:43200
 AREQ A    1 P 95:113:00000 95:120:00000 95:116:28800
 CHUR A    1 P 95:118:00000 95:120:00000 95:119:00000
 DAV1 A    1 P 95:113:00000 95:114:00000 95:113:43200
 DRAO A    1 P 95:113:00000 95:120:00000 95:116:43200
 FAIR A    1 P 95:113:00000 95:120:00000 95:116:43200
 FORT A    1 P 95:113:00000 95:118:00000 95:115:21600
 GOLD B    1 P 95:113:00000 95:120:00000 95:116:43200
 GUAM A    1 P 95:113:00000 95:120:00000 95:116:43200
 HART A    1 P 95:115:00000 95:120:00000 95:117:28800
```

```
*SITE PT SOLN T DATA_START__ __DATA_END__ _MEAN_EPOCH_
 KERG  A    1 P 95:113:00000 95:120:00000 95:116:43200
 KIT3  A    1 P 95:113:00000 95:119:00000 95:116:00000
 KOKB  A    1 P 95:113:00000 95:120:00000 95:116:43200
 KOSG  A    1 P 95:113:00000 95:120:00000 95:116:43200
 MADR  A    1 P 95:113:00000 95:120:00000 95:116:43200
 MCM4  A    1 P 95:113:00000 95:120:00000 95:116:14400
 NRC1  A    1 P 95:113:00000 95:120:00000 95:116:43200
 RCM5  A    1 P 95:113:00000 95:120:00000 95:116:43200
 SANT  A    1 P 95:113:00000 95:120:00000 95:116:43200
 SCHE  A    1 P 95:113:00000 95:116:00000 95:114:43200
 STJO  A    1 P 95:113:00000 95:120:00000 95:116:43200
 TAIW  A    1 P 95:114:00000 95:120:00000 95:117:43200
 TIDB  A    1 P 95:113:00000 95:120:00000 95:116:43200
 TROM  A    1 P 95:113:00000 95:120:00000 95:116:43200
 TSKB  A    1 P 95:113:00000 95:120:00000 95:116:43200
 WETT  A    1 P 95:113:00000 95:120:00000 95:116:00000
 WILL  A    1 P 95:118:00000 95:120:00000 95:119:00000
 YAR1  A    1 P 95:113:00000 95:120:00000 95:116:43200
 YELL  A    1 P 95:113:00000 95:120:00000 95:116:43200
-SOLUTION/EPOCHS
*-------------------------------------------------------------------------------
+SOLUTION/ESTIMATE
*
* The parameter estimates are written here. Parameter types STAX, STAY, STAZ,
* VELX, VELY, VELZ (coordinate and velocity x, y, z) are followed by a
* station reference. Erp types LOD, UT, XPO, YPO have no station. The
* constraint code (0, 1 or 2) is given here for each parameter - the empty
* fields are filled with a data-not-given character (-)
*
*                  *** New to version 1.00 ***
*
*    TYPE increased to 6 chars, ESTIMATED Value field to 21 chars, STD
*    decreased to 11chars (included here for information only) ***
*    The STDS for consistency must be the same as the corresponding values
*    derived from the MATRIX blocks, which are given to full num. precision.
*INDEX TYPE__ CODE PT SOLN _REF_EPOCH__ UNIT S __ESTIMATED VALUE____ _STD_DEV
     1 STAX   ALBH  A    1 95:116:43200 m    2 -.234133292758691E+7 .1845776E-2
     2 STAY   ALBH  A    1 95:116:43200 m    2 -.353904953122971E+7 .1890911E-2
     3 STAZ   ALBH  A    1 95:116:43200 m    2  .474579146627762lE+7 .2075918E-2
     4 STAX   AI-GO A    1 95:116:43200 m    1  .918129492990467 4E+6 .1768625E-2
     5 STAY   ALGO  A    1 95:116:43200 m    1 -.434607120901217E+7 .1797731E-2
     6 STAZ   ALGO  A    1 95:116:43200 m    1  .456197784042848 9E+7 .1878956E-2
     7 STAX   AREQ  A    1 95:116:28800 m    2  .194282668752556 1E+7 .6477347E-2
     8 STAY   AREQ  A    1 95:116:28800 m    2 -.580407019776578E+7 .8829387E-2
     9 STAZ   AREQ  A    1 95:116:28800 m    2 -.179689395509440E+7 .3872643E-2
    10 STAX   CHUR  A    1 95:119:00000 m    2 -.236438707221352E+6 .2190659E-2
    11 STAY   CHUR  A    1 95:119:00000 m    2 -.330761674613259E+7 .2499980E-2
    12 STAZ   CHUR  A    1 95:119:00000 m    2  .543004917038484 5E+7 .3338507E-2
    13 STAX   DAV1  A    1 95:113:43200 m    2  .486854552427363 2E+6 .5143560E-2
    14 STAY   DAV1  A    1 95:113:43200 m    2  .228509936446627 1E+7 .5465295E-2
    15 STAZ   DAV1  A    1 95:113:43200 m    2 -.591495576584752E+7 .8718856E-2
    16 STAX   DRAO  A    1 95:116:43200 m    2 -.205916467723249E+7 .1818058E-2
    17 STAY   DRAO  A    1 95:116:43200 m    2 -.362110834605865E+7 .1859042E-2
    18 STAZ   DRAO  A    1 95:116:43200 m    2  .481443238680934 6E+7 .2053716E-2
    19 STAX   FAIR  A    1 95:116:43200 m    0 -.228162142409438E+7 .2008781E-2
    20 STAY   FAIR  A    1 95:116:43200 m    0 -.145359574941003E+7 .2100198E-2
    21 STAZ   FAIR  A    1 95:116:43200 m    0  .575696193640600 8E+7 .2509140E-2
    22 STAX   FORT  A    1 95:115:21600 m    2  .498538657850238 4E+7 .1084655E-1
```

*INDEX	TYPE	CODE	PT	SOLN	REF EPOCH	UNIT	S	ESTIMATED VALUE	STD_DEV
23	STAY	FORT	A	1	95:115:21600	m	2	-.395499854274894E+7	.9229132E-2
24	STAZ	FORT	A	1	95:115:21600	m	2	-.428426474252779E+6	.2879426E-2
25	STAX	GOLD	B	1	95:116:43200	m	1	-.235361417310070E+7	.2060113E-2
26	STAY	GOLD	B	1	95:116:43200	m	1	-.464138536535744E+7	.2135362E-2
27	STAZ	GOLD	B	1	95:116:43200	m	1	.3676976474604919E+7	.2151652E-2
28	STAX	GUAM	A	1	95:116:43200	m	2	-.507131279252173E+7	.3359775E-2
29	STAY	GUAM	A	1	95:116:43200	m	2	.3568363515536474E+7	.3434317E-2
30	STAZ	GUAM	A	1	95:116:43200	m	2	.1488904271291384E+7	.2465369E-2
31	STAX	HART	A	1	95:117:28800	m	0	.5084625439996016E+7	.3117434E-2
32	STAY	HART	A	1	95:117:28800	m	0	.2670366550990838E+7	.2988406E-2
33	STAZ	HART	A	1	95:117:28800	m	1	-.276849396332954E+7	.2436794E-2
34	STAX	KERG	A	1	95:116:43200	m	2	.1406337354635808E+7	.3228912E-2
35	STAY	KERG	A	1	95:116:43200	m	2	.3918161143630010E+7	.3090251E-2
36	STAZ	KERG	A	1	95:116:43200	m	2	-.481616739541420E+7	.2887894E-2
37	STAX	KIT3	A	1	95:116:00000	m	2	.1944945408967126E+7	.3880638E-2
38	STAY	KIT3	A	1	95:116:00000	m	2	.4556652228809900E+7	.4395018E-2
39	STAZ	KIT3	A	1	95:116:00000	m	2	.4004325952269760E+7	.4075488E-2
40	STAX	KOKB	A	1	95:116:43200	m	0	-.554383812506372E+7	.2572993E-2
41	STAY	KOKB	A	1	95:116:43200	m	0	-.205458735000368E+7	.2349073E-2
42	STAZ	KOK8	A	1	95:116:43200	m	1	.2387809656652860E+7	.2100031E-2
43	STAX	KOSG	A	1	95:116:43200	m	1	.3899225249570046E+7	.1777152E-2
44	STAY	KOSG	A	1	95:116:43200	m	1	.3967318114717967E+6	.1725390E-2
45	STAZ	KOSG	A	1	95:116:43200	m	1	.5015078333904634E+7	.1593831E-2
46	STAX	MADR	A	1	95:116:43200	m	1	.4849202445485532E+7	.1730374E-2
47	STAY	MADR	A	1	95:116:43200	m	1	-.360329133978604E+6	.1739288E-2
48	STAZ	MADR	A	1	95:116:43200	m	1	.4114913089855005E+7	.1417137E-2
49	STAX	MCM4	A	1	95:116:14400	m	2	-.131170323900895E+7	.2978227E-2
50	STAY	MCM4	A	1	95:116:14400	m	2	.3108151420651672E+6	.3072598E-2
51	STAZ	MCM4	A	1	95:116:14400	m	2	-.621325504790322E+7	.4581133E-2
52	STAX	NRC1	A	1	95:116:43200	m	2	.1112777313114861E+7	.1834574E-2
53	STAY	NRC1	A	1	95:116:43200	m	2	-.434147580328482E+7	.1899372E-2
54	STAZ	NRC1	A	1	95:116:43200	m	2	.4522955793195269E+7	.2001532E-2
55	STAX	RCM5	A	1	95:116:43200	m	2	.9613347339731020E+6	.2721087E-2
56	STAY	RCM5	A	1	95:116:43200	m	2	-.567407417401052E+7	.4543879E-2
57	STAZ	RCM5	A	1	95:116:43200	m	2	.2740535190143120E+7	.2918609E-2
58	STAX	SANT	A	1	95:116:43200	m	0	.1769693284302684E+7	.3096912E-2
59	STAY	SANT	A	1	95:116:43200	m	0	-.504457411643344E+7	.3047045E-2
60	STAZ	SANT	A	1	95:116:43200	m	1	-.346832104809249E+7	.2679039E-2
61	STAX	SCHE	A	1	95:114:43200	m	2	.1450982826872315E+7	.2170755E-2
62	STAY	SCHE	A	1	95:114:43200	m	2	-.338693424191906E+7	.2378425E-2
63	STAZ	SCHE	A	1	95:114:43200	m	2	.5189301335610829E+7	.2882939E-2
64	STAX	STJO	A	1	95:116:43200	m	2	.2612631222496210E+7	.1852240E-2
65	STAY	STJO	A	1	95:116:43200	m	2	-.342680699958938E+7	.1909100E-2
66	STAZ	STJO	A	1	95:116:43200	m	2	.4686757814504888E+7	.1941888E-2
67	STAX	TAIW	A	1	95:117:43200	m	2	-.302478192993486E+7	.3600265E-2
68	STAY	TAIW	A	1	95:117:43200	m	2	.4928936907613859E+7	.4052780E-2
69	STAZ	TAIW	A	1	95:117:43200	m	2	.2681234449924764E+7	.2902421E-2
70	STAX	TIDB	A	1	95:116:43200	m	0	-.446099608394879E+7	.2950717E-2
71	STAY	TIDB	A	1	95:116:43200	m	0	.2682557122624863E+7	.2958276E-2
72	STAZ	TIDB	A	1	95:116:43200	m	1	-.367444382121832E+7	.2716867E-2
73	STAX	TROM	A	1	95:116:43200	m	1	.2102940345331658E+7	.2258738E-2
74	STAY	TROM	A	1	95:116:43200	m	1	.7215693988724571E+6	.2336037E-2
75	STAZ	TROM	A	1	95:116:43200	m	0	.5958192085393612E+7	.3604893E-2
76	STAX	TSKB	A	1	95:116:43200	m	2	-.395719924355657E+7	.2924832E-2
77	STAY	TSKB	A	1	95:116:43200	m	2	.3310199709624858E+7	.3038009E-2
78	STAZ	TSKB	A	1	95:116:43200	m	2	.3737711702012423E+7	.2546651E-2
79	STAX	WETT	A	1	95:116:00000	m	1	.4075578580084480E+7	.1776241E-2

```
*INDEX TYPE   CODE PT SOLN REF EPOCH   UNIT S  ESTIMATED VALUE       STD_DEV
    80 STAY   WETT A    155: 116: 00000 m    1  .9318526769029480E+6 .1731380E-2
    81 STAZ   WETT A    1 95:116:00000 m     O  .4801570021461830E+7 .1457045E-2
    82 STAX   WILL A    1 95:119:00000 m     2 -.208425800223933E+7  .2188081E-2
    83 STAY   WILL A    1 95:119:00000 m     2 -.331387295088804E+7  .2351786E-2
    84 STAZ   WILL A    1 95:119:00000 m     2  .501985312109704OE+7 .2824378E-2
    85 STAX   YAR1 A    1 95:116:43200 m     1 -.238902544223632E+7  .2931452E-2
    86 STAY   YAR1 A    1 95:116:43200 m     1  .5043316884438646E+7 .2937762E-2
    87 STAZ   YAR1 A    1 95:116:43200 m     1 -.307853084113885E+7  .2538746E-2
    88 STAX   YELL A    1 95:116:43200 m     1 -.122445249322380E+7  .2055871E-2
    89 STAY   YELL A    1 95:116:43200 m     1 -.268921606751285E+7  .2061675E-2
    90 STA2   YELL A    1 95:116:43200 m     1  .5633638286707014E+7 .3035230E-2
    91 LOD    ---- --   1 95:113:43200 ms    2  .2871055744817214E+1 .1212729E-1
    92 LOD    ---- --   2 95:114:43200 ms    2  .2959652540110830E+1 .1131045E-1
    93 LOD    ---- --   3 95:115:43200 ms    2  .2973492029661421E+1 .1201761E-1
    94 LOD    ---- --   4 95:l16:43200ms     2  .2919511470925497E+1 .1199782E-1
    95 LOD    ---- --   5 95:117:43200 ms    2  .2799350739071390E+1 .1192584E-1
    96 LOD    ---- --   6 95:118:43200 ms    2  .2600397770842830E+1 .1188556E-1
    97 LOD    ---- --   7 95:119:43200 ms    2  .2430330357604413E+1 .1082158E-1
    98 UT     ---- --   1 95:114:43200 ms    2  .8722024405764063E+2 .1318171E-1
    99 UT     ---- --   2 95:115:43200 ms    2  .8430515991559695E+2 .1575504E-1
   100 UT     ---- --   3 95:116:43200 ms    2  .8136510032786199E+2 .1745336E-1
   101 UT     ---- --   4 95:117:43200 ms    2  .7849507028080811E+2 .1867862E-1
   102 UT     ---- --   5 95:118:43200 ms    2  .7572503990368940E+2 .1998887E-1
   103 UT     ---- --   6 95:119:43200 ms    2  .7312024540830212E+2 .2099974E-1
   104 XPo    ---- --   1 95:113:43200 mas   2  .1029608387361842E+3 .7876117E-1
   105 XPo    ---- --   2 95:114:43200 mas   2  .1069725602672064E+3 .7569313E-1
   106 XPO    ---- --   3 95:115:43200 mas   2  .1113899879374726E+3 .7622913E-1
   107 XPo    ---- --   4 95:116:43200 mas   2  .1154778670578098E+3 .7722355E-l
   108 XPO    ---- --   5 95:117:43200 mas   2  .1194089883086856E+3 .7541868E-1
   109 XPo    ---- --   6 95:118:43200 mas   2  .1236303461298091E+3 .7505631E-1
   110 XPO    ---- --   7 95:119:43200 mas   2  .1275168152328533E+3 .7039234E-1
   111 YPo    ---- --   1 95:113:43200 mas   2  .5530926512007116E+3 .9289514E-1
   112 YPo    ---- --   2 95:114:43200 mas   2  .5521110887312243E+3 .8795571E-1
   113 YPo    ---- --   3 95:115:43200 mas   2  .5512599272862197E+3 .8666021E-1
   114 YPo    ---- --   4 95:116:43200 mas   2  .5497716474578965E+3 .8859832E-1
   115 YPo    ---- --   5 95:l17:43200mas    2  .5485830683498143E+3 .8738927E-1
   116 YPO    ---- --   6 95:118:43200 mas   2  .5470190294873472E+3 .8867092E-1
   117 YPo    ---- --   7 95:119:43200 mas   2  .5455323053395770E+3 .8377195E-1
-SOLUTION/ESTIMATE
*-----------------------------------------------------------------------------
+SOLUTION/APRIORI
*
* The same format as the previous block, but parameters given, and their
* order, can be different.
*
* ITRF93(1995.318) coord. constraints for the 13 stations applied (ITRF SSC+
* SSV sigmas used, responsible for correlation in APRIORI matrix)
*                  *** New to version 1.00 ***
*
*    TYPE increased to 6 chars, ESTIMATED Value field to 21 chars, STD
*    decreased to 11chars (included here for information only) ***
*    The STDS for consistency must be the [illegible] as the corresponding values
*    derived from the [illegible] blocks.
*
```

*INDEX	TYPE__	CODE	PT	SOLN	REF_EPOCH	UNIT	S	__ESTIMATED VALUE___	_STD_DEV
1	STAX	ALGO	A	1	95:116:43200	m	2	.91812950316301E+06	.300264E-02
2	STAY	ALGO	A	1	95:116:43200	m	2	-.43460712286616E+07	.300413E-02
3	STAZ	ALGO	A	1	95:116:43200	m	2	.45619778480795E+07	.300413E-02
4	STAX	FAIR	A	1	95:116:43200	m	2	-.22816214309794E+07	.300148E-02
5	STAY	FAIR	A	1	95:116:43200	m	2	-.14535957605986E+07	.300264E-02
6	STAZ	FAIR	A	1	95:116:43200	m	2	.57569619418178E+07	.300264E-02
7	STAX	GOLD	B	1	95:116:43200	m	2	-.23536141750178E+07	.400111E-02
8	STAY	GOLD	B	1	95:116:43200	m	2	-.46413853870781E+07	.500089E-02
9	STAZ	GOLD	B	1	95:116:43200	m	2	.36769764725192E+07	.500089E-02
10	STAX	HART	A	1	95:116:43200	m	2	.50846254292986E+07	.401782E-02
11	STAY	HART	A	1	95:116:43200	m	2	.26703665485452E+07	.400793E-02
12	STAZ	HART	A	1	95:116:43200	m	2	-.27684939831945E+07	.400607E-02
13	STAX	KOKB	A	1	95:116:43200	m	2	-.55438381300644E+07	.300413E-02
14	STAY	KOKB	A	1	95:116:43200	m	2	-.20545873456548E+07	.300264E-02
15	STAZ	KOKB	A	1	95:116:43200	m	2	.23878096512000E+07	.300413E-02
16	STAX	KOSG	A	1	95:116:43200	m	2	.38992252531315E+07	.502860E-02
17	STAY	KOSG	A	1	95:116:43200	m	2	.39673180967945E+06	.502534E-02
18	STAZ	KOSG	A	1	95:116:43200	m	2	.50150783278438E+07	.304205E-02
19	STAX	MADR	A	1	95:116:43200	m	2	.48492024545575E+07	.300595E-02
20	STAY	MADR	A	1	95:116:43200	m	2	-.36032914100548E+06	.300264E-02
21	STAZ	MADR	A	1	95:116:43200	m	2	.41149130953329E+07	.200891E-02
22	STAX	SANTA		1	95:116:43200	m	2	.17696932851836E+07	.405435E-02
23	STAY	SANTA		1	95:116:43200	m	2	-.50445741389849E+07	.403570E-02
24	STAZ	SANTA		1	95:116:43200	m	2	-.34683210399342E+07	.406511E-02
25	STAX	TIDB	A	1	95:116:43200	m	2	-.44609960811534E+07	.400793E-02
26	STAY	TIDB	A	1	95:116:43200	m	2	.26825571044644E+07	.400446E-02
27	STAZ	TIDB	A	1	95:116:43200	m	2	-.36744438230192E+07	.400607E-02
28	STAX	TROM	A	1	95:116:43200	m	2	.21029403520603E+07	.422320E-02
29	STAY	TROM	A	1	95:116:43200	m	2	.72156940310411E+06	.413292E-02
30	STAZ	TROM	A	1	95:116:43200	m	2	.59581920940479E+07	.490313E-02
31	STAX	WETT	A	1	95:116:43200	m	2	.40755785850603E+07	.300264E-02
32	STAY	WETT	A	1	95:116:43200	m	2	.93185266801781E+06	.300148E-02
33	STAZ	WETT	A	1	95:116:43200	m	2	.48015700238753E+07	.200396E-02
34	STAX	YAR1	A	1	95:116:43200	m	2	-.23890254414616E+07	.500803E-02
35	STAY	YAR1	A	1	95:116:43200	m	2	.50433168528356E+07	.501674E-02
36	STAZ	YAR1	A	1	95:116:43200	m	2	-.30785308583027E+07	.401238E-02
37	STAX	YELL	A	1	95:116:43200	m	2	-.12244524961055E+07	.320725E-02
38	STAY	YELL	A	1	95:116:43200	m	2	-.26892160698110E+07	.338846E-02
39	STAZ	YELL	A	1	95:116:43200	m	2	.56336382822123E+07	.484908E-02
40	VELX	ALGO	A	1	95:116:43200	m/y	2	-.21700000000000E-01	.400000E-03
41	VELY	ALGO	A	1	95:116:43200	m/y	2	-.21000000000000E-02	.500000E-03
42	VELZ	ALGO	A	1	95:116:43200	m/y	2	.66000000000000E-02	.500000E-03
43	VELX	FAIR	A	1	95:116:43200	m/y	2	-.28500000000000E-01	.300000E-03
44	VELY	FAIR	A	1	95:116:43200	m/y	2	-.19000000000000E-02	.400000E-03
45	VELZ	FAIR	A	1	95:116:43200	m/y	2	-.10100000000000E-01	.400000E-03
46	VELX	GOLD	B	1	95:116:43200	m/y	2	-.19100000000000E-01	.300000E-03
47	VELY	GOLD	B	1	95:116:43200	m/y	2	.61000000000000E-02	.300000E-03
48	VELZ	GOLD	B	1	95:116:43200	m/y	2	-.47000000000000E-02	.300000E-03
49	VELX	HART	A	1	95:116:43200	m/y	2	-.54000000000000E-02	.120000E-02
50	VELY	HART	A	1	95:116:43200	m/y	2	.17600000000000E-01	.800000E-03
51	VELZ	HART	A	1	95:116:43200	m/y	2	.21600000000000E-01	.700000E-03
52	VELX	KOKB	A	1	95:116:43200	m/y	2	-.12900000000000E-01	.500000E-03
53	VELY	KOKB	A	1	95:116:43200	m/y	2	.61400000000000E-01	.400000E-03
54	VELZ	KOKB	A	1	95:116:43200	m/y	2	.29200000000000E-01	.500000E-03
55	VELX	KOSG	A	1	95:116:43200	m/y	2	-.21800000000000E-01	.170000E-02
56	VELY	KOSG	A	1	95:116:43200	m/y	2	.21200000000000E-01	.160000E-02
57	VELZ	KOSG	A	1	95:116:43200	m/y	2	.12200000000000E-01	.160000E-02

```
*INDEX TYPE_  CODE PT SOLN REF_EPOCH___  UNIT S _ESTIMATED VALUE      _STD_DEV
    58 VELX   MADR  A    1 95:116:43200 m/y  2 -.14100000000000E-01  .600000E-03
    59 VELY   MADR  A    1 95:116:43200 m/y  2  .22200000000000E-01  .400000E-03
    60 VELZ   MADR  A    1 95:116:43200 m/y  2  .20100000000000E-01  .600000E-03
    61 VELX   SANTA      1 95:116:43200 m/y  2  .22800000000000E-01  .210000E-02
    62 VELY   SANTA      1 95:116:43200 m/y  2 -.63000000000000E-02  .170000E-02
    63 VELZ   SANTA      1 95:116:43200 m/y  2  .25600000000000E-01  .230000E-02
    64 VELX   TIDB  A    1 95:116:43200 m/y  2 -.35400000000000E-01  .800000E-03
    65 VELY   TIDB  A    1 95:116:43200 m/y  2 -.17000000000000E-02  .600000E-03
    66 VELZ   TIDB  A    1 95:116:43200 m/y  2  .41200000000000E-01  .700000E-03
    67 VELX   TROM  A    1 95:116:43200 m/y  2 -.25200000000000E-01  .430000E-02
    68 VELY   TROM  A    1 95:116:43200 m/y  2  .16200000000000E-01  .330000E-02
    69 VELZ   TROM  A    1 95:116:43200 m/y  2  .65000000000000E-02  .900000E-02
    70 VELX   WETT  A    1 95:116:43200 m/y  2 -.25200000000000E-01  .400000E-03
    71 VELY   WETT  A    1 95:116:43200 m/y  2  .19100000000000E-01  .300000E-03
    72 VELZ   WETT  A    1 95:116:43200 m/y  2  .12300000000000E-01  .400000E-03
    73 VELX   YAR1  A    1 95:116:43200 m/y  2 -.45900000000000E-01  .900000E-03
    74 VELY   YAR1  A    1 95:116:43200 m/y  2  .90000000000000E-02  .130000E-02
    75 VELZ   YAR1  A    1 95:116:43200 m/y  2  .40300000000000E-01  .100000E-02
    76 VELX   YELL  A    1 95:116:43200 m/y  2 -.28900000000000E-01  .360000E-02
    77 VELY   YELL  A    1 95:116:43200 m/y  2  .60000000000000E-03  .500000E-02
    78 VELZ   YELL  A    1 95:116:43200 m/y  2 -.25000000000000E-02  .870000E-02
-SOLUTION/APRIORI
*-------------------------------------------------------------------------------
+SOLUTION/MATRIX_ESTIMATE L CORR
* Lower triangular correlation matrix elements, referenced by two parameter
* index numbers from SOLUTION/ESTIMATE, are given here.
*                  ***New to version 1.00 ***
*    The PARA fields increased to 21 chars, For CORR STDS must be given on
*    the main diagonal
*
*PARA1 PARA2     PARA2+0______________PARA2+1______________PARA2+2__________
      1     1  .184577690512345-02
      2     1  .29425156137028E-01  .18909112191234E-02
      3     1 -.26004023015799E+00 -.28793741628090E+00  .20759188181234E+01
      4     1  .54687523972711E+00 -.65452884277258E-01 -.43204669126067E-01
      4     4  .17686254341234E-02
      5     1 -.39819911260492E-01  .40433299131131E+00  .11136939059432E+00
      5     4 -.50106659384620E-02  .17977311401234E-02
      6     1 -.35321953180784E-01  .14019789950983E+00  .42813765846990E+00
      6     4  .49918344878102E-01 -.26545148121353E+00  .18789567101234E-02
      7     1  .69393516209264E-01 -.50927698251188E-01 -.18770770478848E-02
      7     4  .11249919556344E+00  .36417010197355E-01 -.96512409551535E-02
* ................2290 lines deleted ......................................
    117     1  .39554853137016E-02 -.14701327842692E+00 -.21849261652602E+00
    117     4  .61854528268407E-01 -.15582766664907E+00 -.35595192513222E+00
    117     7 -.14839162033233E-01  .10088643393429E-01 -.34620521010973E+00
    117    10  .24473678103268E-01 -.17719246220580E+00 -.11471841650685E+00
    117    13  .13124059834379E-01  .19447280189975E+00  .55372167099218E-01
    117    16  .11834483725591E-01 -.15394348548100E+00 -.23577099430936E+00
    117    19 -.69920935880248E-02 -.15152016672011E+00 -.15707791358241E-01
    117    22  .56262209482092E-02  .44664432377454E-01 -.29206116099859E+00
    117    25  .13595733163360E-01 -.36791832813222E-01 -.34302028599229E+00
    117    28  .49976730750360E-01 -.52603056350601E-02  .35995661727203E+00
    117    31  .58434167118809E-01  .79162912401483E-01  .19036198391000E+00
    117    34  .18742319369700E-01  .29877748842137E+00  .27423619442271E+00
    117    37  .37293677828651E-01 -.26370207939877E-01  .28314439940865E+00
    117    40 -.15793512947600E-01  .16902050747741E-01 -.68991757800683E-01
```

```
*PARA1 PARA2      PARA2+0____________       PARA2+1________________    PARA2+2__________
  117  43   .13839204459350E-01  -.90319568728349E-01   .87241280008327E-01
  117  46   .17373506530565E-02   .75995410738772E-02  -.22097307167853E-01
  117  49  -.31558372465614E-02   .33086324692108E+00  -.21155116202680E-01
  117  52   .52662048663150E-01  -.96698061270683E-01  -.38697065241955E+00
  117  55   .17854027402451E-01   .45413441850211E-01  -.39199818754031E+00
  117  58  -.20557084589204E-01   .17772427521895E+00  -.38888132782579E+00
  117  61   .51717169153988E-01  -.12774683850231E+00  -.18640329670510E+00
  117  64   .60566764029226E-01  -.96756801702711E-01  -.31097880769930E+00
  117  67   .15946573701026E-01  -.52959490859687E-01   .43877479729634E+00
  117  70  -.56965234511833E-01   .12258278357446E+00   .20637613018780E+00
  117  73   .10379256768073E-01  -.13337986646258E+00   .34656771257246E-01
  117  76   .45650296192972E-01  -.14097331082148E+00   .31904369696173E+00
  117  79  -.15366288987877E-01  -.76872083582857E-01   .14681131961463E+00
  117  82  -.71521817107470E-02  -.14261694699670E+00  -.12950060100137E+00
  117  85  -.46279787222485E-01   .17675785161574E+00   .43321519299327E+00
  117  88   .17270566844414E-02  -.17956461690783E+00  -.95965022007633E-01
  117  91   .67279754048700E-02   .17105290276520E-01   .96879240353699E-02
  117  94   .46879651728024E-02   .15162522246501E-02   .16405537485657E-01
  117  97  -.33487318865767E-01  -.15479070213606E-01  -.17088921255237E-01
  117 100  -.10651453627699E-01  -.97673708447794E-02  -.44763578708339E-02
  117 103  -.10868132563959E-01   .55392984612278E-01   .38519367197329E-01
  117 106   .56288295168491E-01   .61044503649448E-01   .62180451664303E-01
  117 109   .48458825773687E-01   .64903577511731E-01   .46603628193206E+00
  117 112   .50888540957265E+00   .49512938569870E+00   .49390806153475E+00
  117 115   .49291348118876E+00   .51840633003163E+00   .83771951711234E-01
-SOLUTION/MATRIX_ESTIMATE L CORR
*-----------------------------------------------------------------------------------------
+SOLUTION/MATRIX_APRIORI L CORR
*
* Same format as SOLUTION/MATRIX_ESTIMATE, but a priori values.
*
* Here NRC has only used the first column, This is valid, but wastes space.
*               **New to version 1.00 ***
*   The PARA fields increased to 21 chars, For CORR, STDS must be given on
*   the main diagonal
*PARA1 PARA2      PARA2+0______________PARA2+1______________PARA2+2_________
    1     1 .3002645981234567E-02
    2     2 .3004133331239875E-02
    3     3 .3004133333333333E-02
    4     4 .3001488651234567E-02
    5     5 .3002645982345343E-02
    6     6 .3002645981234567E-02
    7     7 .4001116611234567E-02
    8     8 .5000893333333333E-02
    9     9 .5000893333333333E-02
   10    10 .4017828541234567E-02
   11    11 .4007933581234567E-02
   12    12 .4006075555555556E-02
   13    13 .3004133333333333E-02
   14    14 .3002645981234567E-02
   15    15 .3004133333333333E-02
   16    16 .5028606666666666E-02
   17    17 .5025348391234567E-02
   18    18 .3042059581234567E-02
   19    19 .3005950191234567E-02
   20    20 .3002645981234567E-02
   21    21 .2008914271234567E-02
```

```
*PARA1 PARA2 ____PARA2+0_______________PARA2+1______________PARA2+2__________
    22    22 .4054352301234567E-02
    23    23 .4035701301234567E-02
    24    24 .4065111141234567E-02
    25    25 .4007933581234567E-02
    26    26 .4004464581234567E-02
    27    27 .4006075555555556E-02
    28    28 .4223205911234567E-02
    29    29 .4132920301234567E-02
    30    30 .4903133751234567E-02
    31    31 .3002645981234567E-02
    32    32 .3001488651234567E-02
    33    33 .2003966791234567E-02
    34    34 .5008034271234567E-02
    35    35 .5016748271234567E-02
    36    36 .4012389333333333E-02
    37    37 .3207259781234567E-02
    38    38 .3388466301234567E-02
    39    39 .4849083081234567E-02
-SOLUTION/MATRIX_APRIORI L CORR
*-------------------------------------------------------------------------------
%ENDSNX
```

APPENDIX III

The standard IGS Receiver/Antenna name list (IGSCB information System: ftp igscb.jpl.nasa.gov; file: igscb/station/general/rcvr_ant.tab)

ROGUE Receivers	Description
ROGUE SNR-8	2 unit rack-mounted (big Rogue)
ROGUE SNR-800	1 unit rack-mounted (big Rogue)
ROGUE SNR-8A	MiniRogue -- not CONAN compatible
ROGUE SNR-8C	MiniRogue -- CONAN compatible
ROGUE SNR-8000	TurboRogue (field Unit)
IU3GUESNR-8100	TurboRogue (rack mount)
ROGUE SNR-12	TurboRogue (12 channel)
ROGUE SNR-12 RM	TurboRogue (12 channel, rack mount)

ROGUE Antennae	Description
DORNE MARGOLIN R	Antenna with chokering for Rogues (JPL design)
DORNE MARGOLIN B	Antema with chokering for Rogues (AOA design)
DORNE -LINT	Antenna with chokering for TurboRogues

TRIMBLE Receivers	Description
TRIMBLE 4000s	
TRIMBLE 4000SE	
TRIMBLE 4000SL	
TRIMBLE 4000ST	
TRIMBLE 4000SX	
TRIMBLE 4000SLD	Dual freq. L1 c/a; L2 squaring
TRIMBLE 4000SST	Dual freq. L1 c/a; L2 squaring; L2 p-code optional
TRIMBLE 4000SSE	Dual freq. p-code on L1 and L2; xcr Y-code

TRIMBLE Antennae	Description
4000SE INTERNAL	
4000SLMICRO	(Round)
4000SLD L1/L2	Dual freq. geodetic receiver (SLD series)
4000ST INTERNAL	
4000ST KINEMATIC	Single freq. without a ground plane
4000ST L1 GEODETIC	To use with single freq. geodetic receiver
4000ST L1/L2 GEOD	Dual freq. geodetic receiver (Mod.14532)
4000SX MICRO	(Square)
TR GEOD L1/L2 GP	Geod. L1/L2 compact; grd. plane incl . (Mod.22020)
TR GEOD L1/L2 W/O GP	Geod. L1/L2 compact; grd. plane removed (Mod.22020)
M-PULSE L1/L2 SURVEY	MicroPulse L1/L2 GPS Surveying Antenna 90LL12300
DORNE MARGOLIN TRIM	Antenna with chokering (Trimble design)

MINIMAC Receivers	Description
MINIMAC 2816AT	Rack-mounted (used in CIGNET and NIED)
MINIMAC 2816	Field unit

MINIMAC Antennae	Description
MACROMETER X-DIPOLE	Crossed-dipole antenna with large ground plane
MINIMAC PATCH	Patch antenna

ASHTECH Receivers	Description
ASHTECH xxxxxxxx	xxxxxxxx is the receiver type tobe found in the receiver-generated S-file, e.g. LM-XII3 or L-XII

ASHTECHAntemae	Description
GEODETIC L1/L2 L	Dual freq. with ground plane (LD-XII & MD-XII)
GEODETIC L1/L2 P	Dual freq. with ground plane (P-12)
GEODETIC III L1/L2	Dual freq. with ground plane
DORNE MARGOLIN ASH	Antenna with chokering (Ashtech design)
MARINE/RANGE	Single freq. with a smaller ground plane
A-C L1	Single freq. w/o ground plane for aircraft use
A-C L1/L2	Dual freq. without ground plane for aircraft use

LEICA Receivers	Description
SR299	Geodetic receiver, internal antenna
SR299E	Geodetic receiver, external antenna

LEICAAntenna	Description
INTERNAL	Internal antenna of SR299 receiver
EXTERNAL WITH GP	External antenna of SR299E with groundplane
EXTERNAL WITHOUT GP	External antenna of SR299E, without groundplane

APPENDIX IV

CODING STATION INFORMATION CHANGES IN SINEX V1.00: A SAMPLE

There are THREE valid ways of coding a mid-week station reoeiver/antenna change in weekly SINEX v1.00. To demonstrate this a recent change at GRAZ (week 0859) to show them below. To quote SINEX v1.00 definition "SITE+PT+SOLN defines a unique estimate, SITE+PT is equivalent to DOMES (DOMEX) and uniquely identifies a geodetic mark".

Case (i): To state two separate estimates at a site, assuming the mark has changed. We call these marks GRAZ A and GRAZ B, and don't re-use the old DOMES code, but code the second estimate with unknown DOMES:

```
+SITE/ID
 GRAZ A 11001M002 P GRAZ                    15 29 36.5  47  4  1.7   538.3
 GRAZ B --------- P GRAZ                    15 29 36.5  47  4  1.7   538.3
-SITE/ID
+SITE/RECEIVER
 GRAZ A ---- P 96:174:00000 96:176:86369 ROGUE SNR-8C        ----- -----------
 GRAZ B ---- P 96:177:00000 96:182:86369 ROGUE SNR-8000      ----- -----------
-SITE/RECEIVER
+SITE/ANTENNA
 GRAZ A ---- P 96:174:00000 96:176:86369 DORNE MARGOLIN B     128
 GRAZ B ---- P 96:177:00000 96:182:86369 DORNE MARGOLIN T     457
-SITE/ANTENNA
+SITE/ECCENTRICITY
 GRAZ A ---- P 96:174:00000 96:176:86369 UNE   2.0680   0.0000   0.0000
 GRAZ B ---- P 96:177:00000 96:182:86369 UNE   1.9640   0.0000   0.0000
-SITE/ECCENTRICITY
+SOLUTION/EPOCHS
 GRAZ A    1 P 96:174:00000 96:176:86369 96:175:43185
 GRAZ B    1 P 96:177:00000 96:182:86369 96:179:86385
-SOLUTION/EPOCHS
```

It is illegal to give GRAZ B the sane DOMES as GRAZ A (see quote above).

Case (ii) To state two separate estimates at a site, reduced to a common mark. These are called GRAZ A 1 and GRAZ A 2, and both use a single SITE/ID line because there's only one mark:

```
+SITE/ID
 GRAZ A 11001M002 P GRAZ                    15 29 36.5  47  4  1.7   538.3
-SITE/ID
+SITE/RECEIVER
 GRAZ A 0001 P 96:174:00000 96:176:86369 ROGUE SNR-8C        ----- -----------
 GRAZ A 0002 P 96:177:00000 96:182:86369 ROGUE SNR-8000      ----- -----------
-SITE/RECEIVER
+SITE/ANTENNA
 GRAZ A 0001 P 96:174:00000 96:176:86369 DORNE MARGOLIN B     128
 GRAZ A 0002 P 96:177:00000 96:182:86369 DORNE MARGOLIN T     457
```

```
-SITE/ANTENNA
+SITE/ECCENTRICITY
 GRAZ A 0001 P 96:174:00000 96:176:86369 UNE   2.0680   0.0000   0.0000
 GRAZ A 0002 P 96:177:00000 96:182:86369 UNE   1.9640   0.0000   0.0000
-SITE/ECCENTRICITY
+SOLUTION/EPOCHS
 GRAZ A 0001 P 96:174:00000 96:176:86369 96:175:43185
 GRAZ A 0002 P 96:177:00000 96:182:86369 96:179:86385
-SOLUTION/EPOCHS
```

Case (iii) To state a single estimate at a site, where the station information changed during the data span. In this case there should be only one SOLUTION/EPOCHS entry, for GRAZ A1. As many SITE/... entries may be used as required, in this example we need two in each block .

```
+SITE/ID
 GRAZ A 11001M002 P GRAZ                      1529  36.5   47   4  1.7   538.3
-SITE/ID
+SITE/RECEIVER
 GRAZ A ---- P 96:174:00000 96:176:86369 ROGUE SNR-8C          ----- -----------
 GRAZ A ---- P 96:177:00000 96:182:86369 ROGUE SNR-8000        ----- -----------
-SITE/RECEIVER
+SITE/ANTENNA
 GRAZ A ---- P 96:174:00000 96:176:86369 DORNE MARGOLIN B      128
 GRAZ A ---- P 96:177:00000 96:182:86369 DORNE MARGOLIN T      457
-SITE/ANTENNA
+SITE/ECCENTRICITY
 GRAZ A ---- P 96:174:00000 96:176:86369 UNE   2.0680   0.0000   0.0000
 GRAZ A ---- P 96:177:00000 96:182:86369 UNE   1.9640   0.0000   0.0000
-SITE/ECCENTRICITY
+SOLUTION/EPOCHS
 GRAZ A    1 P 96:174:00000 96:182:86369 96:178:00000
-SOLUTION/EPOCHS
```

Note that in this case no SOLN codes are required in the SITE/... blocks! The records are well orderedby their data start/stop fields. This is a change from the accepted SINEX v0.05 usage.

APPENDIX 2

Towards a new IGS Orbit Model

T.A. SPRINGER, G. BEUTLER, M. ROTHACHER

Astronomical Institute
University of Berne
Sidlerstrasse 5
CH-3012 Bern
Switzerland

March 19, 1996

Why a new IGS Orbit Model ?

- The existing model including Rock4/42 Solar Radiation Pressure was developed **before** the availability of highly accurate orbits.
- It therefore cannot take into account subtleties which became apparent through IGS operations.
- The existing model is **not** suited for long arcs.
- The consistency of individual IGS l-day orbit series and the consistency between these series soon reaches 1–5 cm level rms.

Where are we today?

Within the IGS we are aware of:

- The CODE Extended Orbit Model Beutler et al, 1993) on which the IGS long-arc analysis is based,
- developments at MIT (used by SIO) leading o a dramatic improvement of the SIO orbit series,
- developments at JPL to model satelli es during their "eclipse seasons"

- Subsequently we wi l discuss the experiences made with he CODE Extended Orbit Model

History of the Extended CODE Orbit Model

- Developed in 1993 (!) at CODE.
- Used since early 1994 for the long arc analysis of the IGS orbit combination.
- Routinely used at CODE to check orbit quality of the routine IGS processing.
- In January 1996 fully integrated into the Bernese software.

The Extended CODE Orbit Model

The radiation pressure model may be written as:

$$a_{rpr} = a_{ROCK} + a_D + a_Y + a_X$$

where a_{ROCK} is the acceleration due to the Rock-model, and

$$a_D = [a_{D0} + a_{DC}\cos u + a_{DS}\sin u]e_D = D(u)e_D$$
$$a_Y = [a_{Y0} + a_{YC}\cos u + a_{YS}\sin u]e_Y = Y(u)e_Y$$
$$a_X = [a_{X0} + a_{XC}\cos u + a_{XS}\sin u]e_X = X(u)e_X$$

where a_{D0} $a_{DC}, a_{DS}, a_{Y0}, a_{YC}, a_{YS}, a_{X0}, a_{XC}$, and a_{XS} are the **nine parameters** of the Extended Model,

e_D is the unit vector sun-satellite,
e_y is the unit vector along the spacecraft 's solar-panel axis,
$e_X = e_Y \times e_D$,
u is the argument of latitude at time t.

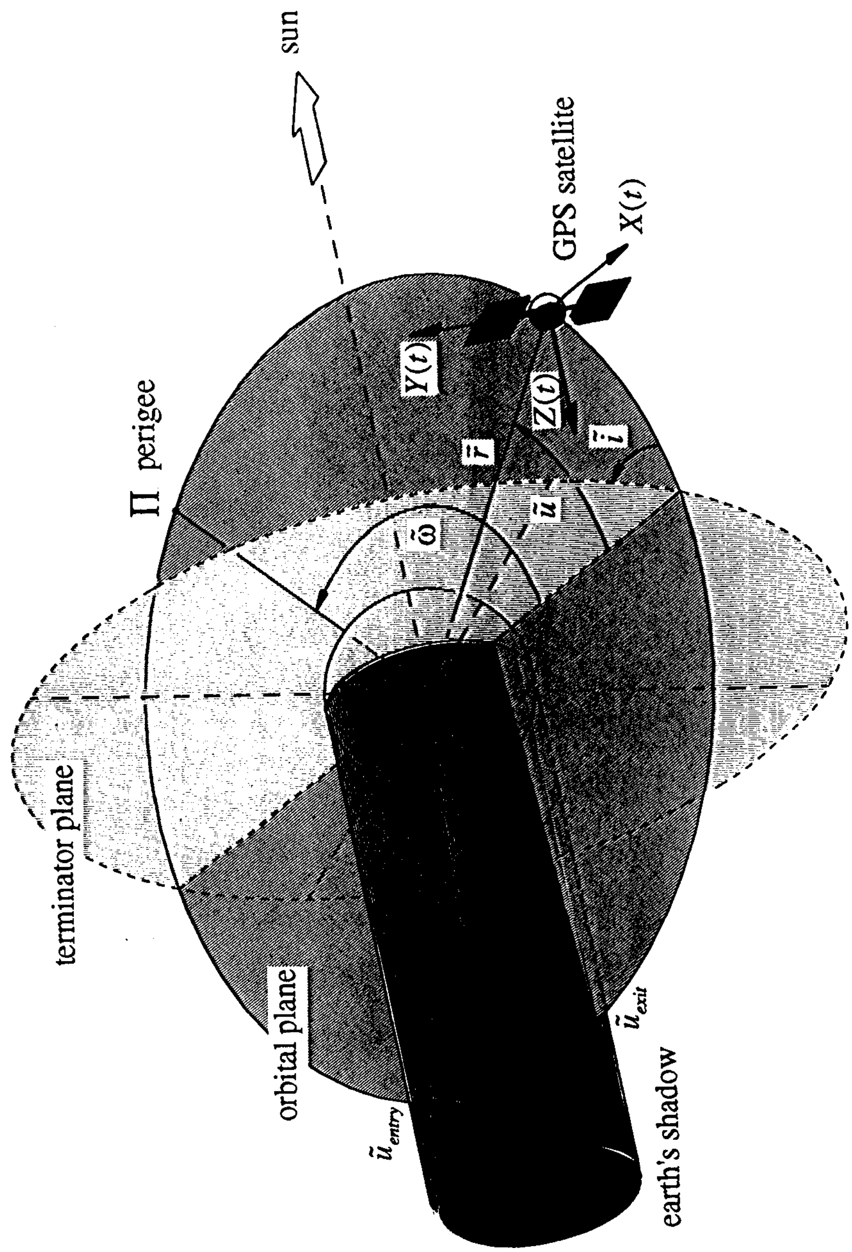

sun
GPS satellite
$X(t)$
$Y(t)$
$Z(t)$
Π perigee
$\tilde{r}$
$\tilde{i}$
$\tilde{u}$
$\tilde{\omega}$
terminator plane
orbital plane
$\tilde{u}_{entry}$
$\tilde{u}_{exit}$
earth's shadow

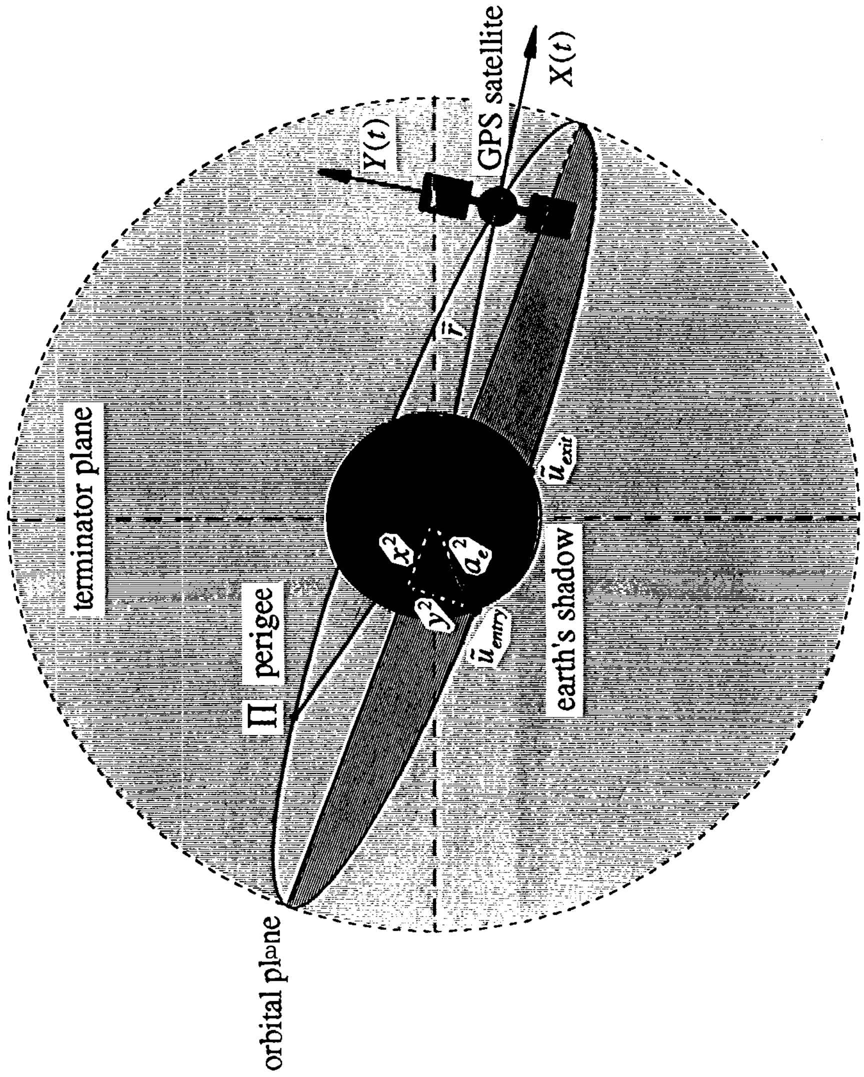
orbital plane
Π perigee
terminator plane
earth's shadow
GPS satellite
$X(t)$
$Y(t)$
$\vec{r}$
x^2
y^2
a_e^2
$\vec{u}_{exit}$
$\vec{u}_{entry}$

Why the Extended CODE Orbit Model

- Conventional 8 or 9 parameter orbit models are no longer adequate for high precision orbits ($< 10cm$),
- "stochastic" pulses are capable of absorbing orbit model deficiencies but a better "deterministic" model is preferable,
- in more than 2 years of IGS orbit combinations, the model has shown that it is capable of modeling the satellites over 7 days at the few centimeter level,
- all days of an n-day arc have the same quality,
- it removes the so called "y-shift" of the orbit- and coordinate-systems,
- it allows much better orbit predictions.

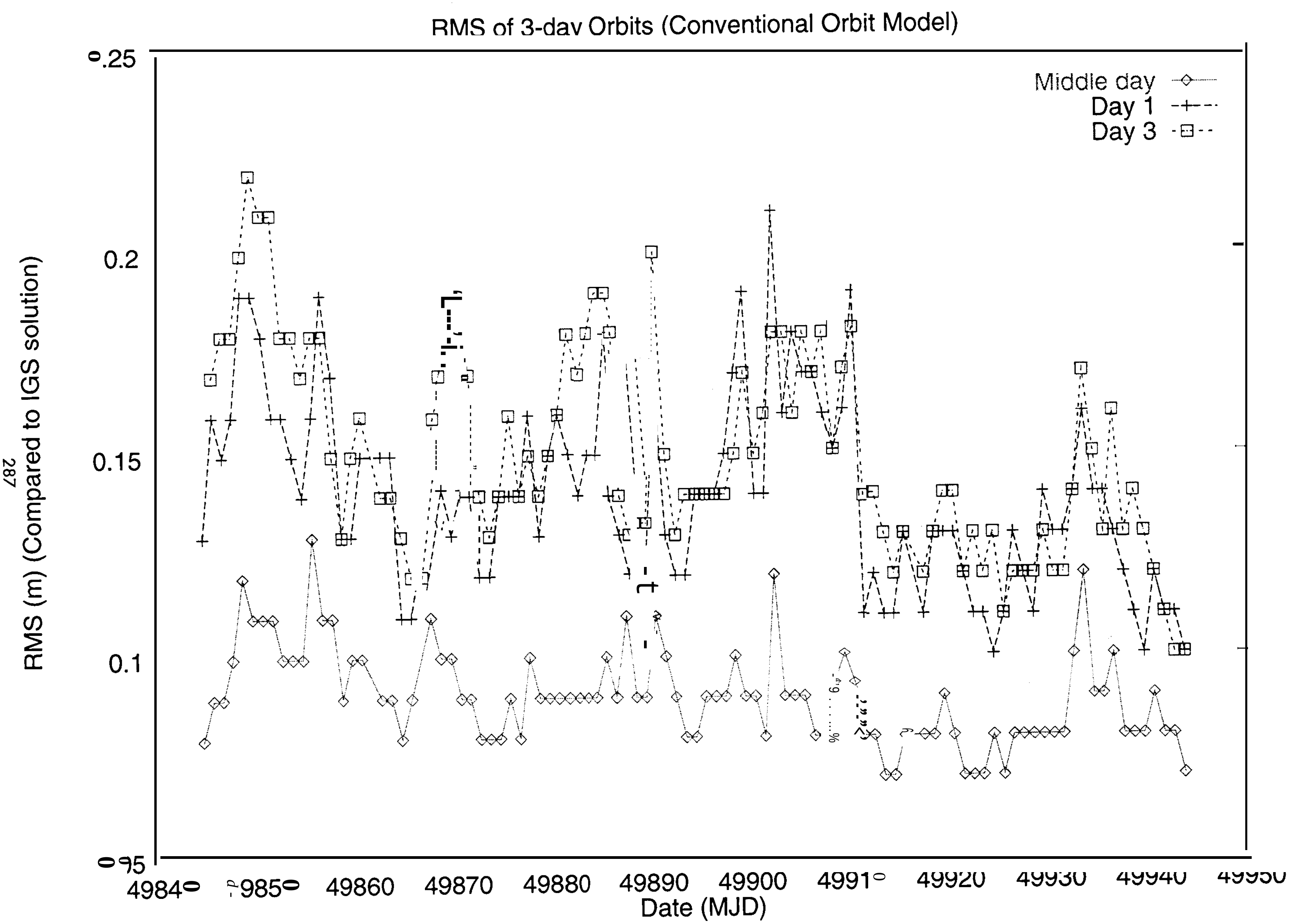
RMS of 3-dav Orbits (Conventional Orbit Model)
Middle day
Day 1
Day 3
0.25
0.2
0.15
0.1
0.05
49840
49850
49860
49870
49880
49890
49900
49910
49920
49930
49940
49950
Date (MJD)
RMS (m) (Compared to IGS solution)

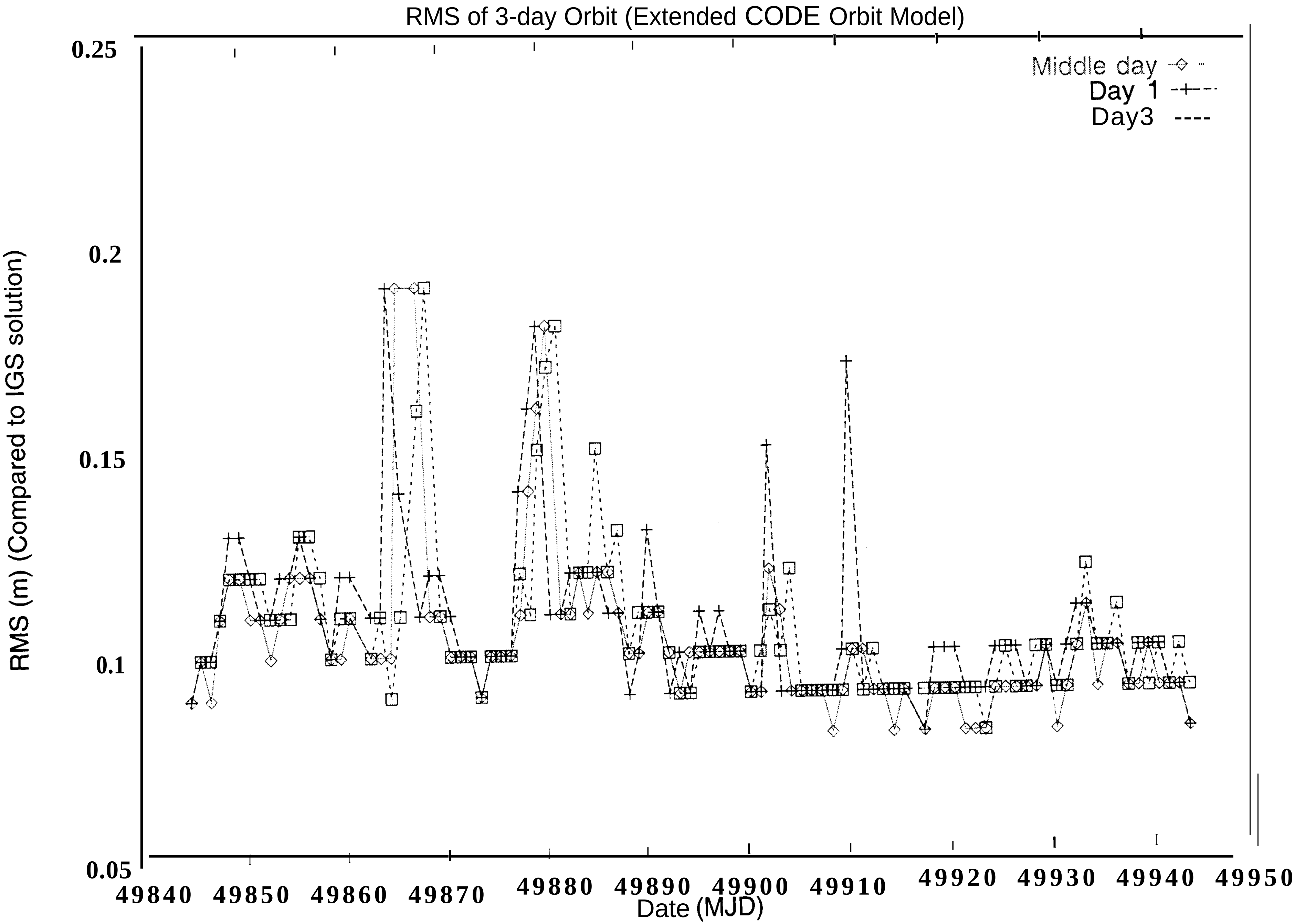
RMS of 3-day Orbit (Extended CODE Orbit Model)
Middle day
Day 1
Day3
0.25
0.2
0.15
0.1
0.05
RMS (m) (Compared to IGS solution)
49840
49850
49860
49870
49880
49890
49900
49910
49920
49930
49940
49950
Date (MJD)

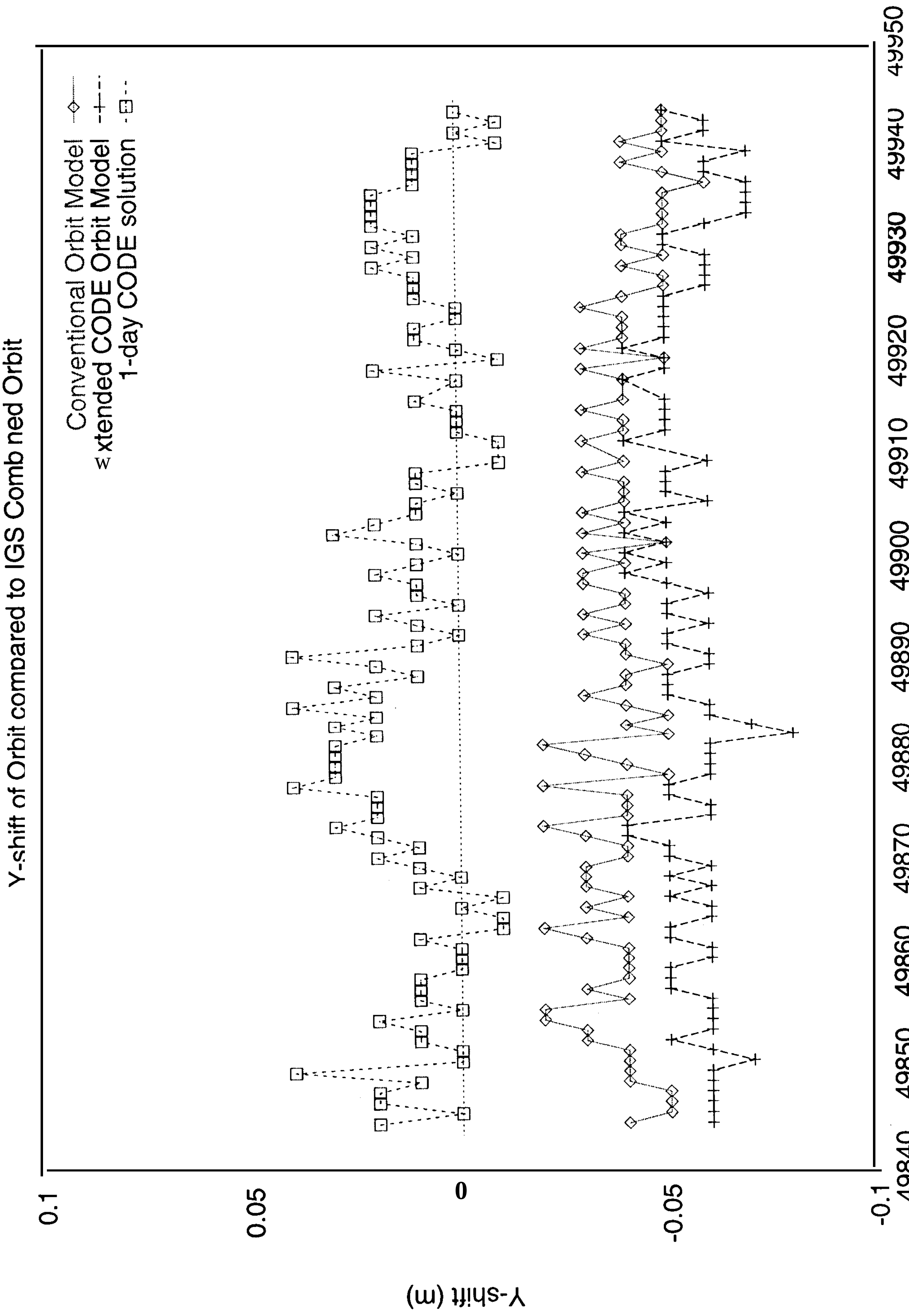

Y-shift of Orbit compared to IGS Comb ned Orbit
Conventional Orbit Model
xtended CODE Orbit Model
1-day CODE solution
Y-shift (m)
0.1
0.05
0
-0.05
-0.1
Date (MJD)
49840
49850
49860
49870
49880
49890
49900
49910
49920
49930
49940
49950

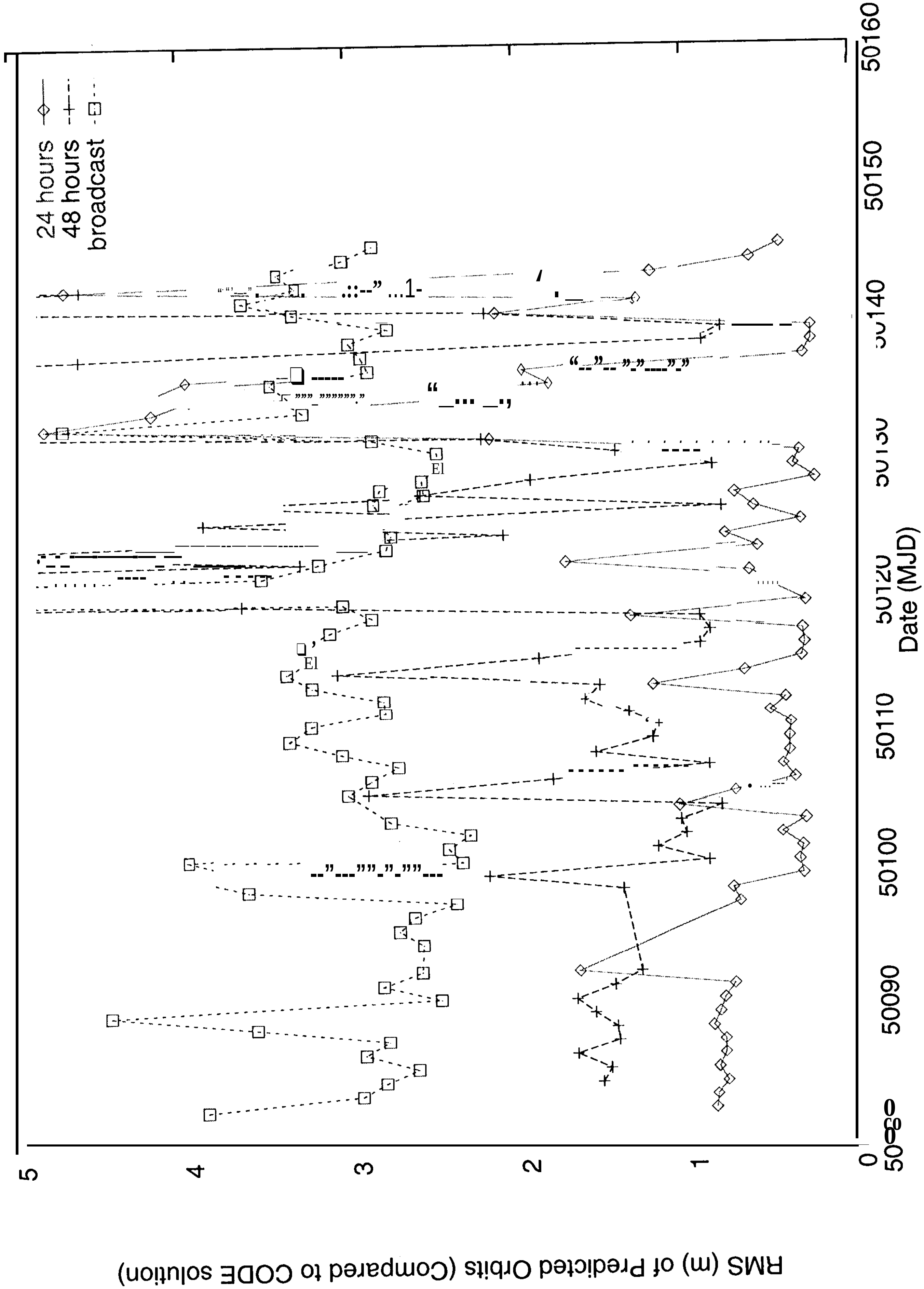
24 hours
48 hours
broadcast
RMS (m) of Predicted Orbits (Compared to CODE solution)
Date (MJD)
0
1
2
3
4
5
50080
50090
50100
50110
50120
50130
50140
50150
50160

Use of the Extended CODE Orbit Model for Rapid Orbits

- Rapid Orbits at CODE are orbits generated around 12 hours UT for the preceding day.
- Possibility to use long(er) arcs because all days show the same quality,
- with longer arcs the (Rapid) Orbit becomes much less sensitive to the number of available stat ions.
- Currently we use a 5-day arc, where our contribution to the IGS Preliminary Orbit is the last day of this arc.
- Solution is created using normal equation stacking (AD DNEQ). The final 5-day solution takes only 5 min of CPU (on a Alpha 600 5/266).
- Possibility to use two days of our official IGS processing which contain our full network (currently at maximum 76 stations).

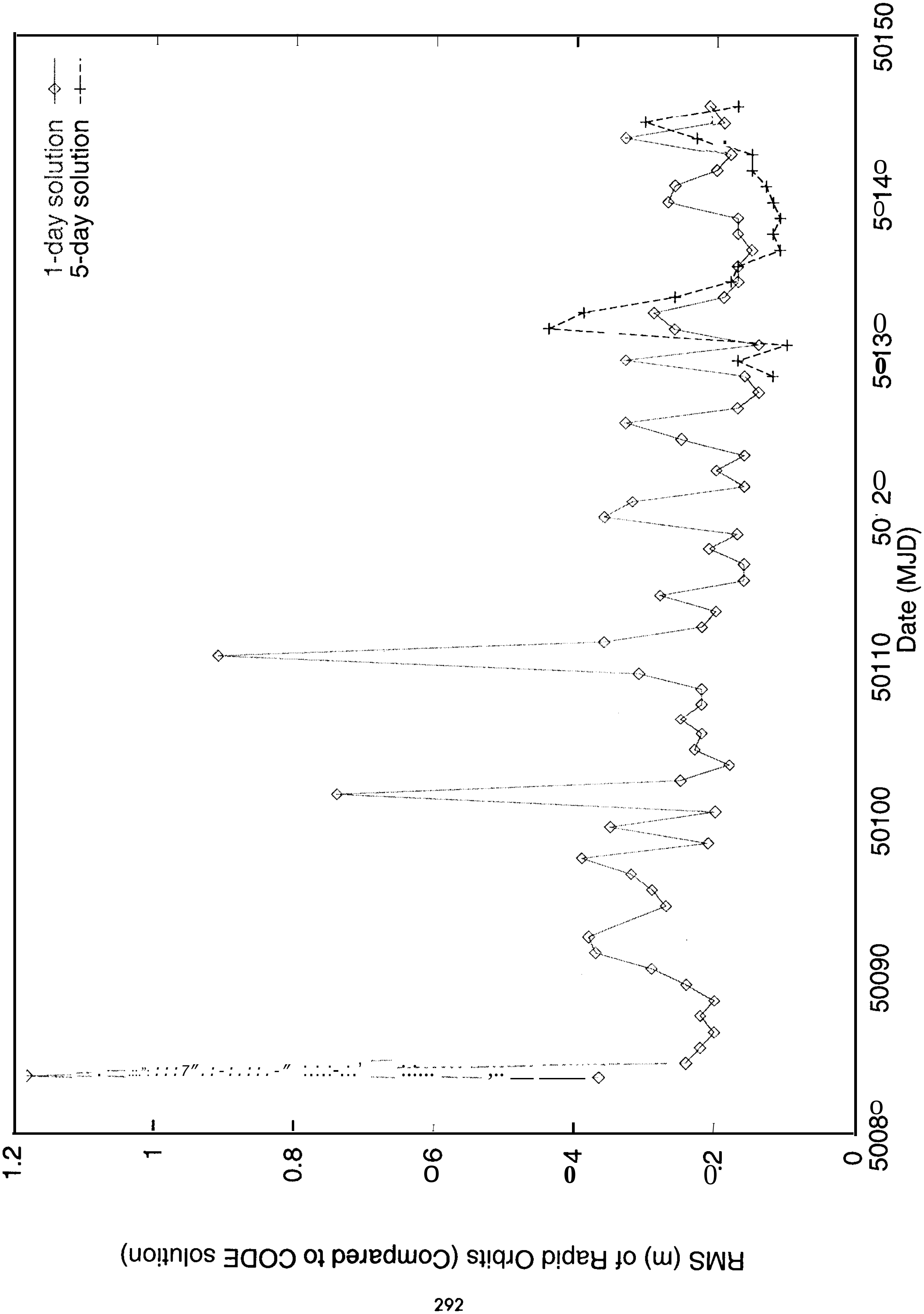
1-day solution
5-day solution
Date (MJD)
RMS (m) of Rapid Orbits (Compared to CODE solution)
50080
50090
50100
50110
50150
0
0.2
0.6
0.8
1
1.2

Problem areas with Orbit Modeling

- In general each acceleration term (dynamical parameter) will create an out-of-plane (W) component which may implicitly (through a resulting net rotation of all orbital planes) affect the transformation parameters between the inertial and the terrestrial reference frames (ICRF and ITRF):
- Motion of node for satellite k over 1 revolution:

$$\delta\Omega_k(t_0, t) = \frac{1}{n_k \cdot a_k \cdot \sin i_k} \cdot \int_{t_0}^{t} \sin u_k \cdot W_k(t) \cdot dt'$$

- Mean motion of the entire GPS orbit system:

$$\dot{\Omega}_{mean}(t) = \frac{1}{n_{sat}} \cdot \sum_{k=1}^{n_{sat}} \frac{1}{U_k} \cdot \delta\Omega_k(t - \frac{1}{2}U_k, t + \frac{1}{2}U_k)$$

- Similar equations maybe extracted for change of inclination (correlation with nutation!).

UTI – UTC **differences to Bulletin** A EOP Series

and resulting Orbit Rotation due to RPR – Model

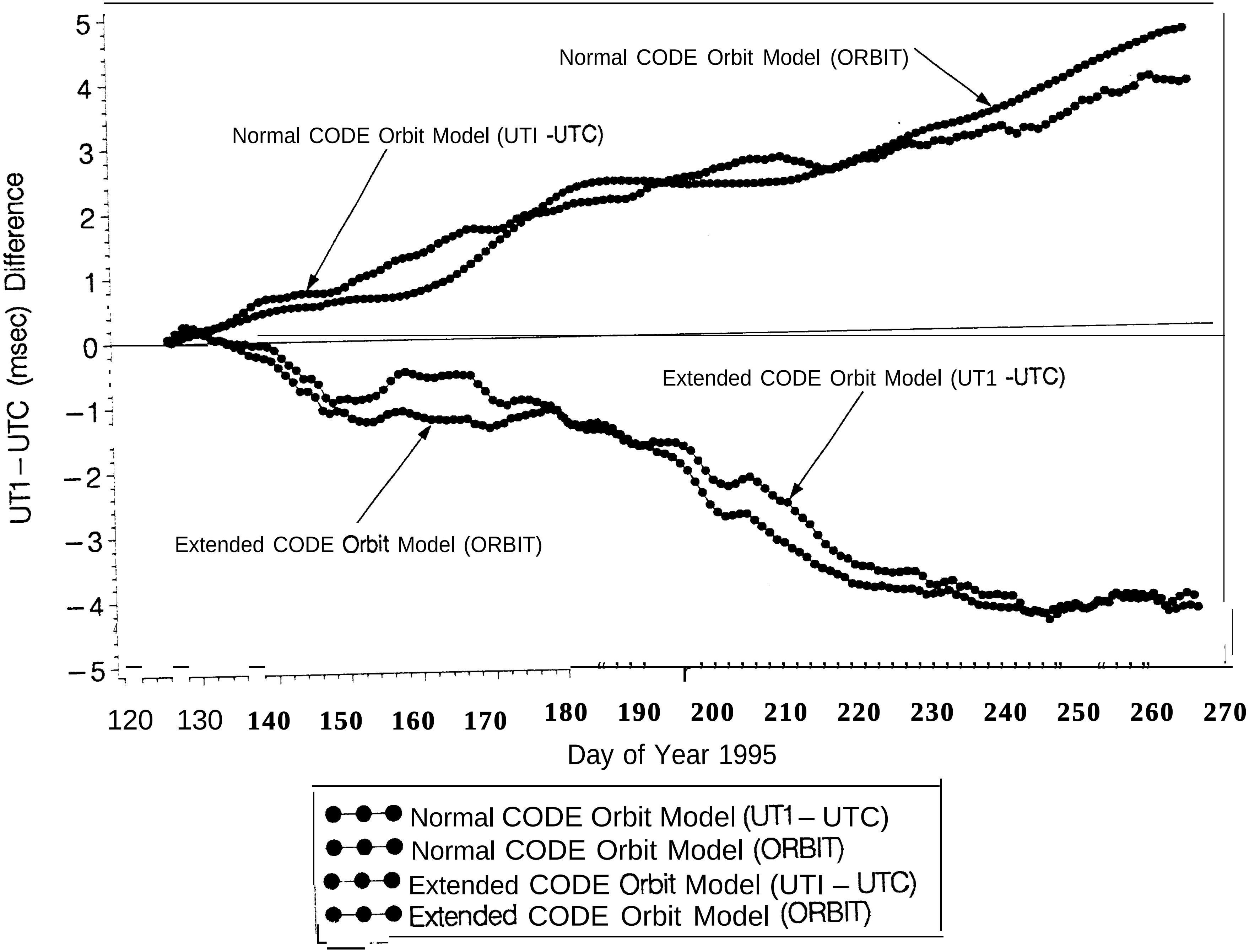

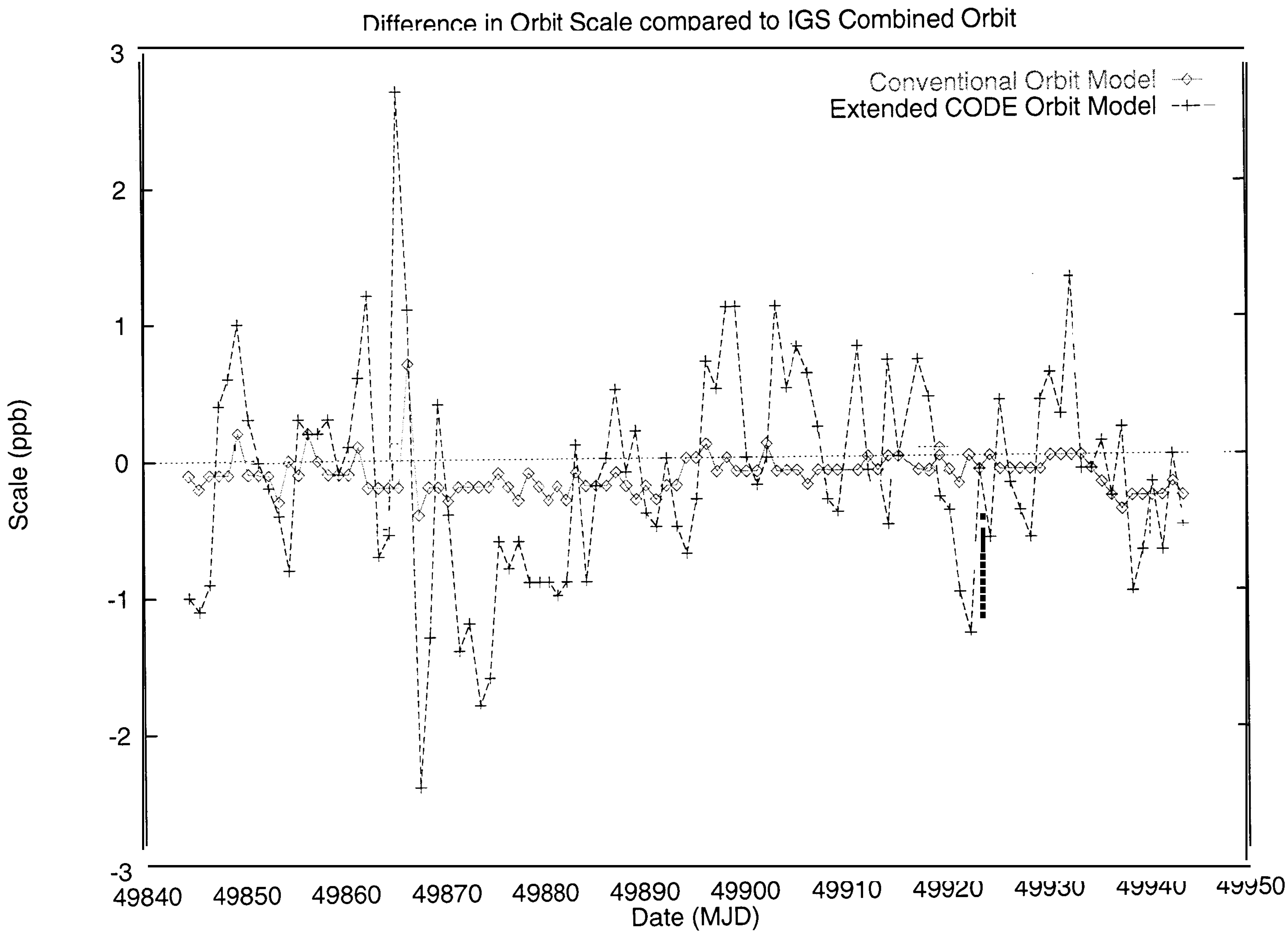
Difference in Orbit Scale compared to IGS Combined Orbit
Conventional Orbit Model
Extended CODE Orbit Model
Scale (ppb)
3
2
1
0
-1
-2
-3
49840
49850
49860
49870
49880
49890
49900
49910
49920
49930
49940
49950
Date (MJD)

Conclusions concerning Extended CODE Orbit Model

- All individual days of an n-day arc are of the same (high) quality.
- Possibility to meat e arcs of at least 7 days.
- No "y-shift" problem.
- Rapid orbits within 12 hours at the 10 cm level.
- (Rapid) Orbit predictions for the next 24 hours are at the 30 cm level.
- Correlations with UT1-UTC and nutation series exist, but additional constraints will cope with this problem (to be shown).

Conclusions concerning the IGS Orbit Model

- We believe that a new IGS Orbit Model should be ~~**defined.**~~
- This model may be general in the sense that it will leave some degree of freedom to each IGS Analysis Center.
- We believe that all experiences gained in the context of GPS high accuracy orbit modeling should be used to develop this ~~**new** IGS **Standard.**~~
- **We** believe that the new model also should become part of the ~~**new** IERS **standards.**~~

MULT -TECHNIQUE EOP COMB NAT ON

D. Gambis

Central Burean of IERS, Paris Observatory, FRANCE

IGS Workshop, Silver Spring, March 19-2 1996

UT1 based on both VLBI and GPS

The approach

- GPS high-frequency variations associated with long-term VLBI variations

- Procedure has to be the most simple as possible for clarity of the process.

- High frequency terms are removed in VLBI series while they are kept for internal GPS “UTI” series.

The critical point concerns the threshold determination within which the high-frequency information contained in the GPS series is valuable.